TGAL-88-03

YIELD ESTIMATION OF NOVAYA ZEMLYA EXPLOSIONS FROM SHORT-PERIOD BODY WAVES

W.W. Chan, K.L. McLaughlin, R.K. Cessaro, M.E. Marshall, and A.C. Lees

Teledyne Geotech Alexandria Laboratories
314 Montgomery Street
Alexandria, Virginia 22314-1581

JUNE 1988

FINAL TECHNICAL REPORT: TASKS 1 and 2
ARPA ORDER NO: A05143
PROJECT TITLE: Yield Estimation and Regional Location
CONTRACT: MDA903-87-C-0069

Approved for Public Release; Distribution Unlimited

Prepared for:
DEFENSE ADVANCED RESEARCH PROJECTS AGENCY
1400 Wilson Boulevard
Arlington, VA 22209

Monitored by:
Defense Supply Service - Washington
Room 1D 245, The Pentagon
Washington, D.C. 20310

Unclassified
SECURITY CLASSIFICATION OF THIS PAGE

ADA203393

REPORT DOCUMENTATION PAGE

Form Approved
OMB No 0704-0188
Exp Date Jun 30, 1986

1a REPORT SECURITY CLASSIFICATION Unclassified	1b RESTRICTIVE MARKINGS
2a SECURITY CLASSIFICATION AUTHORITY	3 DISTRIBUTION / AVAILABILITY OF REPORT Approved for Public Release; Distribution Unlimited
2b DECLASSIFICATION / DOWNGRADING SCHEDULE	
4 PERFORMING ORGANIZATION REPORT NUMBER(S) TGAL-88-03	5 MONITORING ORGANIZATION REPORT NUMBER(S)
6a NAME OF PERFORMING ORGANIZATION Teledyne Geotech Alexandria Laboratories 6b OFFICE SYMBOL (If applicable)	7a NAME OF MONITORING ORGANIZATION Defense Supply Service - Washington
6c ADDRESS (City, State, and ZIP Code) 314 Montgomery Street Alexandria, VA 22314	7b ADDRESS (City, State, and ZIP Code) Room 1D245, The Pentagon Washington, D.C. 20310
8a NAME OF FUNDING / SPONSORING ORGANIZATION DARPA 8b OFFICE SYMBOL (If applicable) NMRO	9 PROCUREMENT INSTRUMENT IDENTIFICATION NUMBER MDA903-87-C-0069
8c ADDRESS (City, State, and ZIP Code) 1400 Wilson Boulevard Arlington, VA 22209	10 SOURCE OF FUNDING NUMBERS PROGRAM ELEMENT NO / PROJECT NO / TASK NO / WORK UNIT ACCESSION NO
11 TITLE (Include Security Classification) Yield Estimation of Novaya Zemlya Explosions from Short-Period Body Waves	
12 PERSONAL AUTHOR(S) W.W. Chan, K.L. McLaughlin, R.K. Cessaro, M.E. Marshall, A.C. Lees	
13a TYPE OF REPORT Final Technical 13b TIME COVERED FROM June 87 TO June 88 14 DATE OF REPORT (Year, Month, Day) August 1988 15 PAGE COUNT 103	
16 SUPPLEMENTARY NOTATION	
17 COSATI CODES FIELD / GROUP / SUB-GROUP	18 SUBJECT TERMS (Continue on reverse if necessary and identify by block number) Yield estimation, Novaya Zemlya, Body Waves

19 ABSTRACT (Continue on reverse if necessary and identify by block number)

This study investigates the characteristics of Novaya Zemlya explosions using various body wave phases. This information will be used to calibrate the yields of these explosions. The azimuthal variation of amplitude for the Novaya Zemlya explosions as seen from WWSSN recordings indicates that there is a strong component of near-source heterogeneity due to multiple source excitation, near-source structural heterogeneity, or source anisotropy. The systematic azimuthal variation in amplitude may be modeled with a $\sin(2\theta)$ curve, which allows an estimate of the magnitude bias due to certain network station distributions. Several events that have an azimuthal variation in amplitude which departs from a $\sin(2\theta)$ curve may be possible multiple explosions.

20 DISTRIBUTION / AVAILABILITY OF ABSTRACT ☒ UNCLASSIFIED/UNLIMITED ☐ SAME AS RPT ☐ DTIC USERS	21 ABSTRACT SECURITY CLASSIFICATION
22a NAME OF RESPONSIBLE INDIVIDUAL Dr. Robert R. Blandford	22b TELEPHONE (Include Area Code) (202) 697-7523 22c OFFICE SYMBOL NMRO

DD FORM 1473, 84 MAR 83 APR edition may be used until exhausted
All other editions are obsolete

SECURITY CLASSIFICATION OF THIS PAGE
Unclassified

(19. Continued)

Clear pP and pPcP depth phases can be observed in deconvolved teleseismic P-wave and PcP-wave source time functions from Novaya Zemlya events. With few exceptions, pP and pPcP delay times show a systematic increase with increasing size. The two largest southern Novaya Zemlya events observed ($m_b > 6.7$) show delay times of about 0.6 sec., and most large events ($6.0 < m_b < 6.9$) have depth phase delays between 0.35 and 0.55 sec.

Relative explosion source size estimates are presented based on spectral measures of P, PcP, and P_{diff} at EKA and WRA arrays. These spectral energy measurements may be correlated with the m_b estimates to provide an independent calibration of magnitudes. By comparing the spectral energy levels between Novaya Zemlya and Amchitka events, it is found that the largest Novaya Zemlya event is larger than CANNIKIN.

The time domain measurements of P'P' for Novaya Zemlya recorded on WWSSN stations are used to provide a calibration of the m_b estimates from P-waves which are quite often clipped for large events. Using a distance-amplitude correction obtained from the data set, the m_b estimates for P'P' are computed using a generalized linear model. A different approach is to solve for the station-path effects and m_b's for P'P' simultaneously. Both magnitude estimates are well correlated with the m_b estimates from the P-waves.

SUMMARY

This study investigates the characteristics of Novaya Zemlya explosions using various body wave phases. This information will be used to calibrate the yields of these explosions. The azimuthal variation of amplitude for the Novaya Zemlya explosions as seen from WWSSN recordings indicates that there is a strong component of near-source heterogeneity due to multiple source excitation, near-source structural heterogeneity, or source anisotropy. The systematic azimuthal variation in amplitude may be modeled with a $\sin(2\theta)$ curve, which allows an estimate of the magnitude bias due to certain network station distributions. Several events that have an azimuthal variation in amplitude which departs from a $\sin(2\theta)$ curve may be possible multiple explosions.

Clear pP and pPcP depth phases can be observed in deconvolved teleseismic P-wave and PcP-wave source time functions from Novaya Zemlya events. With few exceptions, pP and pPcP delay times show a systematic increase with increasing size. The two largest southern Novaya Zemlya events observed ($m_b > 6.7$) show delay times of about 0.6 sec., and most large events ($6.0 < m_b < 6.9$) have depth phase delays between 0.35 and 0.55 sec.

Relative explosion source size estimates are presented based on spectral measures of P, PcP, and P_{diff} at EKA and WRA arrays. These spectral energy measurements may be correlated with the m_b estimates to provide an independent calibration of magnitudes. By comparing the spectral energy levels between Novaya Zemlya and Amchitka events, it is found that the largest Novaya Zemlya event is larger than CAN-

NIKIN.

The time domain measurements of P'P' for Novaya Zemlya recorded on WWSSN stations are used to provide a calibration of the m_b estimates from P-waves which are quite often clipped for large events. Using a distance-amplitude correction obtained from the data set, the m_b estimates for P'P' are computed using a generalized linear model. A different approach is to solve for the station-path effects and m_b's for P'P' simultaneously. Both magnitude estimates are well correlated with the m_b estimates from the P-waves.

TABLE OF CONTENTS

	Page
SUMMARY	iii
TABLE OF CONTENTS	v
LIST OF FIGURES	vi
LIST OF TABLES	x
INTRODUCTION	1
AZIMUTHAL CHARACTERISTICS OF NOVAYA ZEMLYA P-WAVE AMPLITUDES	4
Explosive Source Directivity	7
Multiple Events	31
SPECTRAL ESTIMATES OF NOVAYA ZEMLYA EXPLOSION SOURCE SIZE FROM P, PcP, and P_{diff}	39
Source Time Function Deconvolutions	40
P- and PcP-Wave Spectral Estimates	49
P_{diff}-Wave Spectral Estimates	56
Comparison with Amchitka Events	57
MAGNITUDE SCALING FOR NOVAYA ZEMLYA EXPLOSIONS FROM P'P'	63
P'P' Amplitude-Distance Relationship	65
Maximum-Likelihood Estimates of m_b(P'P')	72
CONCLUSIONS	78
REFERENCES	80
DISTRIBUTION LIST	83

LIST OF FIGURES

Figure No.	Title	Page
1	Composite plot of P(a) amplitude versus distance for 17 Novaya Zemlya explosions recorded at WWSSN stations. The amplitude decay assumes a 1/r geometrical spreading factor similar to the Veith and Clawson (1972) relationship which is plotted in dashed line.	6
2a	Plots of sin(2θ) least squares fit to the southern Novaya Zemlya amplitude data (solid circles) after correcting for geometrical spreading. The Y's indicate measurements within the noise level and upward arrows indicate clipped measurements.	8 & 9
2b	Plots of the amplitude for each station on a focal sphere for the southern Novaya Zemlya events. The size of the symbol indicates the amplitude in mμ. The circles are well recorded P_a amplitudes, the triangles are for stations with clipped measurements, and the diamonds are for stations with measurements within the noise level.	10 & 11
3a	Plots of sin(2θ) fit to the northern Novaya Zemlya amplitude data (solid circles) after correcting for geometrical spreading. The Y's indicate measurements within the noise level and upward arrows indicate clipped measurements.	12-20
3b	Plots of the amplitude for each station on a focal sphere for the northern Novaya Zemlya events. The size of the symbol indicates the amplitude in mμ. The circles are well recorded P_a amplitudes, the triangles are for stations with clipped measurements, and the diamonds are for stations with measurements within the noise level.	21-29
4a	Partitioning according to equal area quadrant (upper) and equal station distribution (lower) and the m_b estimates associated with each quadrant for the northern Novaya Zemlya event of 07 Nov 68.	33

4b	Partitioning according to equal area quadrant (upper) and equal station distribution (lower) and the m_b estimates associated with each quadrant for the northern Novaya Zemlya event of 19 Oct 80.	34
4c	Partitioning according to equal area quadrant (upper) and equal station distribution (lower) and the m_b estimates associated with each quadrant for the northern Novaya Zemlya event of 14 Oct 70.	35
4d	Partitioning according to equal area quadrant (upper) and equal station distribution (lower) and the m_b estimates associated with each quadrant for the southern Novaya Zemlya event of 18 Oct 75.	36
5a	Comparison of deconvolved P and PcP phases recorded at the array EKA from events located at the Novaya Zemlya test sites.	41
5b	Deconvolutions of P phases recorded at the array EKA from events located at the Novaya Zemlya test sites.	42
5c	Deconvolutions of PcP phases recorded at the array EKA from events located at the Novaya Zemlya test sites.	43 & 44
5d	Deconvolutions of P_{diff} phases recorded at the array WRA from events located at the Novaya Zemlya test sites.	45
6	pP-P and pPcP-PcP time delays versus Lilwall and Marshall (1986) m_b measured from the P and PcP deconvolutions of Figure 5. Events at the southern Novaya Zemlya test site are indicated with "stars", northern Novaya Zemlya test site events are indicated with "boxes". Measurements made on deconvolved PcP waves are indicated by open stars or boxes, while those made on deconvolved P waves are solid stars or solid boxes. With the exception of one northern event and the two large southern events, the data exhibit a trend indicating larger events have longer delay times.	48
7a	Maximum-likelihood P-wave averaged spectra for Novaya Zemlya event 73270 recorded at 19 EKA stations. The upper and lower error bars are indicated for each discrete spectral amplitude.	50

7b	Maximum-likelihood PcP-wave averaged spectra for Novaya Zemlya event 73270 recorded at 20 EKA stations. The upper and lower error bars are indicated for each discrete spectral amplitude.	51
7c	P-wave spectra for event in Fig. 7a recorded at EKA. The spectra is corrected for instrument response, attenuation, and estimated RDP. The horizontal bar indicates the bandwidth used to estimate the spectral amplitude of the phase.	52
7d	PcP-wave spectra for event in Fig. 7a recorded at EKA. The spectra is corrected for instrument response, attenuation, and estimated RDP. The horizontal bar indicates the bandwidth used to estimate the spectral amplitude of the phase.	53
8	P and PcP spectral estimates at EKA versus Lilwall and Marshall (1986) m_b. The dotted line serves to separate P and PcP spectral level estimates. Events at the northern test site are identified with "boxes", the southern test site with "stars". P-wave spectral levels inferred from PcP spectral levels are identified by either open "stars" or "boxes".	55
9	P spectral levels at WRA corrected for t*=0.45 sec, and estimated RDP, versus Lilwall and Marshall (1986) m_b.	58
10	Ray paths for P′P′ (PKPPKP). The phase is best recorded at distance range of 40° to 80°. The underside reflection from the 650 discontinuity is generally denoted as the P′P′ precursor.	64
11	An example of P′P′ trace from the WWSSN station BOZ (Δ = 60.6°)	66
12	P′P′ amplitude-distance relationship for eight events in Novaya Zemlya. These are uncorrected amplitudes measured from the analog WWSSN film chips.	67
13	Composite P′P′ data scaled to m_b = 6 after correcting for instrument response and gain. A rms fit to the data yields an empirical distance-amplitude relationship for P′P′	68
14	Predicted P, PKP, and P′P′ peak amplitudes from WKBJ theory for a perturbed PEM (Choy and Cormier, 1983). Note the PKP caustic at 145° and the P′P′ caustic at 70° .	70

15	Observed P(max)/P′P′ amplitude ratios at WWSSN stations between 30° and 80°, for the eight large Novaya Zemlya explosions. Only on scale P(max) and P′P′ data are plotted. The ratios decrease drastically near the caustics of about 60° to 70°.	71
16	Least squares fit of m_b(P)'s versus m_b(P′P′) using (a) *a priori* constraints from estimated station corrections and amplitude-distance correction (left) and (b) no station and path constraints (right).	73
17	Station-path effects versus distance obtained from ML-GLM estimates of m_b(P′P′) using 7 northern Novaya Zemlya events. The dashed line indicates the P′P′ distance-amplitude relationship from Figure 13.	77

LIST OF TABLES

Table No.	Title	Page
1	Novaya Zemlya m_b's.	5
2	Sin(2θ) Fit to the Novaya Zemlya Data.	30
3	Novaya Zemlya m_b by Quadrant.	37
4	Novaya Zemlya pP and pPcP Amplitudes and Delays.	46
5	Novaya Zemlya Explosion P and PcP Spectral Levels at EKA.	56
6	Novaya Zemlya P_{diff} Spectral Estimates at WRA.	57
7	Log(Ψ_∞) Spectral Estimates.	60
8	Comparison of Amchitka Surface waves and P-wave.	62
9	m_b(P'P') Estimates Using Amplitude-Distance Corrections.	74
10	m_b(P'P') Estimates Corrected for Station-Path Effects.	75

INTRODUCTION

Novaya Zemlya, an archipelago located between the Barents Sea and Kara Sea, has been a frequent site for large nuclear explosions detonated by the Soviet Union. The high tonnage of the explosions there may provide a constraint on the high end of the magnitude-yield relationship. However, on account of its remoteness in the Arctic, Novaya Zemlya remains one of the most poorly monitored test sites in the world. Thick and low velocity sediments (Eldholm and Talwani, 1977; Chan and Mitchell, 1985) perturb surface waves propagation. The lack of regional station coverage has also limited most studies of Novaya Zemlya to teleseismic data. In determining a regional magnitude scale for Novaya Zemlya, Nuttli (1988) found the available data set for Novaya Zemlya to have a limited distance and azimuthal coverage, which makes it more difficult to assess than the other test sites. The paucity of information regarding local geology adds to the difficulty in determining a magnitude scaling relationship for the region. This study undertakes a manifold approach to understanding the characteristics and yield estimation of Novaya Zemlya explosions by applying several methods to the study of various body wave phases.

Azimuthal variations in body-wave amplitude are detected for some Novaya Zemlya events and may be attributed to one of more of the following effects: tectonic release, source directivity, or local structural heterogeneity. The observed azimuthal amplitude variation has a strong impact on the construction of a magnitude:yield calibration curve for these events. As a direct result of the biased station locations, yield estimations for the Novaya Zemlya events may be biased low, if the $\sin(2\theta)$ variation is a proper parameterization of the amplitude variation. In the case of double events,

which may be the source function for some of the Novaya Zemlya explosions, m_b estimates are further complicated due to interference effects. These effects should be taken into account in the estimation of explosive yields.

In order to utilize seismic magnitudes to estimate explosive yield, a magnitude:yield relationship must be established for each test site. Two of the most important contributions to systematic offsets in the m_b:Log(yield) relationship are (1) the intrinsic attenuation in the mantle directly beneath the test site, and (2) the interference effects of the free-surface reflection (pP) with the direct P wave. This report presents estimates of these two effects for the Novaya Zemlya test sites. The maximum-likelihood deconvolution procedure of Shumway and Der (1985) is used to examine directly the pP phase from explosions at Novaya Zemlya test sites, and the attenuation parameter $\overline{t^*}$ is determined from the observed spectrum. Estimates may then be formulated for the yield of each event, once these two primary effects on the magnitude:yield relationship have been determined.

The largest Novaya Zemlya explosions clipped a substantial fraction (over 50%) of the WWSSN network as well as an unknown number of stations that report amplitudes to NEIS and ISC. As a consequence, the magnitudes for these events are suspect unless the data censoring effects are taken into account. The magnitudes presented by Chan *et al.* (1988) showed that these events had magnitudes as large as, or larger than, CANNIKIN (5 Mt). In order to provide further confidence in that result, we have examined other plausible means to determine relative explosion source sizes based on phases that are not clipped for the largest events. These phases provide additional independent measures of source size to complement the traditional m_b

measurements made using P-waves.

The core phases PcP and P′P′ (PKPPKP) are examined as possible alternative measures of the radiated P-wave energy from explosions at Novaya Zemlya. We extend the method developed by Gupta *et al.* (1985) to study NTS and Eastern Kazakh P-wave and P-coda spectra to PcP-wave spectra. By referencing the PcP spectral levels at the EKA array to the P-wave spectral levels for events where both P and PcP remain on scale, the (clipped) P-wave spectral level for large events can be inferred from their corresponding unclipped PcP-waves. When geometrical spreading is applied to the P-wave and PcP-wave spectral levels, the P-wave moments for the events can be estimated.

For the high-tonnage Novaya Zemlya explosions, many of the analog recordings of P arrivals are clipped. The core reflected phase, P′P′ with its easily observable on-scale recordings, may prove suitable as an independent calibration of the source size. The P′P′ magnitude estimates may then offer an independent calibration of the m_b estimates.

AZIMUTHAL CHARACTERISTICS OF NOVAYA ZEMLYA P-WAVE AMPLITUDES

Long-period surface wave data from explosions have been found to contain a strong anisotropic component (Press and Archambeau, 1962; Aki, 1964; Nuttli, 1969; Hirasawa, 1971; Toksöz and Kehrer, 1972; Masse', 1981), and may be due to triggered earthquakes (Brune and Pomeroy, 1963; Aki and Tsai, 1972) or stress relaxation (Press and Archambeau, 1962; Archambeau, 1972). Interference between the anisotropic component and the explosion has also been demonstrated by Wallace *et al.* (1983) using long period body wave data from Pahute Mesa events. For short-period body wave, Lay *et al.* (1984) also found azimuthal variation of amplitude for the Pahute Mesa events, which they attributed to tectonic release or local heterogeneity in the structure.

As has been demonstrated by Bache (1976), Murphy *et al.* (1983), and Wallace *et al.* (1983), the level of the anisotropic component may bias the m_b estimations due to its interference effect on the explosive-generated P waves. This finding is important for the estimation of energy from explosions in Novaya Zemlya, which are known to be associated with strong azimuthal variation (Burger *et al.*, 1986). These variations may be interpreted in terms of near-source structural inhomogeneity or tectonic release.

In order to examine the azimuthal dependence of Novaya Zemlya explosive P-waves, we studied the variation of the "a" phase amplitudes for 17 of these events. The MLE-GLM magnitudes estimates (Chan *et al.*, 1988) for these events are listed in Table 1 with those from Lilwall and Marshall (1986).

Table 1. Novaya Zemlya m_b's

	MLE-GLM						Lilwall and Marshall(1986)	
Date	m_b(a)	σ	m_b(b)	σ	m_b(max)	σ	m_b(b)	σ
Southern								
27 Sep 73	5.18	0.05	5.47	0.05	5.72	0.05	5.83	0.03
27 Oct 73	6.65	0.05	6.88	0.05	7.10	0.05	6.90	0.03
02 Nov 74	6.50	0.05	6.80	0.05	7.02	0.05	6.75	0.02
18 Oct 75	6.23	0.05	6.52	0.05	6.84	0.05	6.70	0.02
Northern								
27 Oct 66	6.07	0.04	6.31	0.04	6.45	0.04	6.47	0.03
21 Oct 67	5.40	0.04	5.60	0.04	5.77	0.04	5.99	0.03
07 Nov 68	5.60	0.04	5.85	0.04	6.04	0.04	6.11	0.02
14 Oct 69	5.76	0.04	5.96	0.04	6.13	0.04	6.18	0.03
14 Oct 70	6.43	0.04	6.65	0.04	6.83	0.04	6.77	0.03
27 Sep 71	6.27	0.05	6.49	0.05	6.64	0.05	6.63	0.02
28 Aug 72	5.99	0.05	6.25	0.05	6.38	0.05	6.46	0.02
12 Sep 73	6.37	0.05	6.70	0.05	6.79	0.05	6.96	0.03
29 Aug 74	6.13	0.05	6.40	0.05	6.58	0.05	6.54	0.02
23 Aug 75	6.12	0.05	6.38	0.05	6.51	0.05	6.55	0.02
21 Oct 75	6.11	0.05	6.35	0.05	6.56	0.05	6.59	0.02
20 Oct 76	4.03	0.04	4.35	0.04	4.66	0.04	4.89	0.03
01 Sep 77	5.09	0.06	5.43	0.06	5.57	0.06	5.71	0.02
10 Aug 78	5.39	0.04	5.63	0.04	5.86	0.04	6.04	0.02
11 Oct 80	5.19	0.05	5.45	0.05	5.66	0.05	5.80	0.02
01 Oct 81	5.23	0.05	5.49	0.05	5.65	0.05	5.91	0.02
18 Aug 83	5.33	0.05	5.53	0.05	5.71	0.05	5.84	0.02
25 Oct 84	5.16	0.06	5.43	0.06	5.61	0.06	-	-

Given the strong component of apparent tectonic release associated with the Novaya Zemlya explosions, we seek to understand the possible correlation between the azimuthal amplitude variation and tectonic release taking the approach of Lay *et al.* (1984). We also investigate its relationship to various other near-source parameters, including local structural heterogeneities, double event, and focusing effects. We construct an amplitude-distance relationship for Novaya Zemlya data from the amplitude data, as shown in Figure 1, that resembles the more global model of Veith and Clawson (1972). The anomalous low amplitude values are probably miscalibrated data.

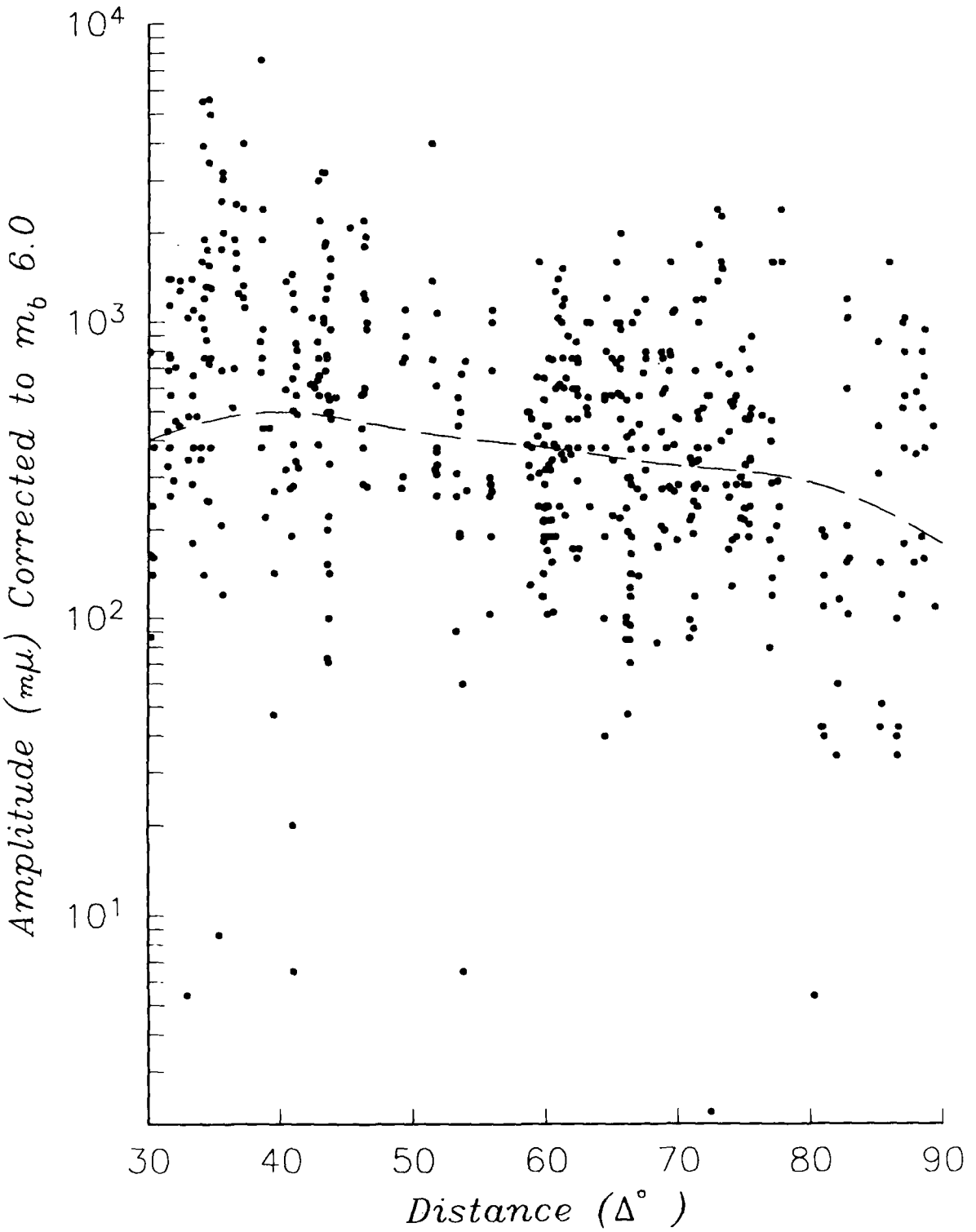

Figure 1. Composite plot of P(a) amplitude versus distance for 17 Novaya Zemlya explosions recorded at WWSSN stations. The amplitude decay assumes a 1/r geometrical spreading factor similar to the Veith and Clawson (1972) relationship which is plotted in dashed line.

Explosive Source Directivity

The initial "a" phase amplitude data are read from analog film chips for 17 Novaya Zemlya explosions. These amplitudes are corrected for the simple geometrical spreading relationship used in Langston and Helmberger (1975). The corrected amplitude data are plotted both against azimuth (Figures 2a and 3a) and on a focal sphere (Figures 2b and 3b) for 4 southern and 18 northern Novaya Zemlya events. From Figures 2a and 3a, these data display a systematic azimuthal amplitude variation that may not be attributed simply to scatter of the data. The corresponding plots of the amplitudes on the focal sphere as shown in Figures 2b and 3b do not show any systematic azimuthal and distance relationship. Following Lay *et al.* (1984), we apply a $\sin(2\theta)$ rms fit to each individual set of censored data where each curve may be parameterized by

$$y = A\ (1 + x \times \sin(2(\ \alpha - \theta\ )))$$

where A is the amplitude of the modulation in millimicrons, θ is the phase of the modulation in degrees and alpha is the station azimuth. The amplitude, phase, and statistics of each best fitting curve are listed in Table 2. The $\sin(2\theta)$ term appears to fit the data with good confidence level for most of the events, as indicated in Table 2.

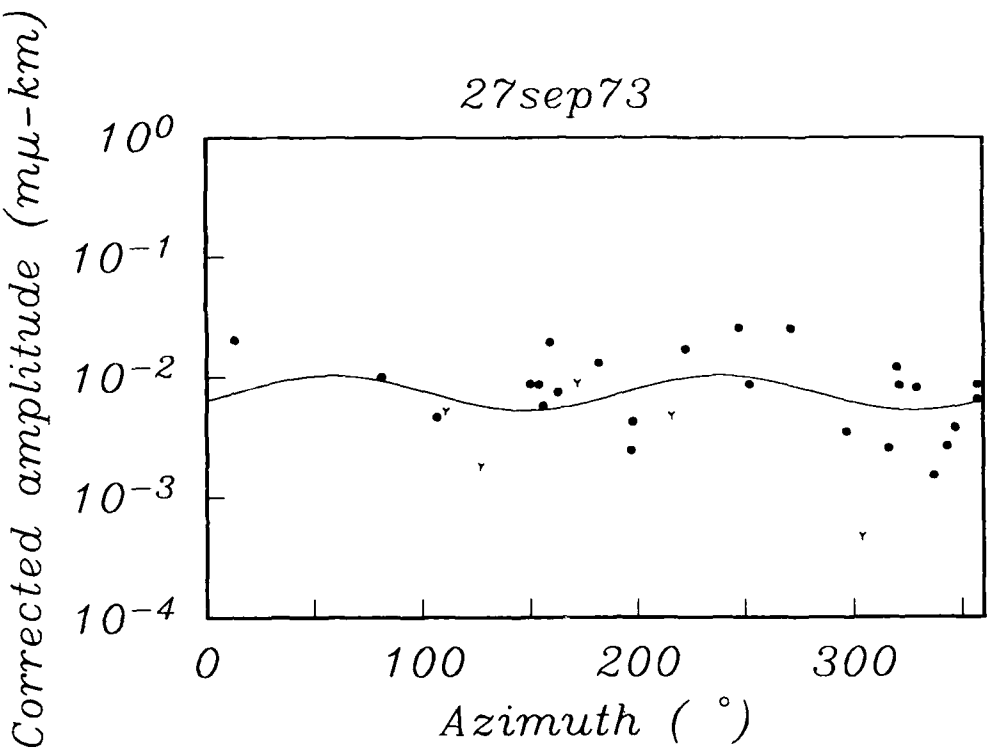

(a)

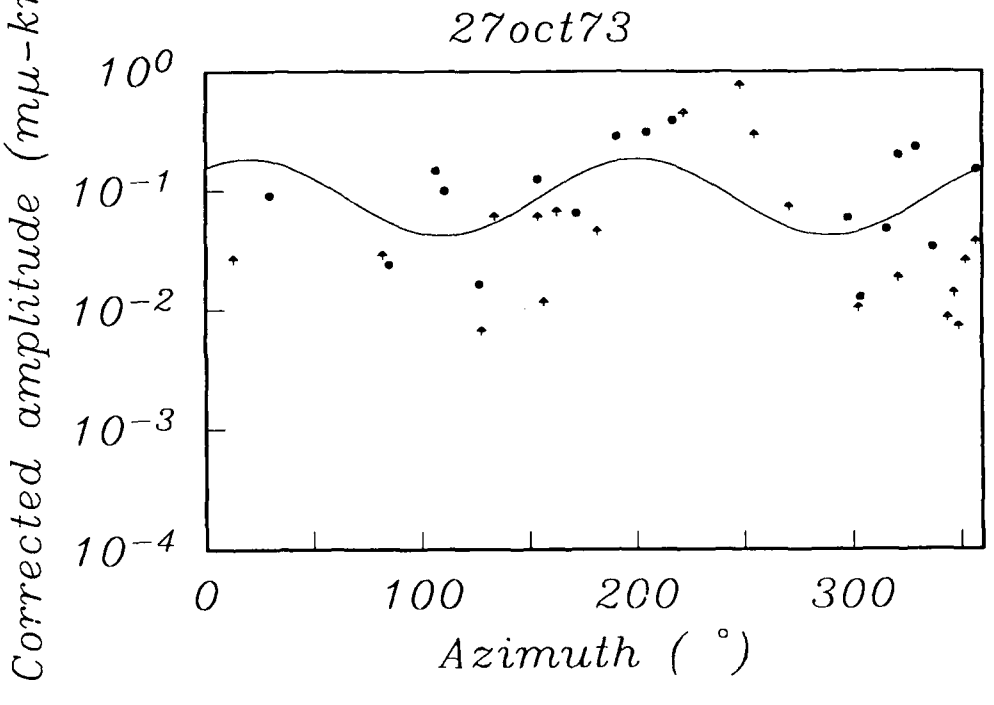

(b)

Figure 2a. Plots of sin(2θ) least squares fit to the southern Novaya Zemlya amplitude data (solid circles) after correcting for geometrical spreading. The Y's indicate measurements within the noise level and upward arrows indicate clipped measurements.

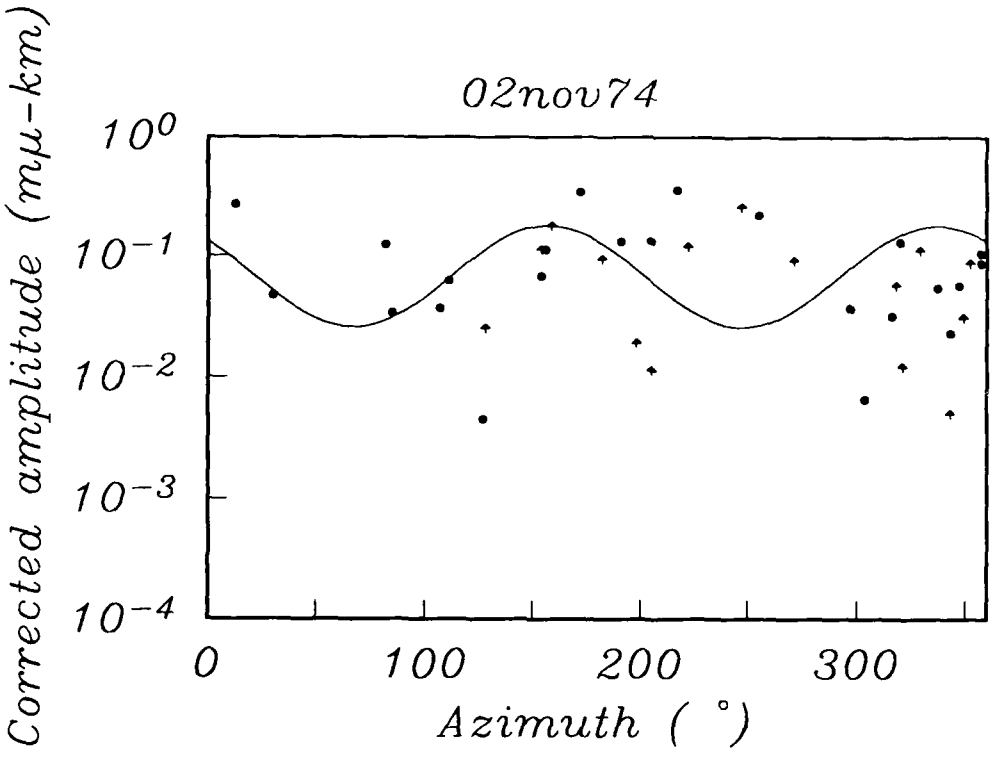

(c)

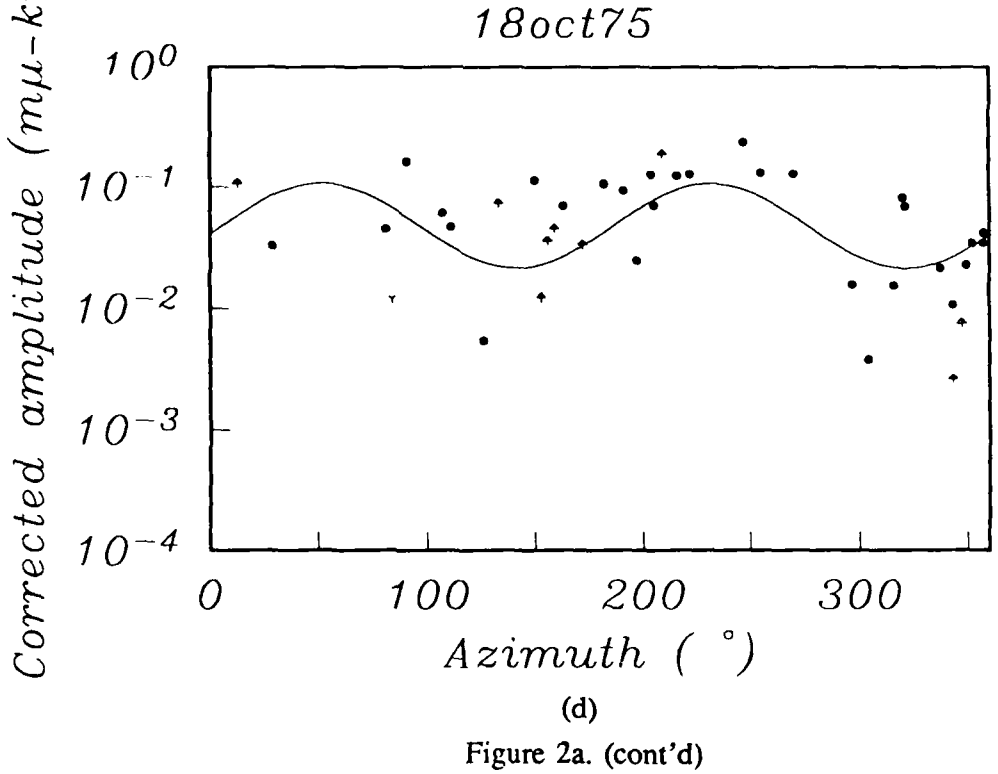

(d)

Figure 2a. (cont'd)

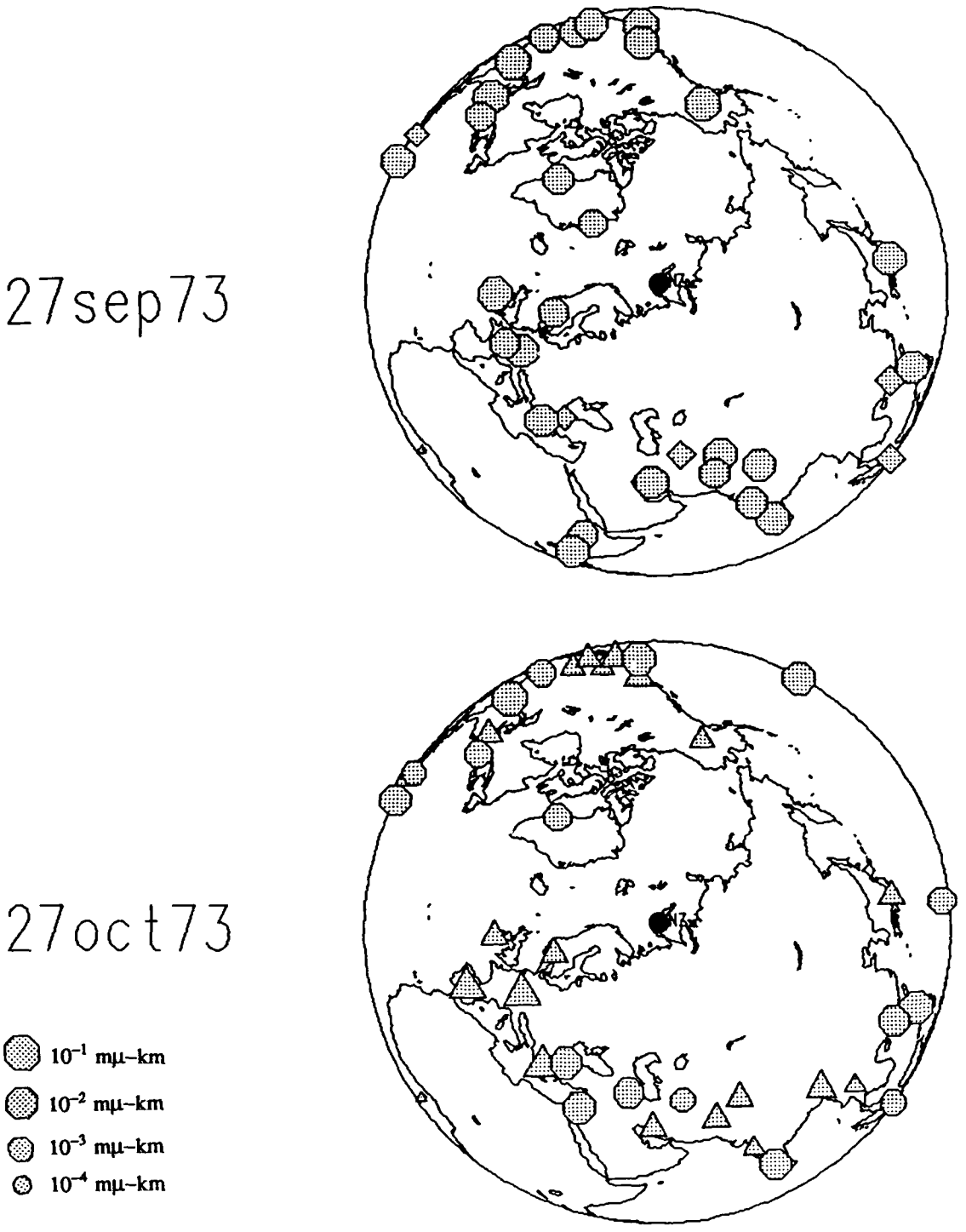

Figure 2b. Plots of the amplitude for each station on a focal sphere for the southern Novaya Zemlya events. The size of the symbol indicates the amplitude in mμ. The circles are well recorded P_a amplitudes, the triangles are for stations with clipped measurements, and the diamonds are for stations with measurements within the noise level.

02nov74

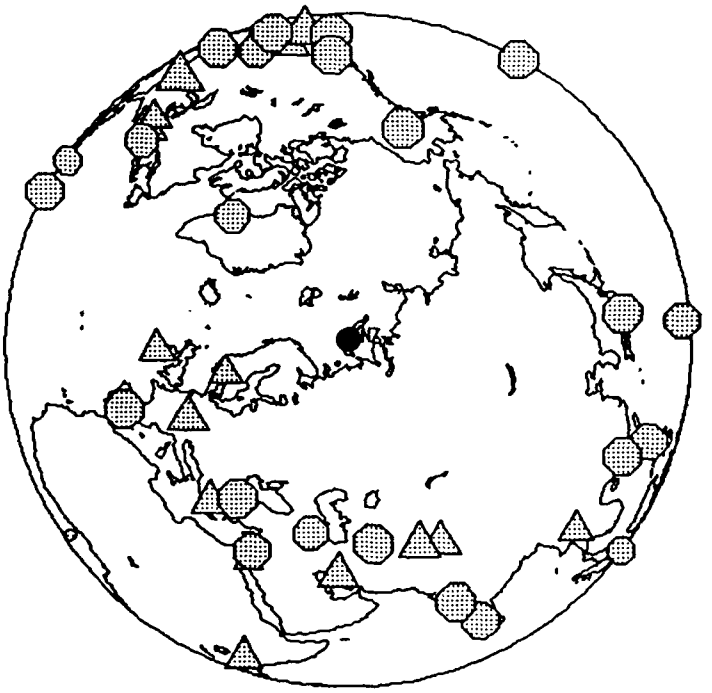

18oct75

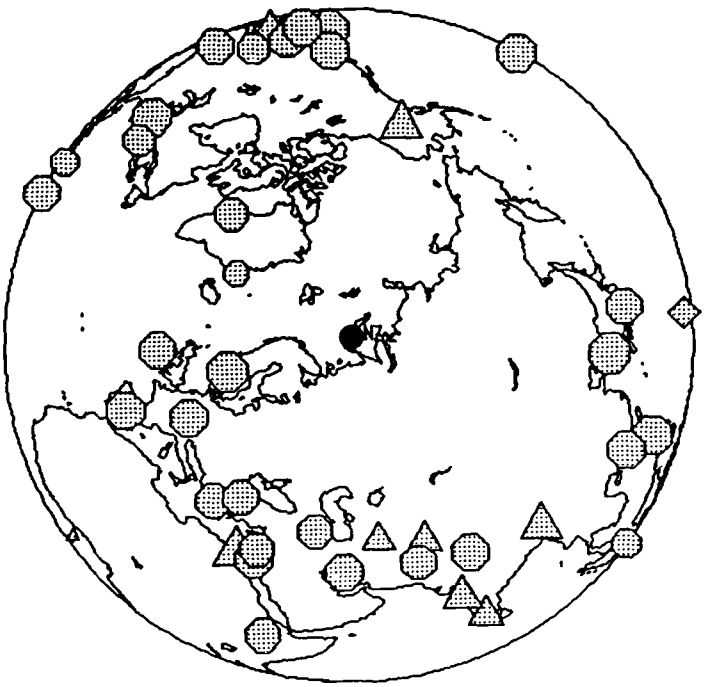

Figure 2b. (cont'd)

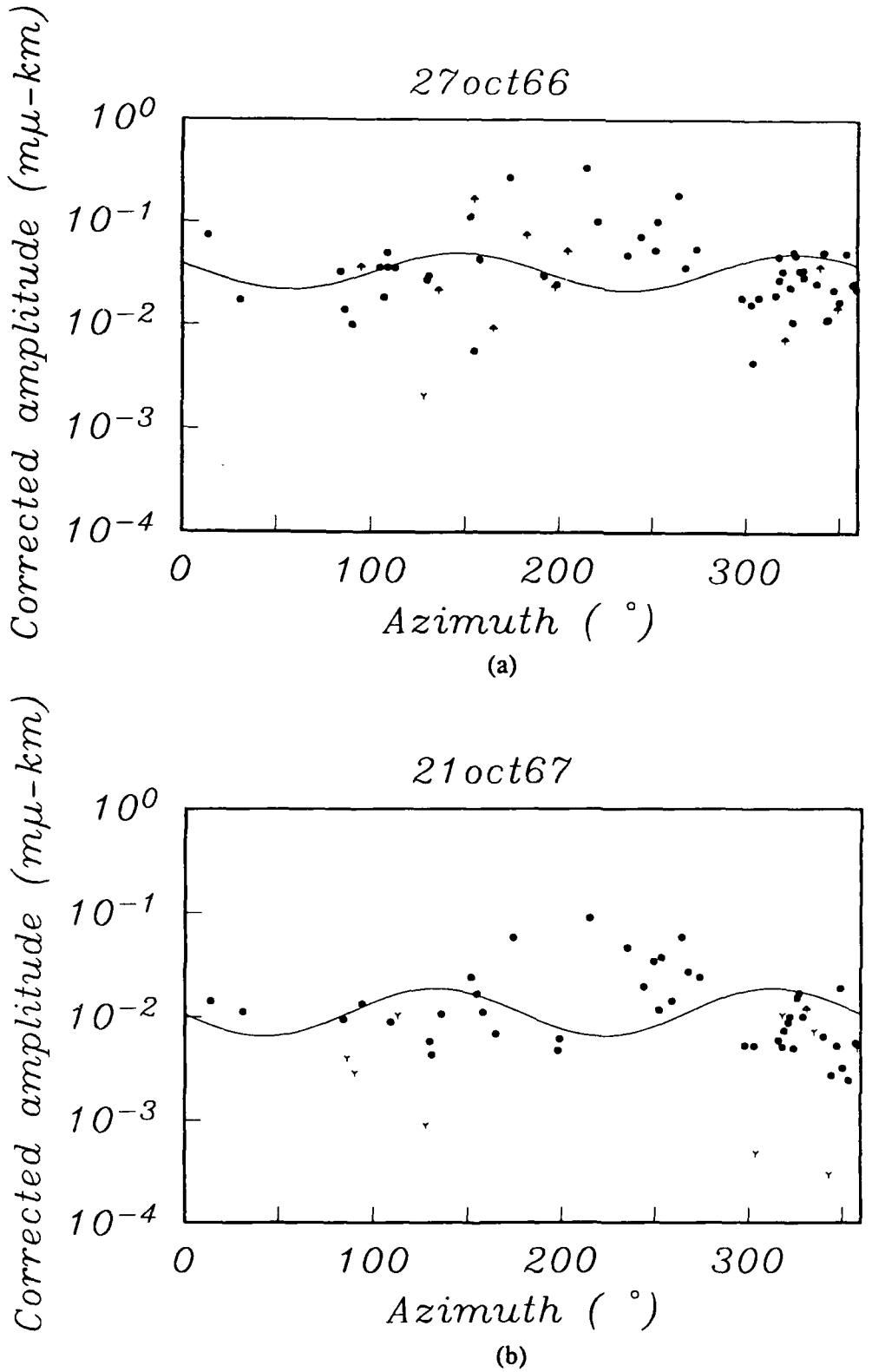

Figure 3a. Plots of sin(2θ) fit to the northern Novaya Zemlya amplitude data (solid circles) after correcting for geometrical spreading. The Y's indicate measurements within the noise level and upward arrows indicate clipped measurements.

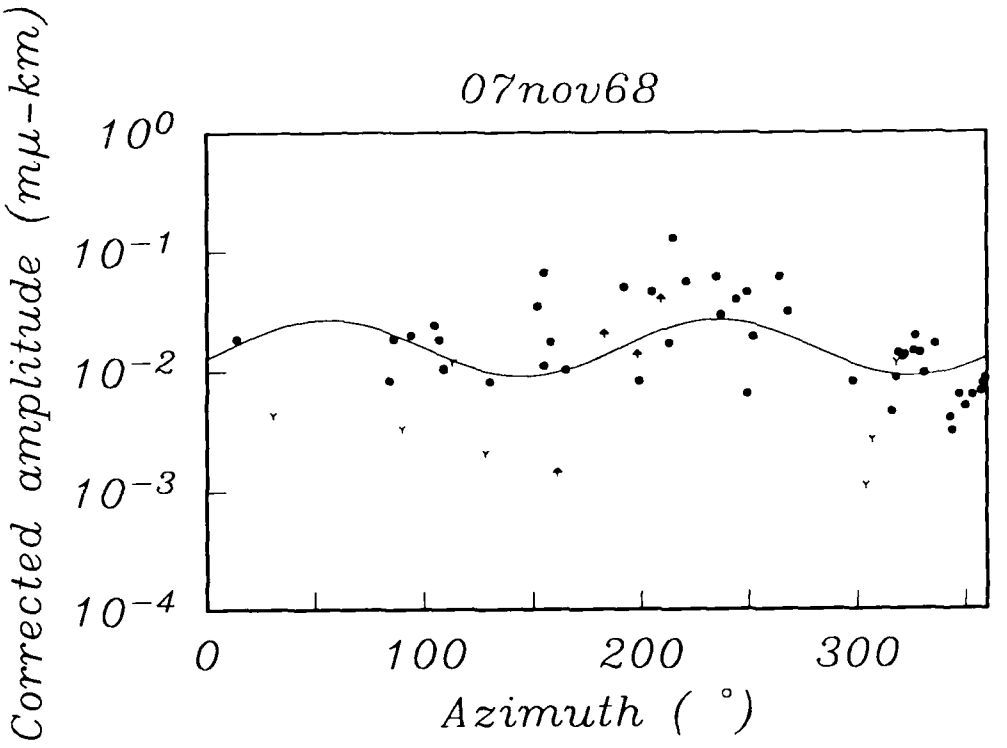

(c)

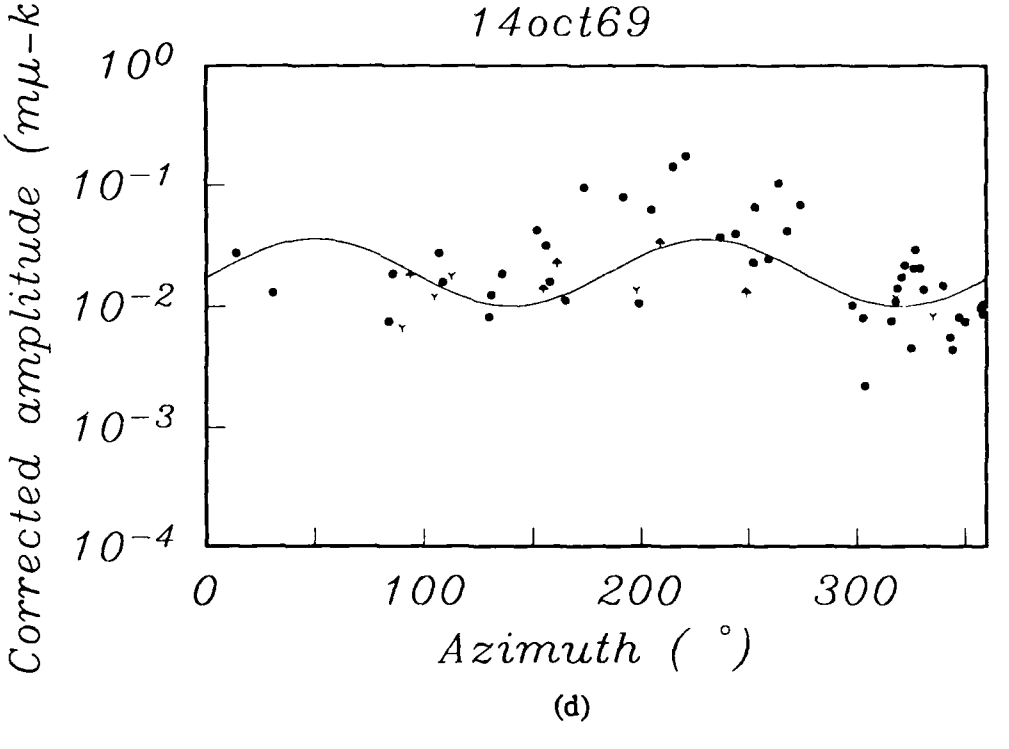

(d)

Figure 3a. (cont'd)

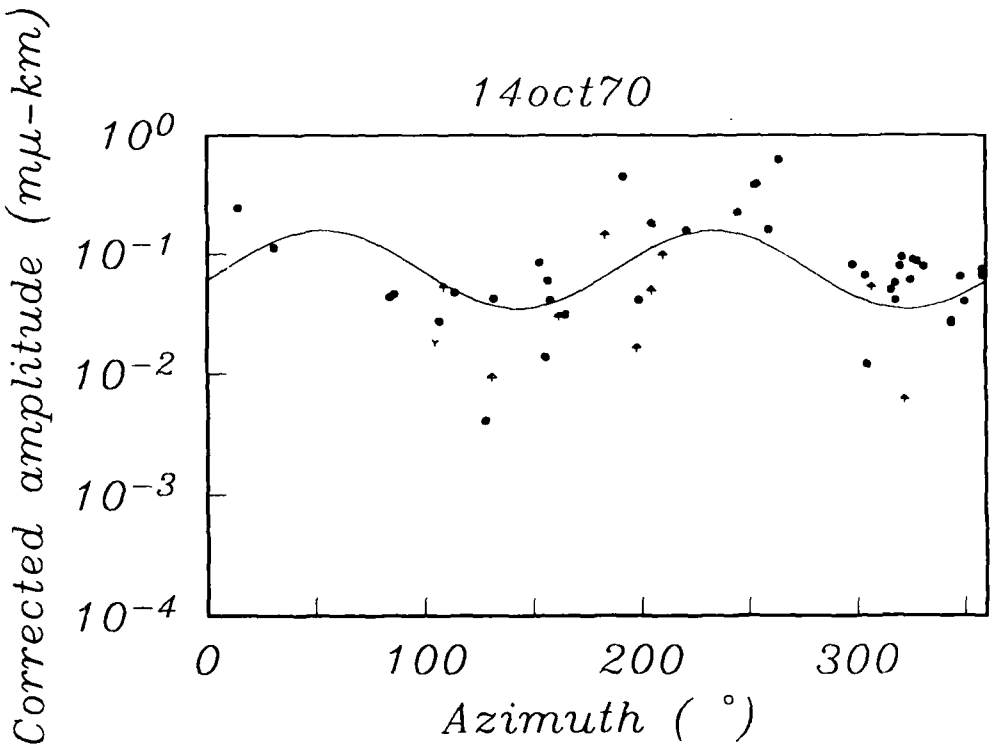

(e)

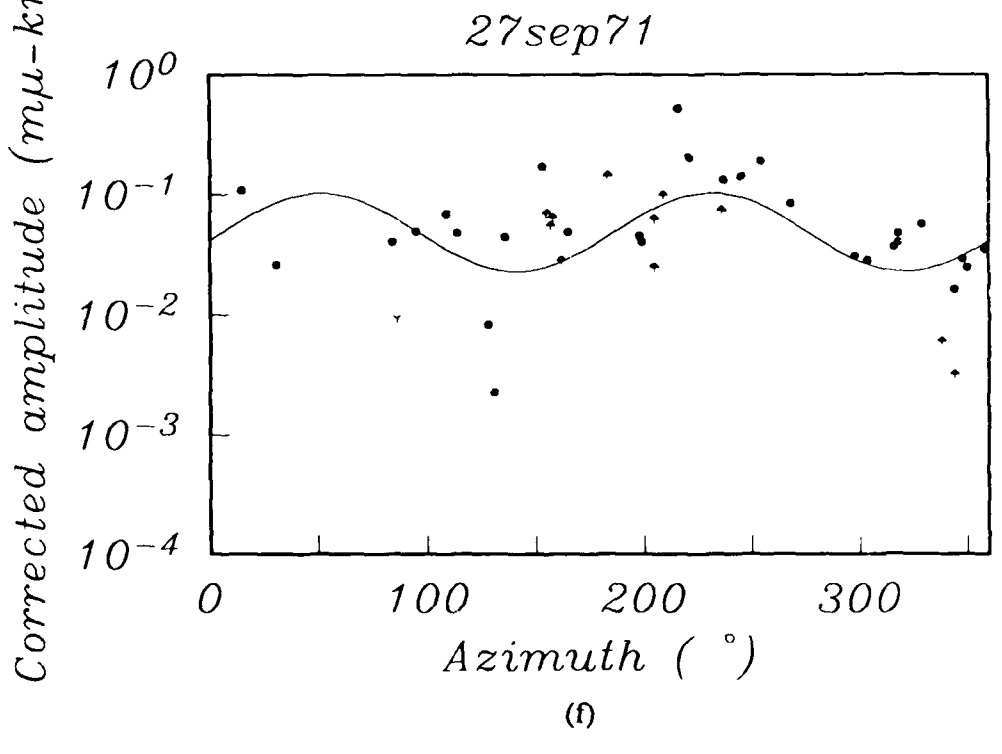

(f)

Figure 3a. (cont'd)

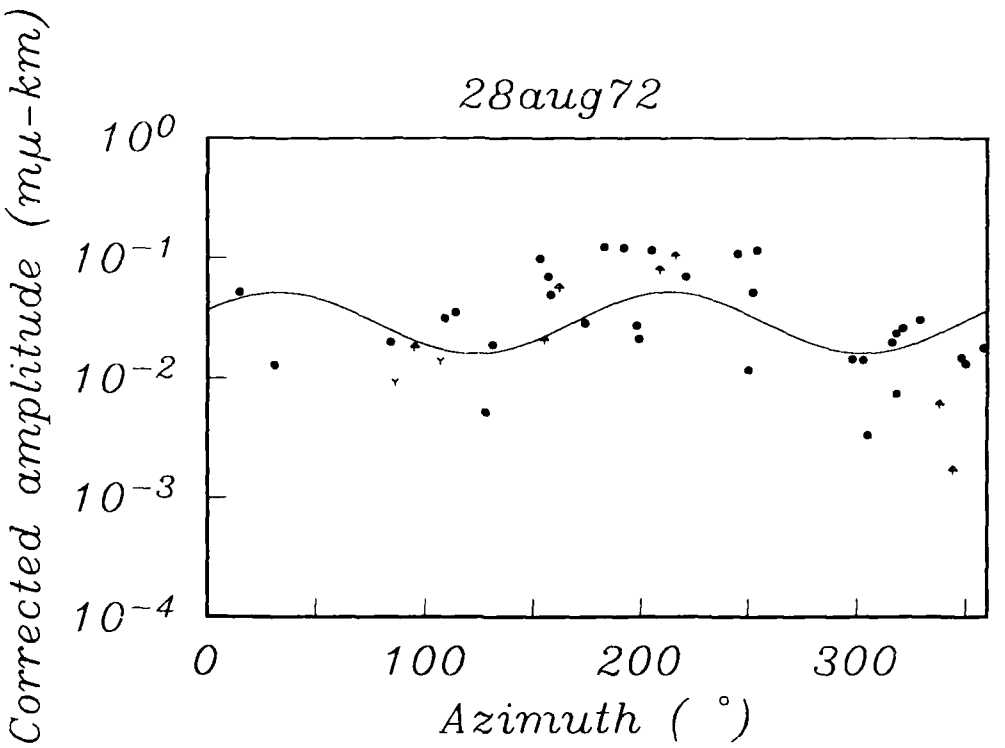

(g)

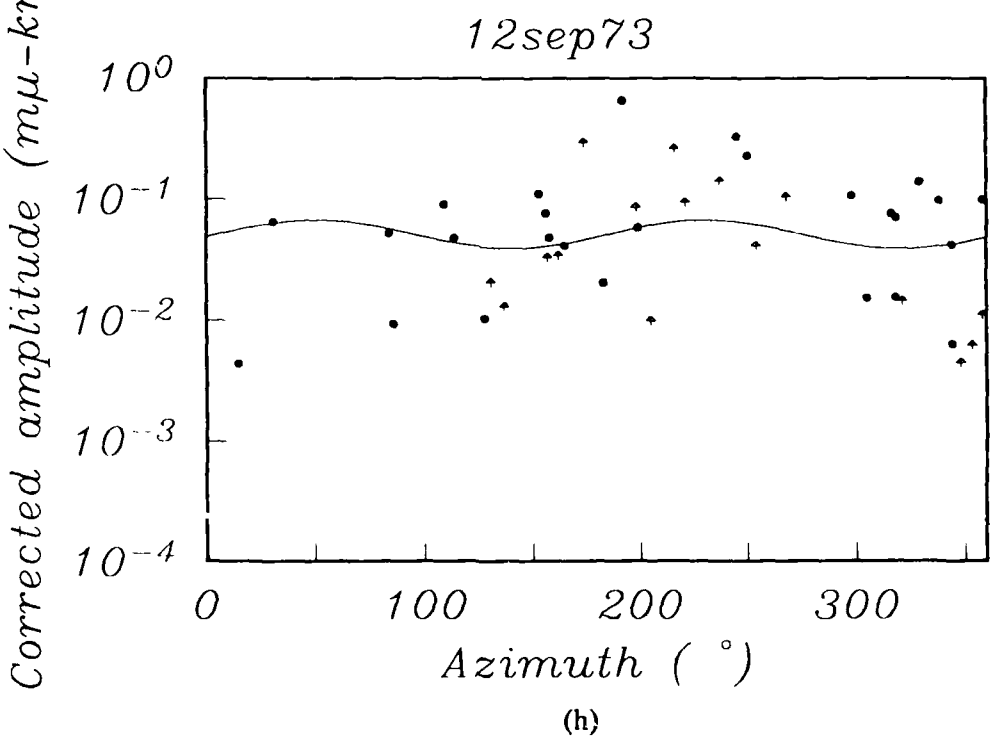

(h)

Figure 3a. (cont'd)

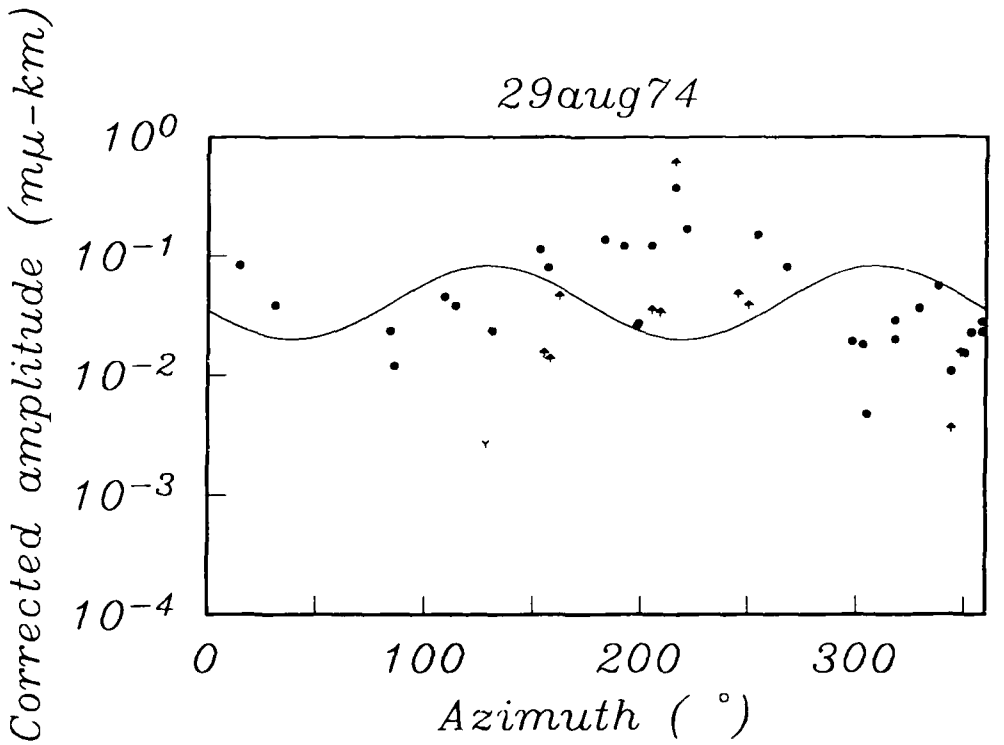

(i)

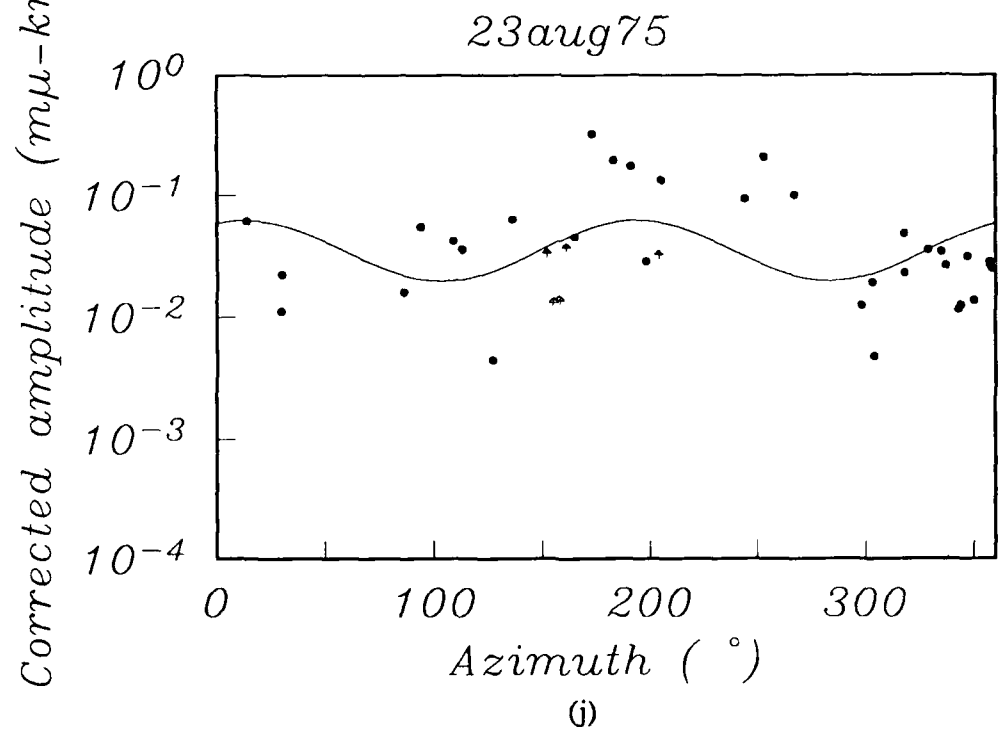

(j)

Figure 3a. (cont'd)

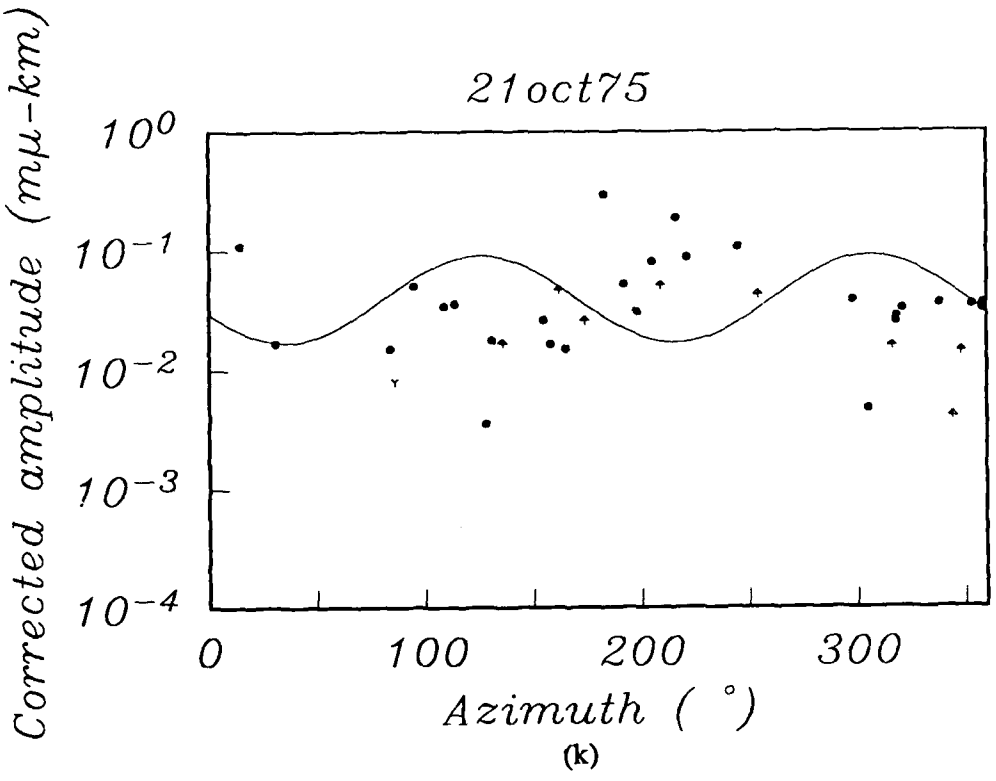

(k)

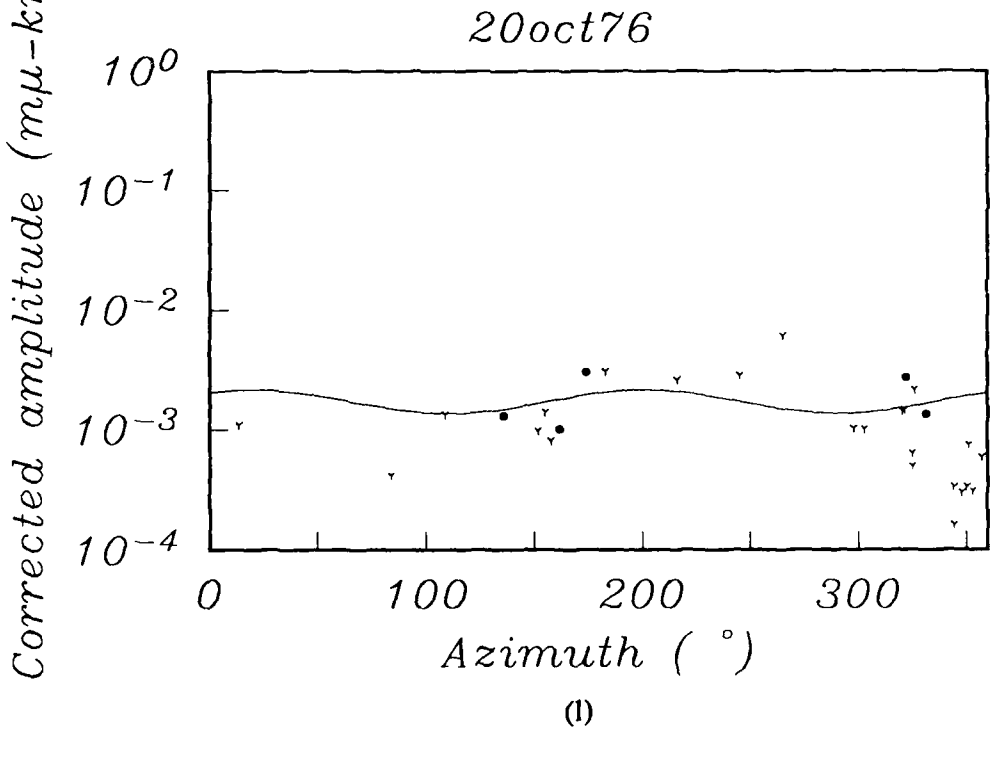

(l)

Figure 3a. (cont'd)

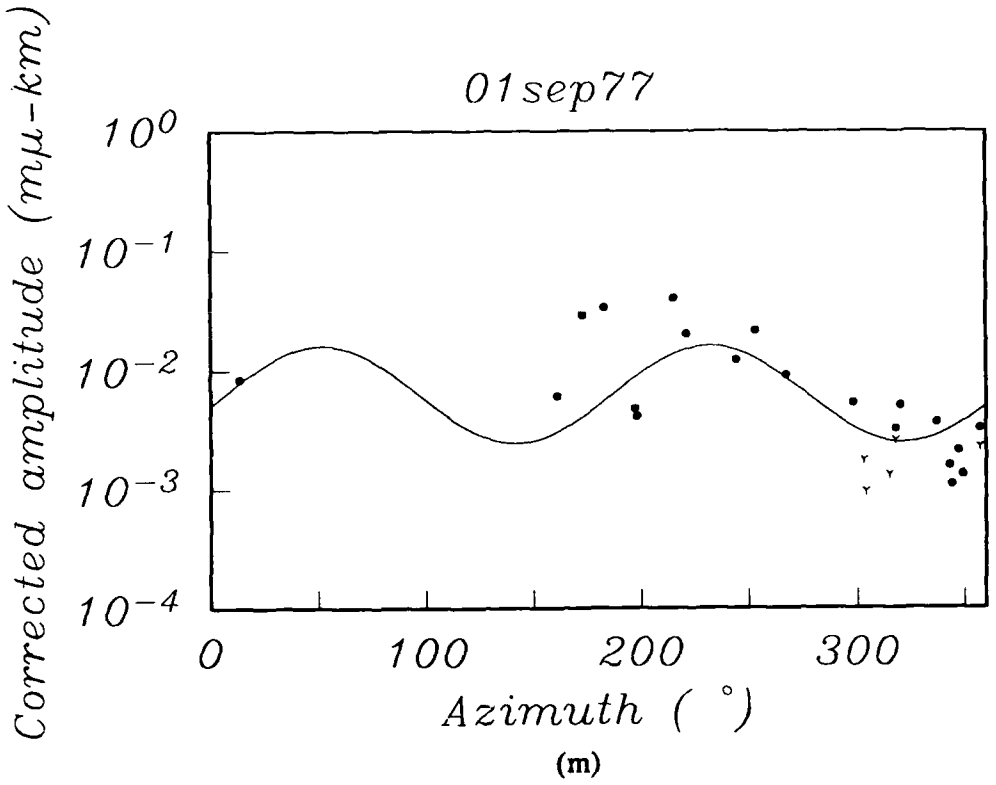

(m)

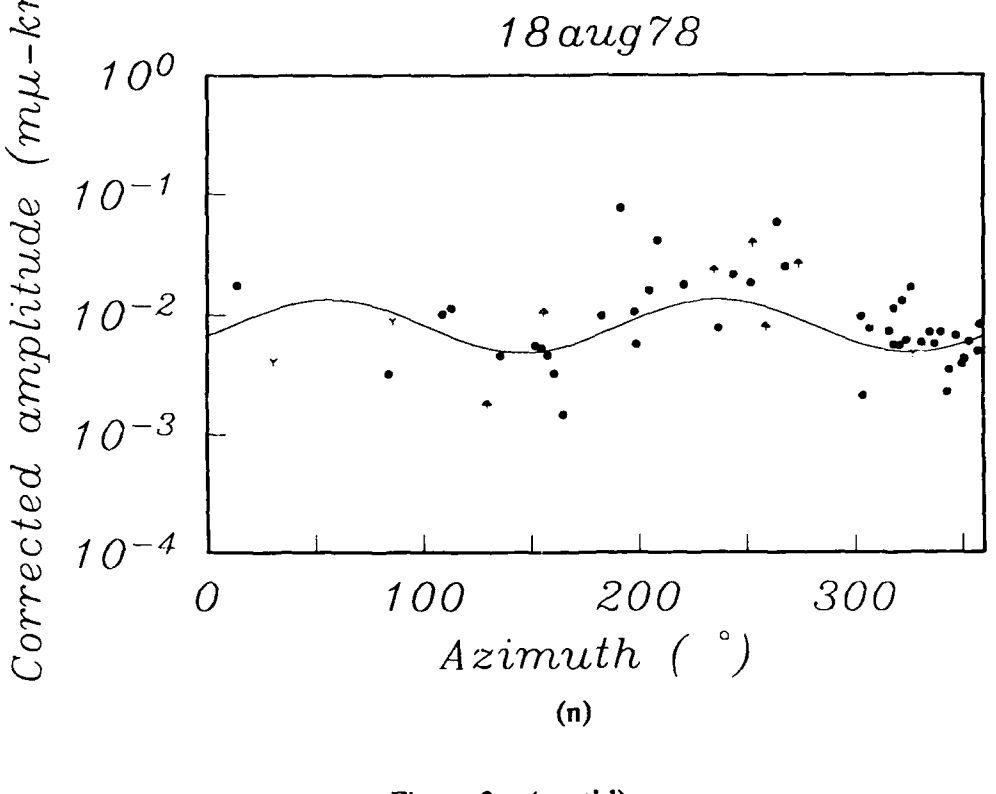

(n)

Figure 3a. (cont'd)

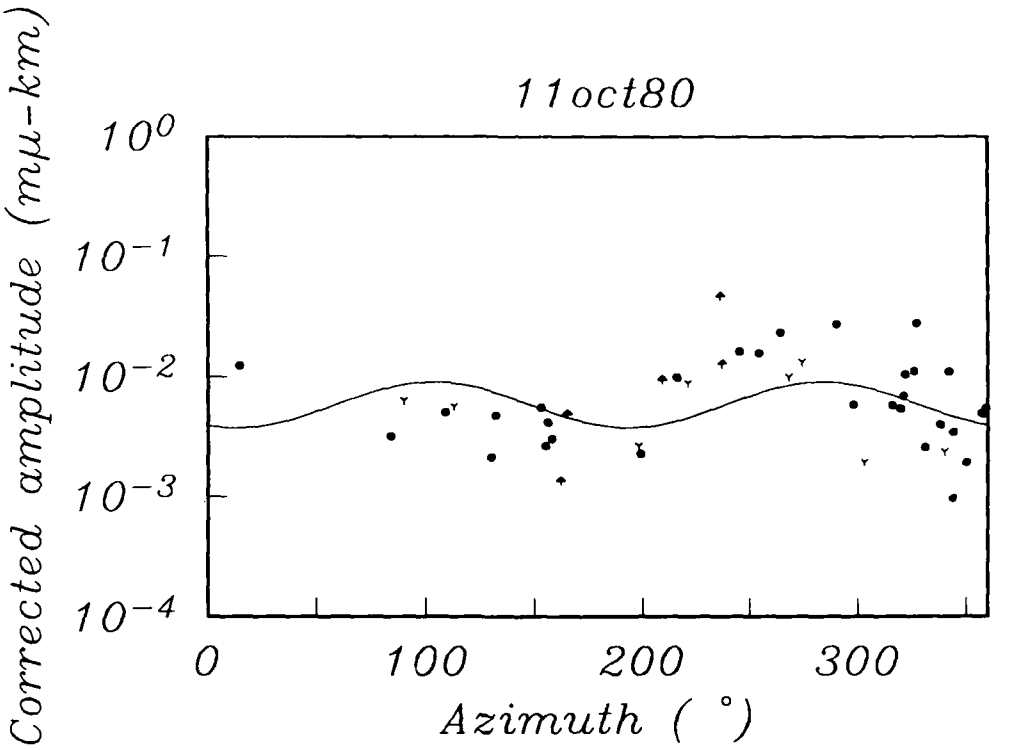

(o)

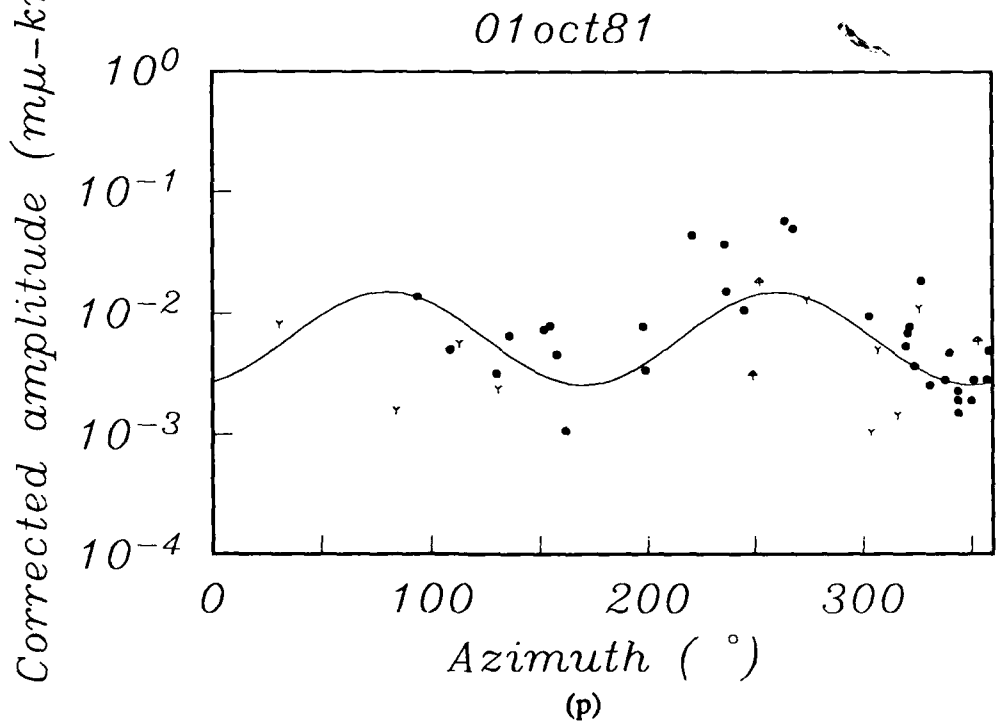

(p)

Figure 3a. (cont'd)

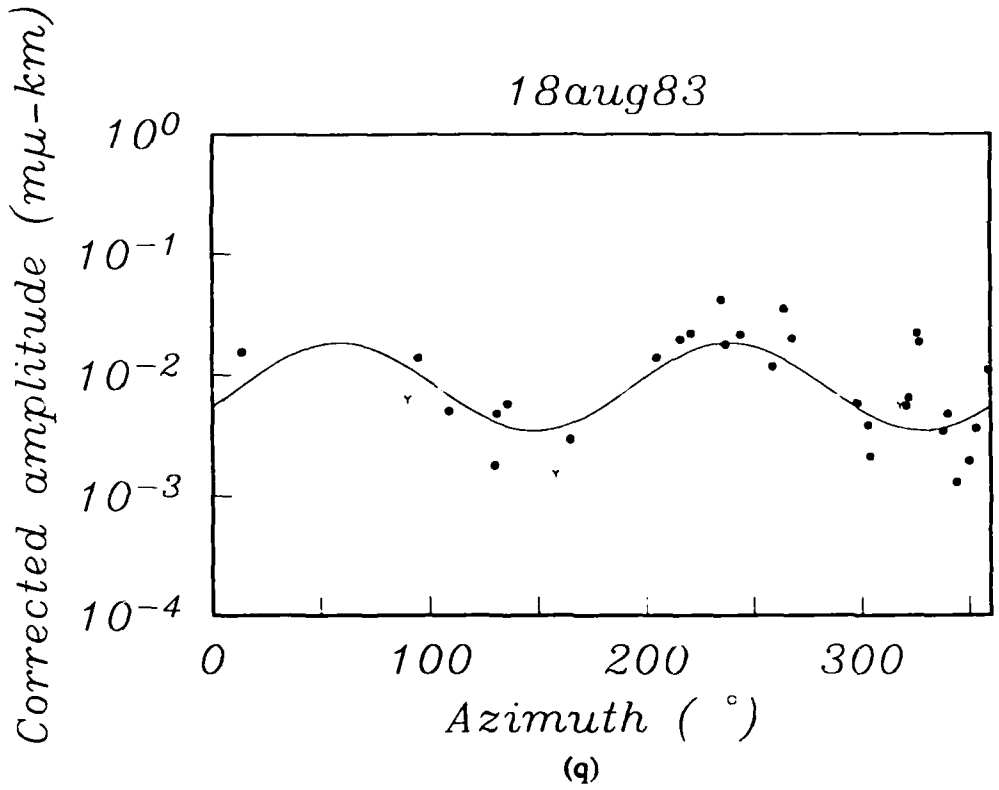

(q)

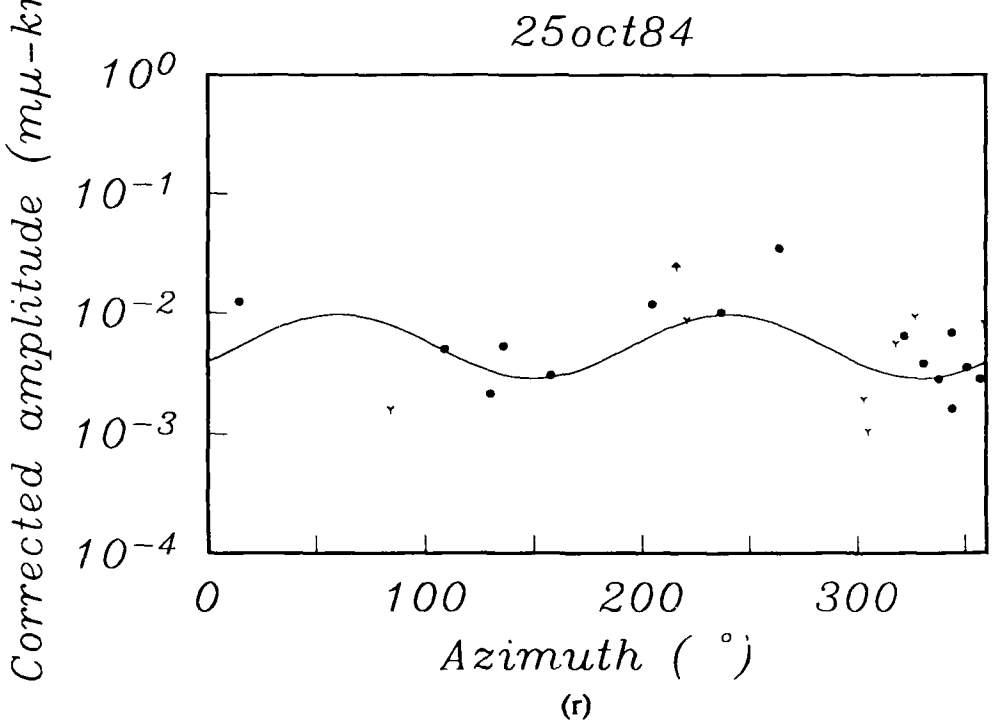

(r)

Figure 3a. (cont'd)

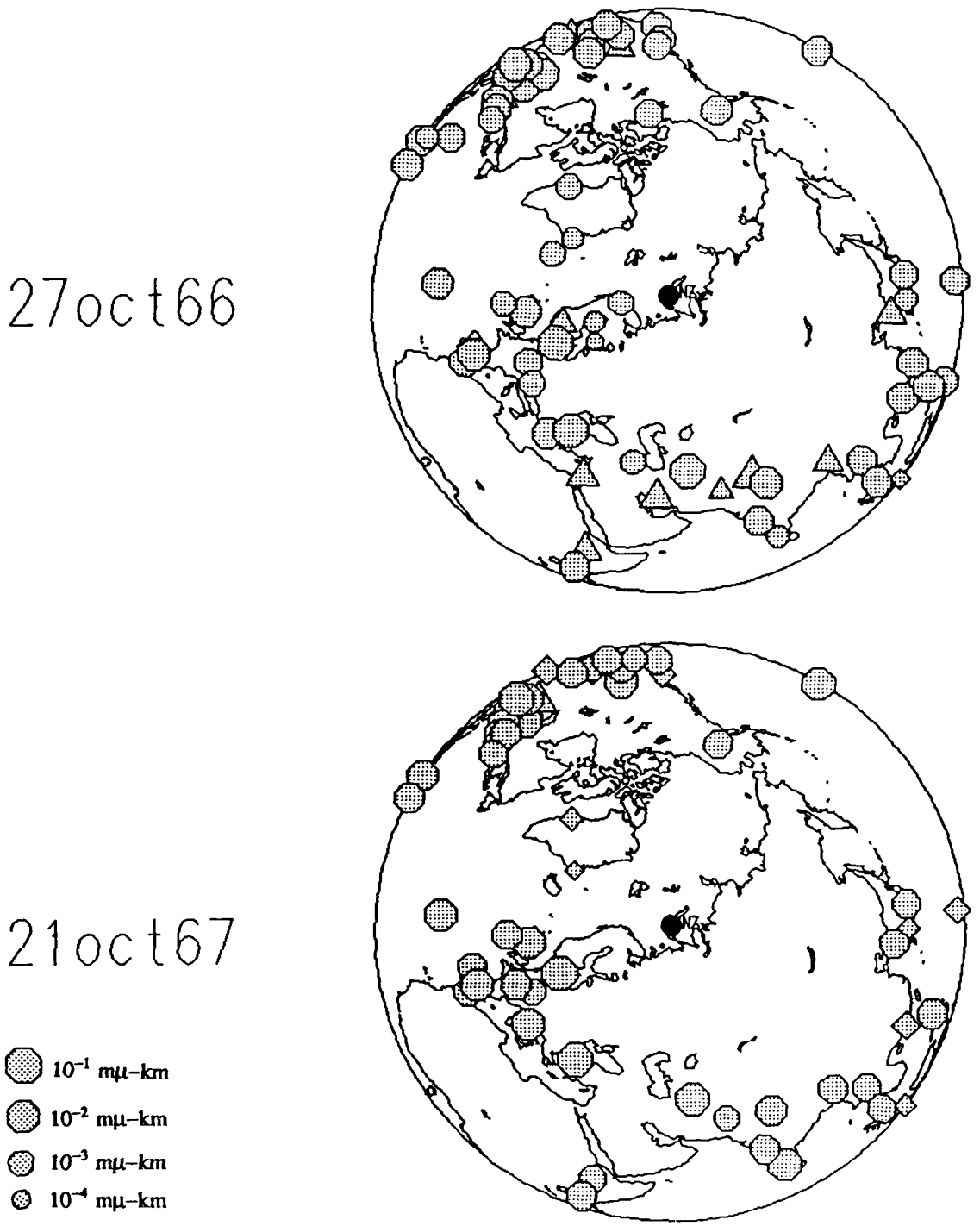

Figure 3b. Plots of the amplitude for each station on a focal sphere for the northern Novaya Zemlya events. The size of the symbol indicates the amplitude in mμ. The circles are well recorded P_a amplitudes, the triangles are for stations with clipped measurements, and the diamonds are for stations with measurements within the noise level.

07nov68

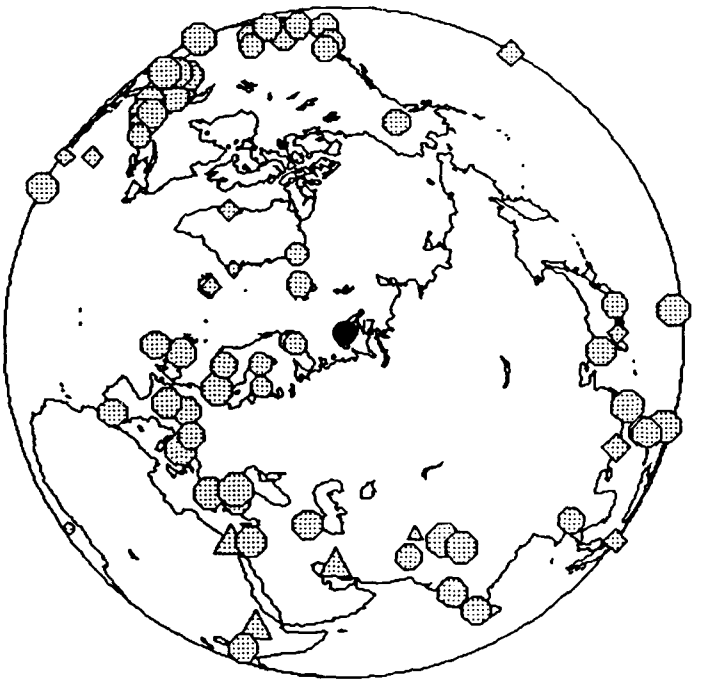

14oct69

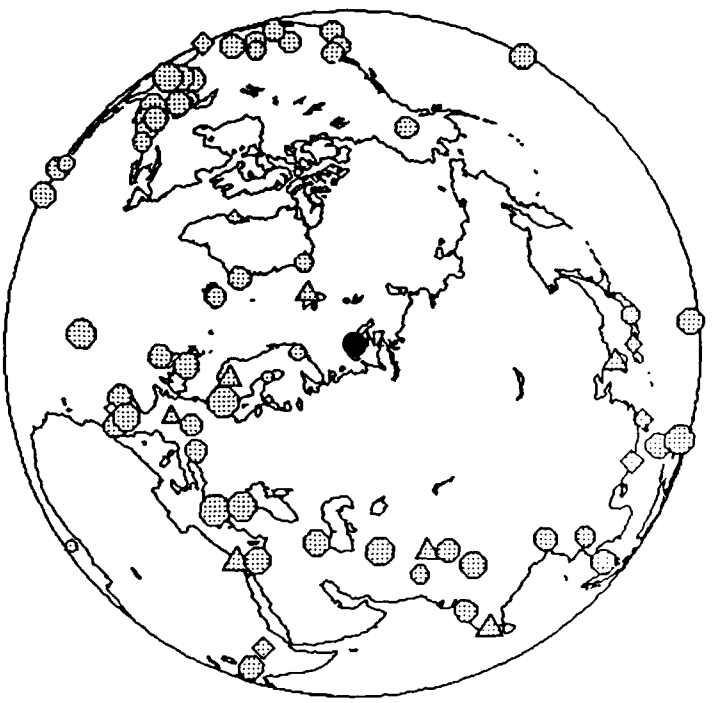

Figure 3b. (cont'd)

14oct70

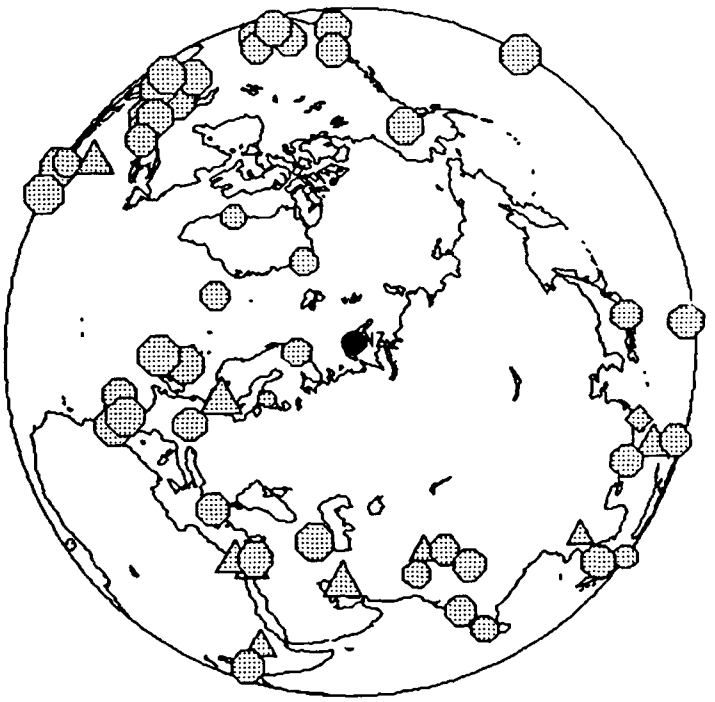

27sep71

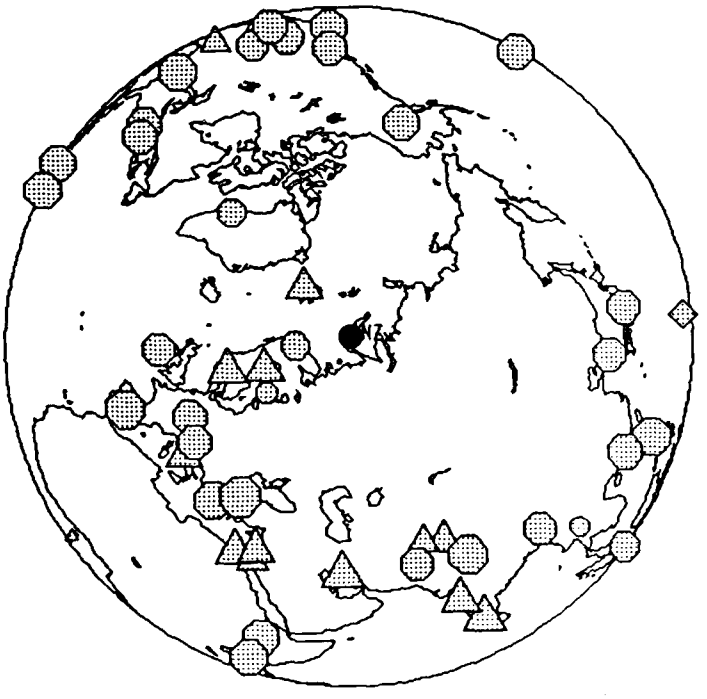

Figure 3b. (cont'd)

28aug72

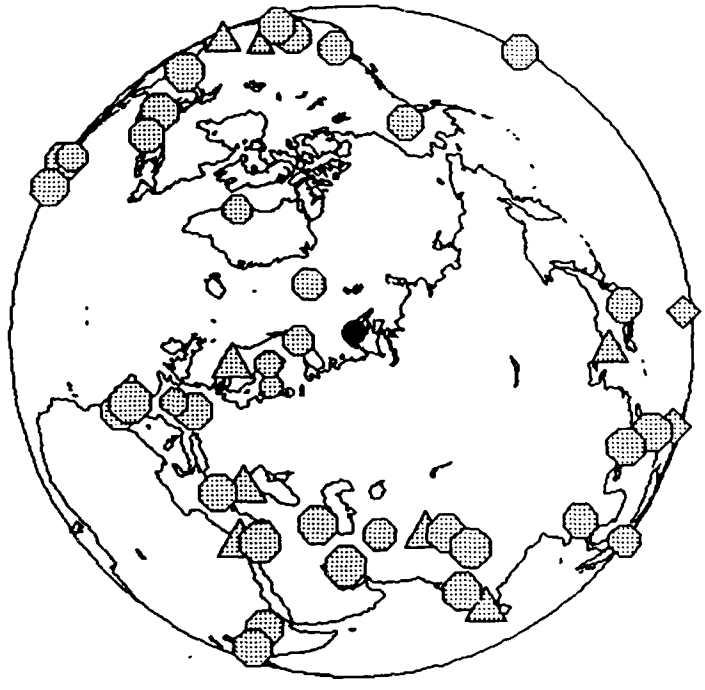

12sep73

Figure 3b. (cont'd)

29aug74

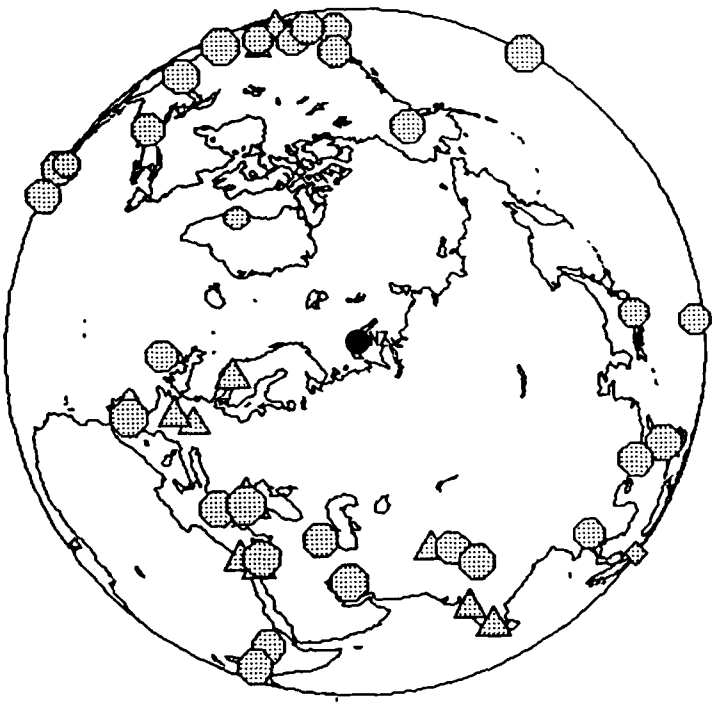

23aug75

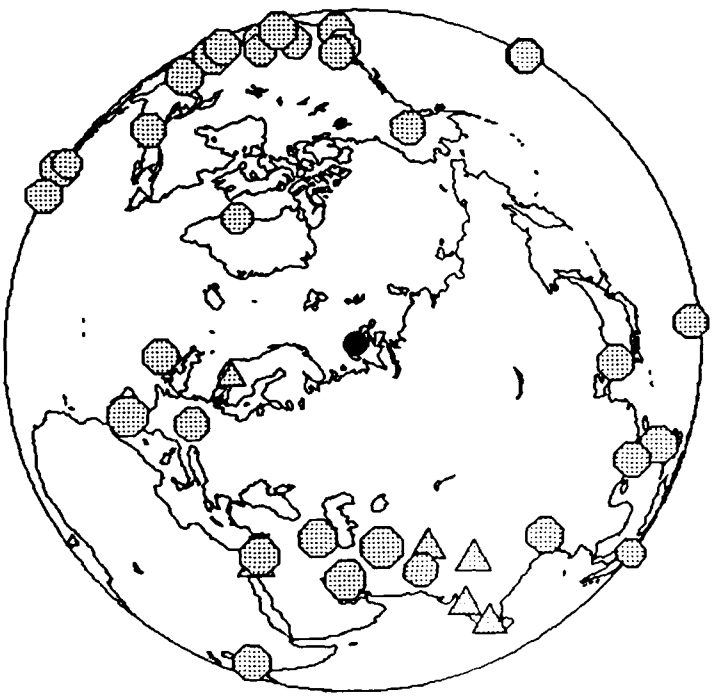

Figure 3b. (cont'd)

21oct75

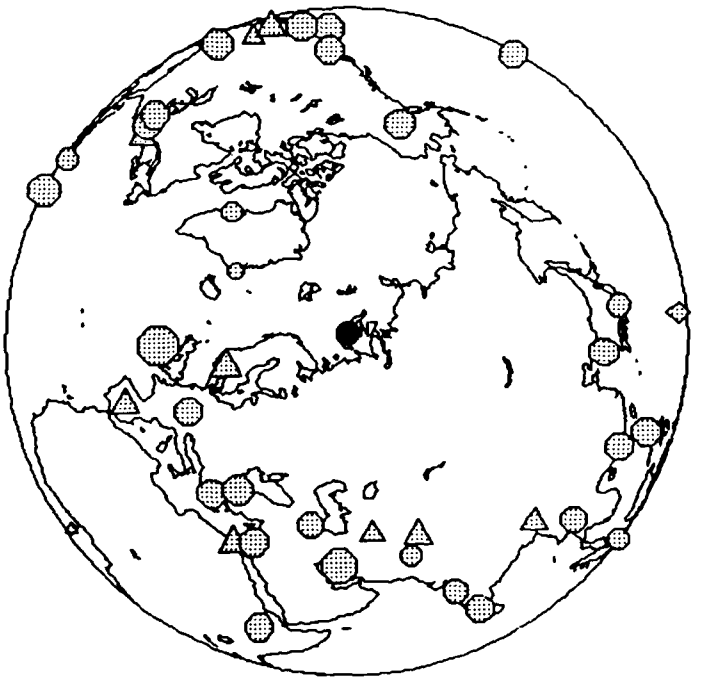

20oct76

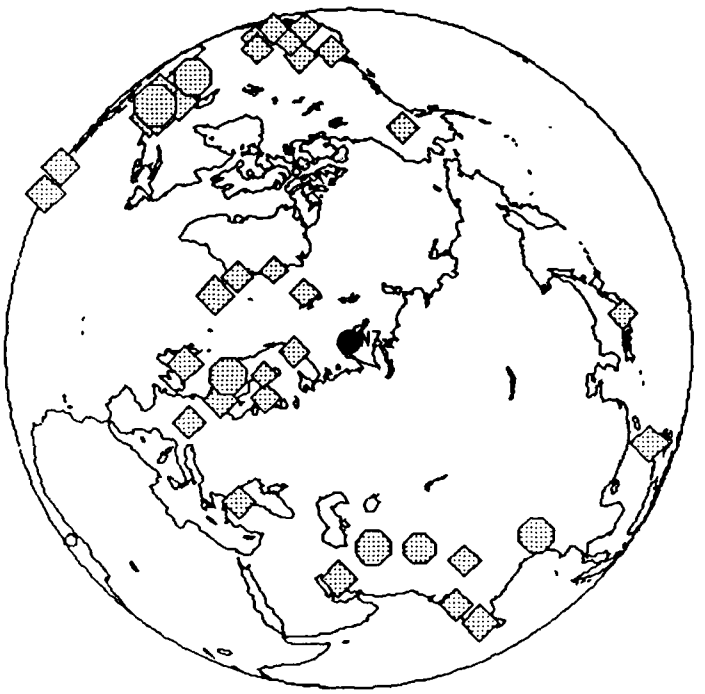

Figure 3b. (cont'd)

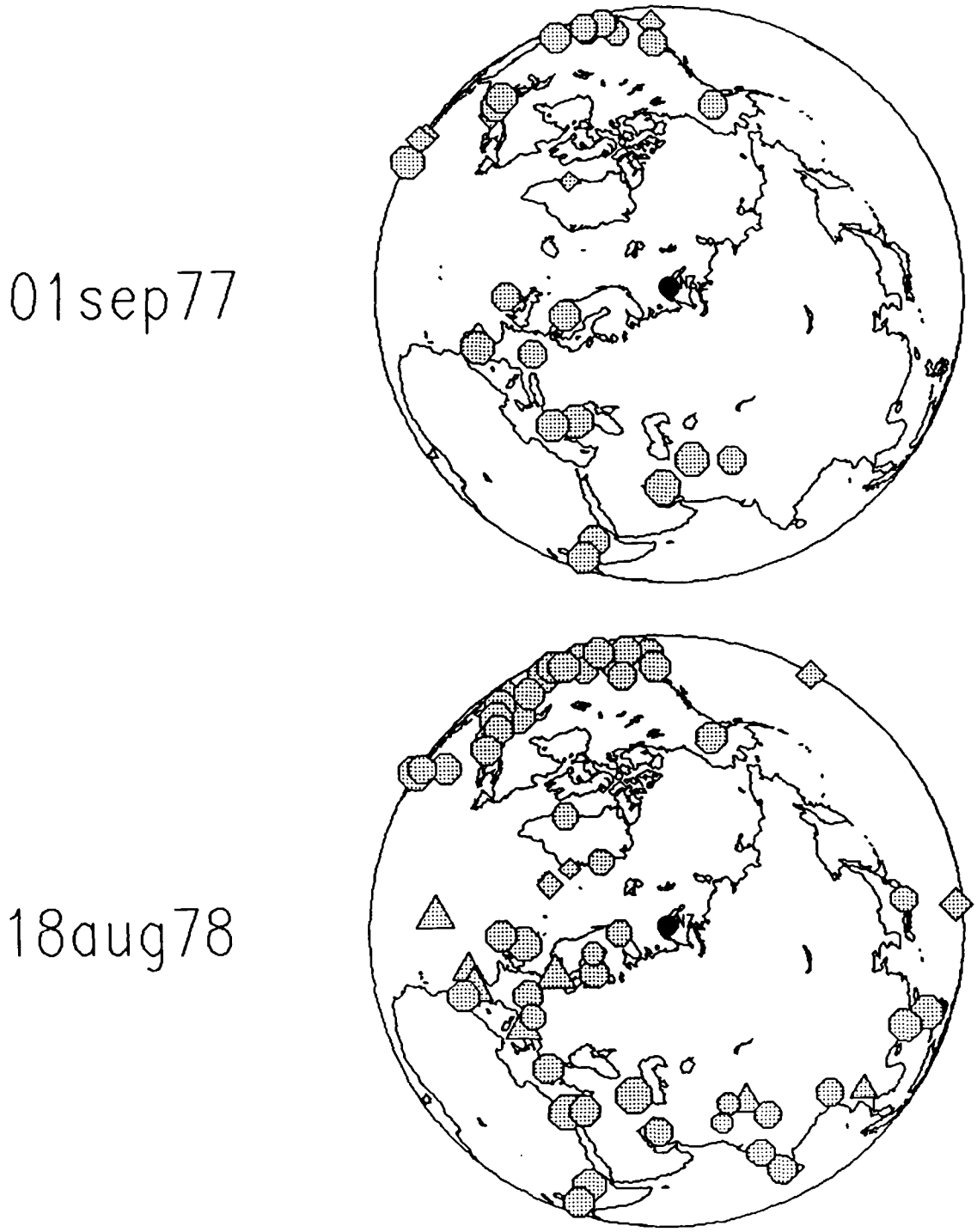

Figure 3b. (cont'd)

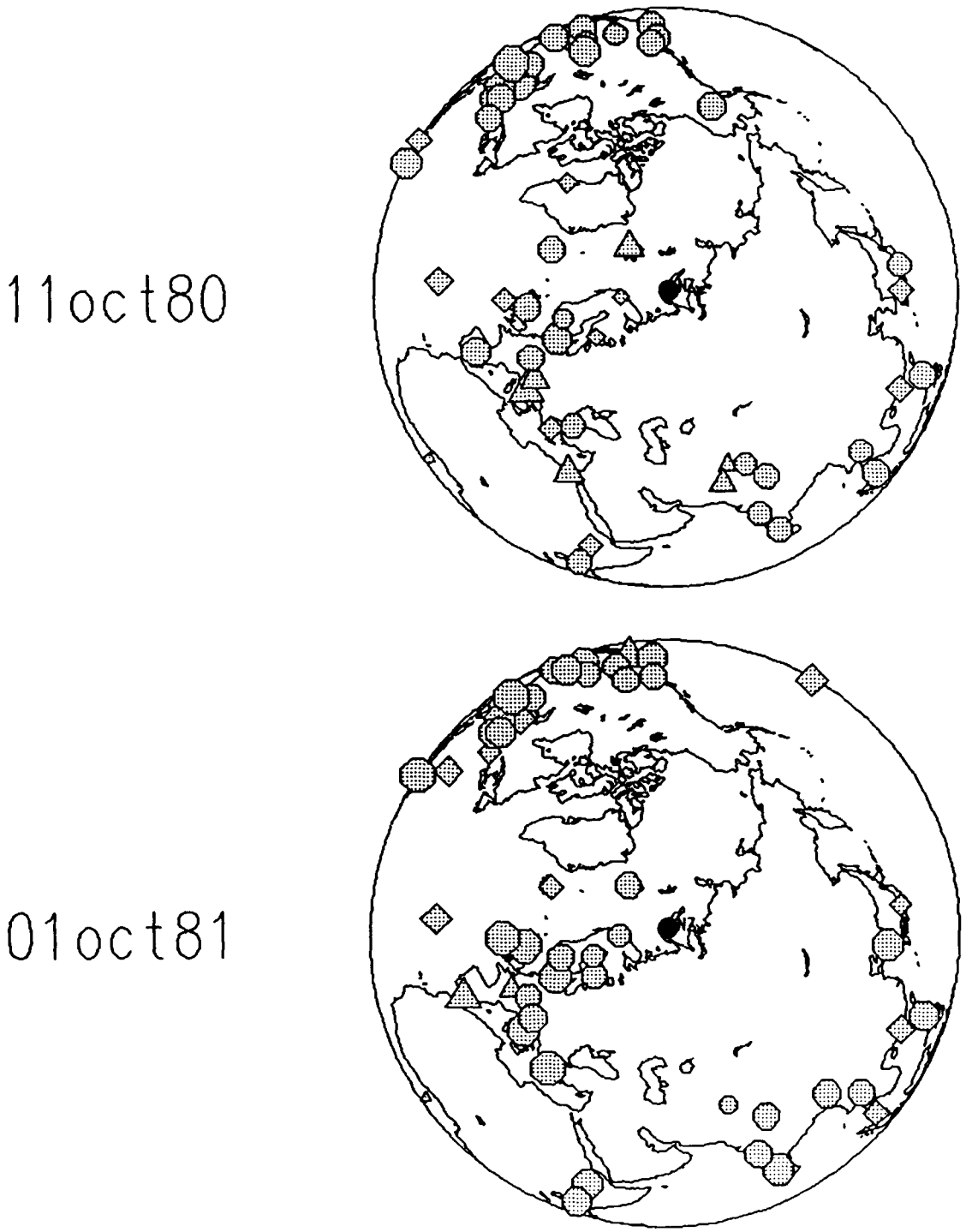

Figure 3b. (cont'd)

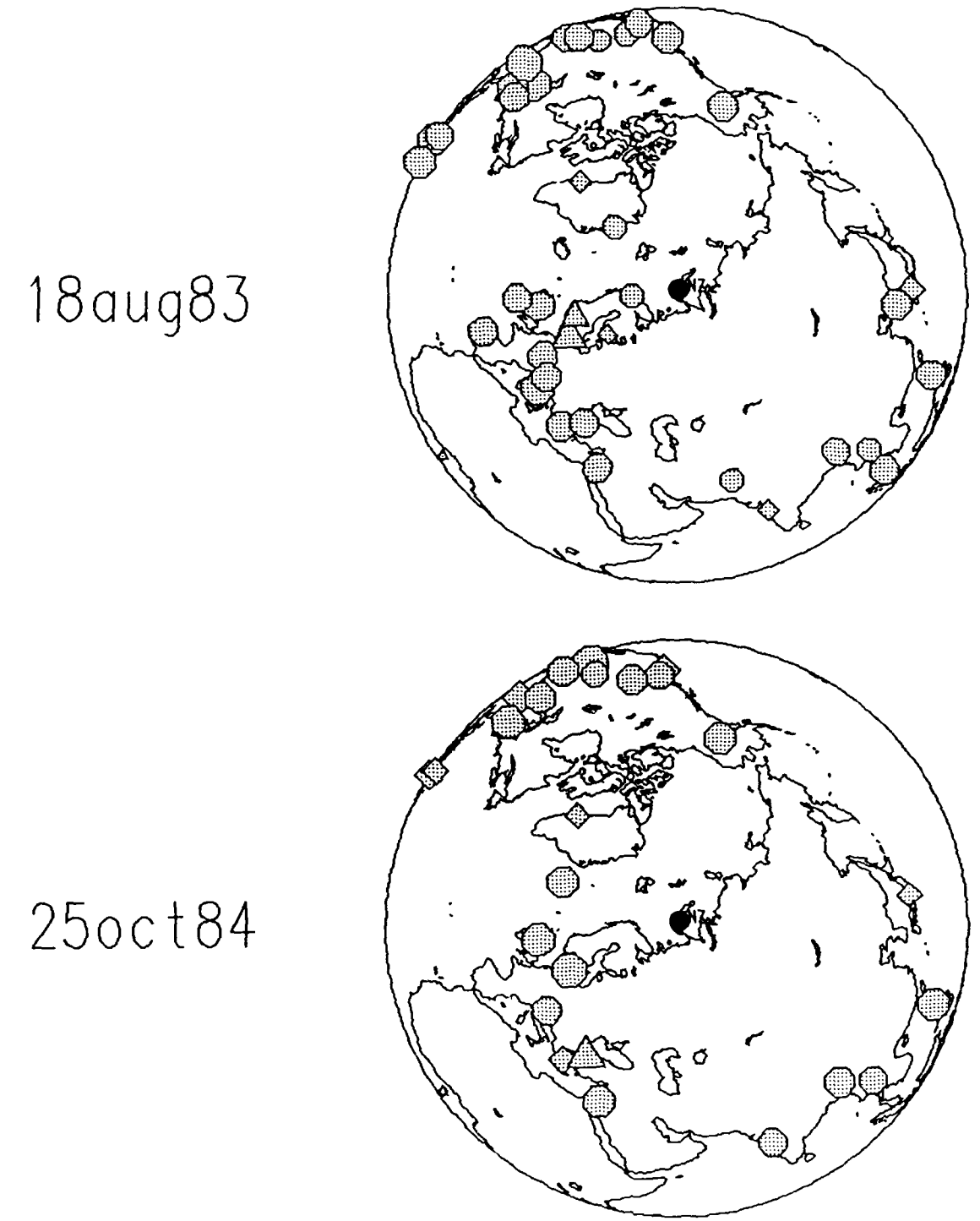

Figure 3b. (cont'd)

Table 2. Sin(2θ) Fit to the Novaya Zemlya Data

Date	Day of year	m_b	Amplitude (μ)	Phase θ (degree)	F-ratio
Southern					
27 Sep 73	270	5.18	1.40	13.2	1.45‡
27 Oct 73	300	6.65	2.09	-24.9	3.12‡
02 Nov 74	306	6.50	2.63	-13.8	6.22
18 Oct 75	291	6.23	2.24	6.4	5.40§
Northern					
27 Oct 66	275	6.07	1.51	-1.4	3.39
21 Oct 67	294	5.40	1.70	17.2	6.55
07 Nov 68	312	5.60	1.72	10.4	7.01
14 Oct 69	287	5.77	1.89	5.1	7.46
14 Oct 70	287	6.44	2.12	8.2	7.71
27 Sep 71	270	6.27	2.12	6.2	5.77
28 Aug 72	241	5.99	1.80	-12.2	3.81§
12 Sep 73	255	6.37	1.31	5.6	0.33‡
29 Aug 74	241	6.13	2.03	-4.8	4.85
23 Aug 75	235	6.12	1.78	-3.7	2.39
21 Oct 75	294	6.11	2.32	4.6	4.18
20 Oct 76	294	4.03	1.26	-24.3	0.06‡
01 Sep 77	244	5.09	2.56	6.7	4.93§
10 Aug 78	222	5.39	1.67	11.3	6.04
11 Oct 80	285	5.19	1.55	220.9	2.61‡
01 Oct 81	274	5.23	2.42	35.3	12.33
18 Aug 83	230	5.33	2.30	13.5	11.27
25 Oct 84	299	5.16	1.84	14.9	3.68‡

§ Fails F-statistic test at 99th percentile.

‡ Fails F-statistic test at 95th percentile.

Most of the phase estimates (θ) from the best fitting curves fall within the range between 5° and 15° for the northern Novaya Zemlya test site. The same conclusion may not be drawn for the southern test site due to a lack of data. For a spherical symmetric Earth, the observed azimuthal pattern indicates that there may be a component of near-source effects or varying attenuation along the paths with different azimuthal distribution. The choice of a sin(2θ) fit is arbitrary and may be assessed if the azimuth

amplitude pattern pertains to near-source effects, eg. tectonics release (Lay *et al.*, 1984). The phase and amplitude of the sin(2θ) modeling also bear no apparent relationship to the size of the explosions.

The sensitivity of an m_b estimate bias that results from a symmetric sin(2θ) amplitude variation are expected to be reduced if a well-distributed network is used because the nodes would tend to cancel. However, in the case of Novaya Zemlya, as shown in Figures 2b and 3b, the receiving stations are biased towards North America and Europe, and little data are available within the 0° to 80° range. If the sin(2θ) model is appropriate to explain the observed azimuthally dependent amplitude variation of the Novaya Zemlya data, it would predict a local amplitude maximum in this azimuth range. Consequently, m_b estimates obtained for Novaya Zemlya with the present station configuration would tend to be biased low.

Multiple Events

Although most of the events may be explained by the sin(2θ) model quite well statistically, as is shown in Figures 2a and 3a and Table 2, there are a few exceptions. One of them is the 18 Oct, 1975 event in southern Novaya Zemlya which was described as a double event by Hurley (1977). Although the sin(2θ) fit to the data without censoring information falls within a 95% confidence interval, if the true amplitude of the censoring information were included, the amplitudes for this event between azimuths of 100° and 170° would then appear to be biased low. This effect may be caused by the simultaneous detonation of two spatially separated explosions which would exhibit constructive and destructive interference at certain azimuths. The other

events that show a possible deviation from the sin(2θ) model are 7 Nov 1968, 14 Oct 1969, and 27 Sep 1971. The 11 Oct 1980 event, which Lilwall and Marshall (1986) indicate may also be a double event, does not show azimuthal characteristics similar to those of the 18 Oct 1975 event.

We have performed azimuthal partitioning of the first motion amplitudes that are used in the maximum-likelihood estimation of the m_b's for four Novaya Zemlya events. The azimuthal pattern is presumed to be due to local geological structure or tectonic release and an attempt is made to model it by a sin(2θ) symmetric function. Therefore, when there is an uniform azimuthal station coverage, the azimuthal effects on the m_b would be averaged with accordant bias reduction. In the case of a double event, the symmetry is not preserved due to the interference effect. The partitioning is designed to demonstrate the azimuthal dependence of m_b as shown in Figure 4. The quadrants are divided into azimuthal range of 0°–90°, 90°–180°, 180°–270°, 270°–360° (Figure 4a) and 314°–74°, 74°–134°, 134°–254°, 254°–314° (Figure 4b). The amplitude readings for the stations within each quadrant are grouped together and input to the MLEGLM estimation (Chan *et al.*, 1988) to arrive at m_b estimate for each quadrant. The m_b values for each quadrant are shown in each figure and are listed in Table 3.

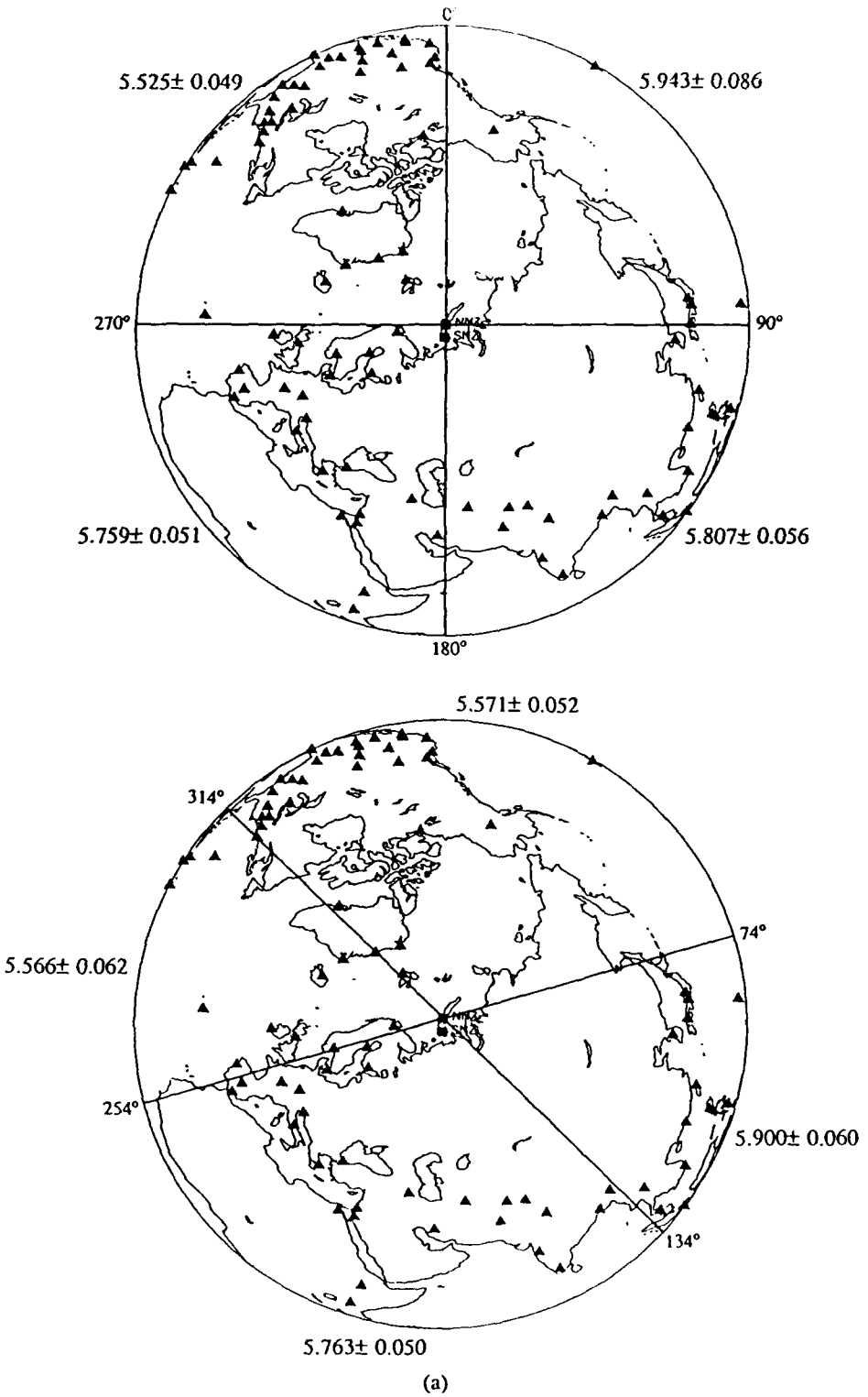

Figure 4a. Partitioning according to equal area quadrant (upper) and equal station distribution (lower) and the m_b estimates associated with each quadrant for the northern Novaya Zemlya event of 07 nov 68.

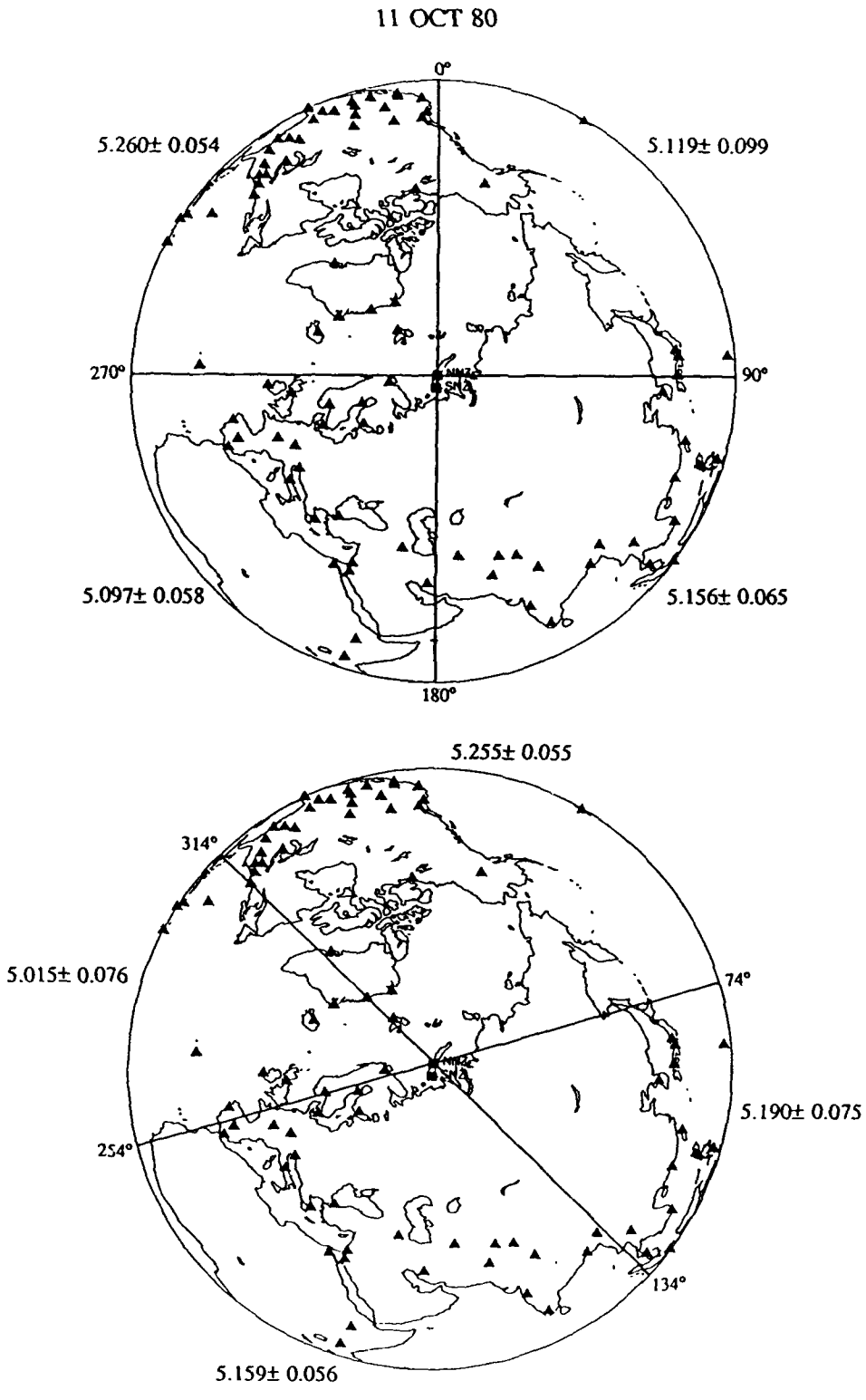

Figure 4b. Partitioning according to equal area quadrant (upper) and equal station distribution (lower) and the m_b estimates associated with each quadrant for the northern Novaya Zemlya event of 11 oct 80.

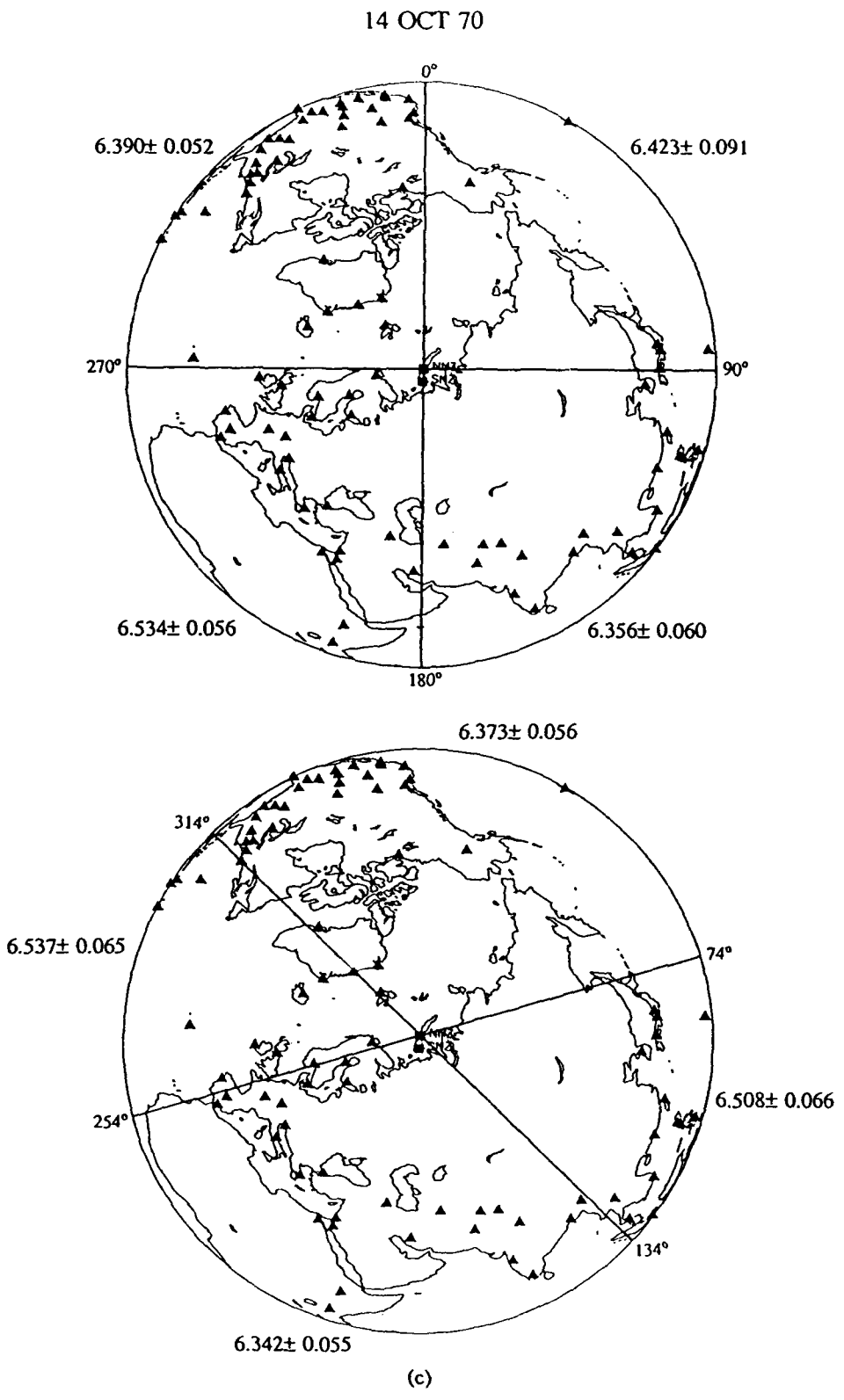

Figure 4c. Partitioning according to equal area quadrant (upper) and equal station distribution (lower) and the m_b estimates associated with each quadrant for the northern Novaya Zemlya event of 14 oct 70.

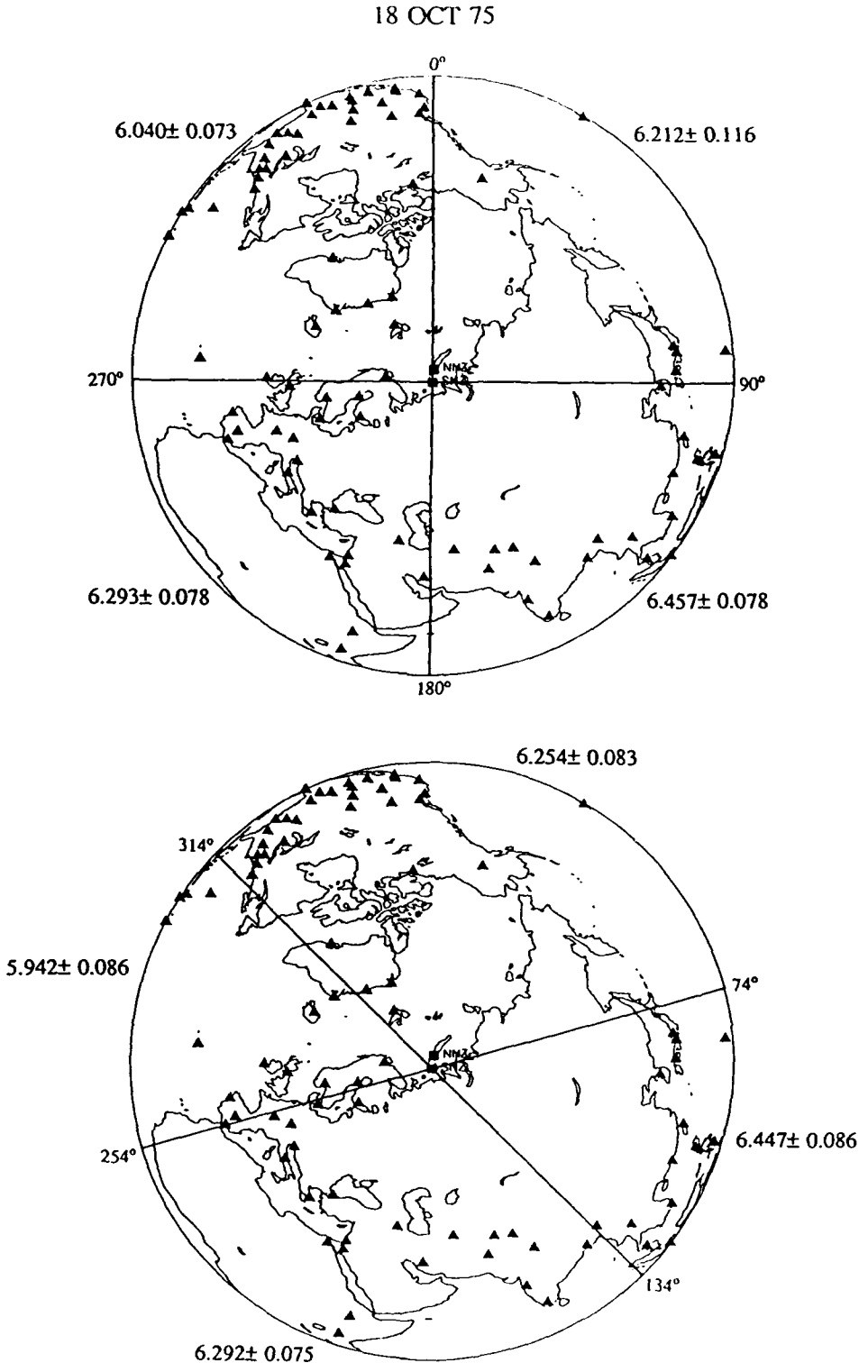

(d)

Figure 4d. Partitioning according to equal area quadrant (upper) and equal station distribution (lower) and the m_b estimates associated with each quadrant for the southern Novaya Zemlya event of 18 oct 75.

Table 3a. Novaya Zemlya m_b by Quadrant				
	m_b			
Date	0°-90°	90°-180°	180°-270°	270°-360°
07 Nov 68	5.943	5.807	5.759	5.525
	±0.086	±0.056	±0.051	±0.049
14 Oct 70	6.423	6.365	6.534	6.390
	±0.091	±0.060	±0.056	±0.052
11 Oct 80	5.119	5.156	5.097	5.260
	±0.099	±0.065	±0.058	±0.054
18 Oct 75	6.212	6.457	6.293	6.040
	±0.116	±0.078	±0.078	±0.073

Table 3b. Novaya Zemlya m_b by Quadrant				
	m_b			
Date	314°-74°	74°-134°	134°-254°	254°-314°
07 Nov 68	5.571	5.900	5.763	5.566
	±0.052	±0.060	±0.050	±0.062
14 Oct 70	6.373	6.508	6.342	6.537
	±0.056	±0.066	±0.055	±0.056
11 Oct 80	5.255	5.190	5.159	5.015
	±0.055	±0.075	±0.056	±0.076
18 Oct 75	6.254	6.447	6.292	5.942
	±0.083	±0.086	±0.075	±0.086

The variations in m_b's for events 11 Oct 80 and 14 Oct 70 are about 0.15 m_b unit whereas for events 07 Nov 68 and 18 Oct 75, the variations are up to 0.4 m_b unit from the 90° quadrant partition. Similar variation is observed using the optimal partitioning taking into account station distribution. The quadrant m_b's for 14 Oct 70 display a symmetry that roughly follows the sin(2θ) distribution, as is shown in Figure 3a(c) for this event. For azimuths 90° to 180° and 270° to 360°, we obtain a lower m_b than for the other two quadrants. Since quadrant 0° to 90° is not well covered by seismic stations, the m_b estimates within this quadrant may be as high as that of the opposite quadrant if the sin(2θ) model is appropriate. The same speculation may be made for the

11 Oct 80 event due to its low yield.

An asymmetric m_b pattern is observed in the case of the double event, 18 Oct 75. The m_b estimates for quadrants 90° to 180° and 180° to 270° are high, as expected from the amplitude-azimuth relationship obtained in Figure 2a(c). The extreme amplitude difference is observed for opposing quadrants of 90° to 180° and 270° to 360° as well as 74° to 134° and 254° to 314° , where the variations are up to 0.5 m_b unit. If the data observed for 18 Oct 75 indeed consist of observations of two events detonated simultaneously, the analysis here indicates that they were separated in space in a NW-SE direction, as the quadrant m_b estimates are the most biased in this direction. A similar asymmetric pattern is observed for the event on 07 Nov 68, where the quadrant m_b bias is up to 0.3 unit. It is speculated that this may have been a double event separated in a NW-SE direction also.

SPECTRAL ESTIMATES OF NOVAYA ZEMLYA EXPLOSION SOURCE SIZE FROM P, PcP, and P_{diff}

The attenuation of body waves from Novaya Zemlya was studied by Der *et al.* (1985) as part of a study of P-wave spectra from several test sites. They concluded that the attenuation parameterized by $\bar{t}^*$ did not differ significantly from the Eastern Kazakh or Amchitka test sites. Given that Novaya Zemlya is a high Q test site then near-source attenuation adjustments must first be made to properly compare tests at NTS to Novaya Zemlya.

The largest Novaya Zemlya explosions have maximum-likelihood magnitudes that exceed the magnitude of CANNIKIN (m_b 6.6, 5 Mt). Because MILROW and CANNIKIN were the largest U.S. shots detonated away from NTS in what is considered a high Q region, the Amchitka shots have assumed a great importance for magnitude:yield determination. Along with the megaton range events at NTS, they constitute a reference set of explosions for determining the yields of Novaya Zemlya explosions. All three Amchitka explosions, including CANNIKIN, had distinct and late depth phases (Bakun and Johnson, 1973; Douglas *et al.*, 1987). The strong P+pP interference for these Amchitka shots makes understanding the P+pP interference of the Novaya Zemlya explosions of prime importance when making attenuation comparisons between these events as well as those at NTS.

Source Time Function Deconvolutions

The Shumway-Der deconvolution procedure (Shumway and Der, 1985; Der *et al.*, 1987b) has been used to study the explosion P-wave source function at NTS, Eastern Kazakh, and Novaya Zemlya as well as other test sites. The algorithm provides a maximum-likelihood estimate of the equivalent teleseismic explosion reduced displacement potential (RDP) corrected for attenuation, instrument response, and variations in site response across an array. Details of the deconvolutions of the explosions are discussed in Der *et al.* (1987a). We present results for Novaya Zemlya explosions deconvolved at two arrays, EKA and WRA. The delays for pP and pPcP as well as the relative pP/P amplitudes are measured from the deconvolved seismograms. These characteristics are intended for use in formulating a magnitude:yield relationship for the Novaya Zemlya test sites.

Some examples of deconvolutions of P- and PcP-waves from Novaya Zemlya events recorded at the array EKA (Δ = 29°) are shown in Figures 5a through 5d. A causal attenuation operator (Azimi *et al.*, 1968) with a t* of 0.23 sec has been removed from the waveforms along with the instrument response and estimates of the individual site responses (see Der *et al.*, 1987a). Measured pP-P and pPcP-PcP delays and relative amplitudes from these maximum-likelihood multichannel deconvolutions derived from recordings at the EKA array are listed in Table 4. The events located at the southern Novaya Zemlya test site are indicated by "(S)" in Table 4. The 1975291 event, regarded by Lilwall and Marshall (1986) as a double event, was clipped for both the P and PcP arrivals at EKA.

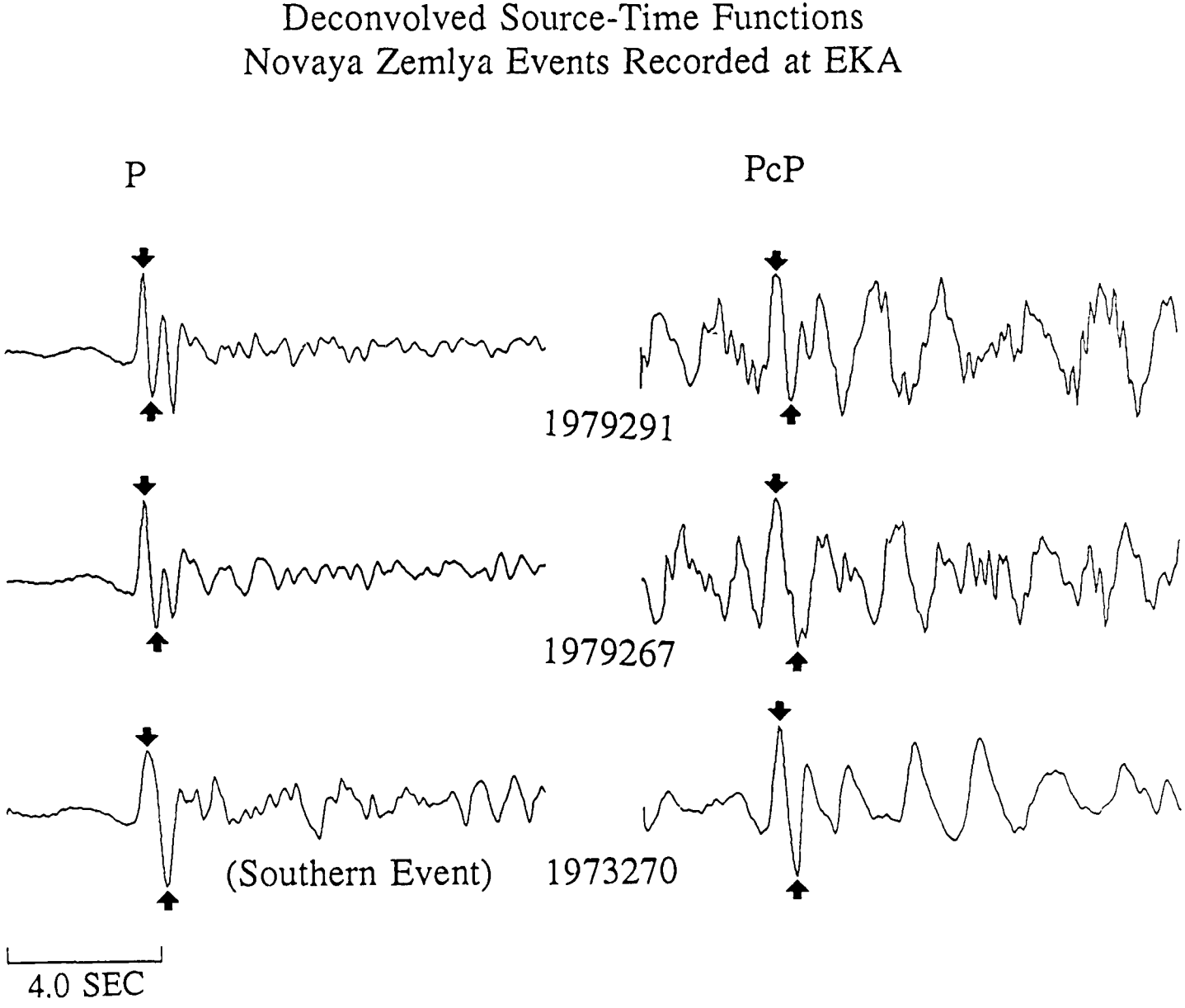

Figure 5a. Comparison of deconvolved P and PcP phases recorded at the array EKA from events located at the Novaya Zemlya test sites.

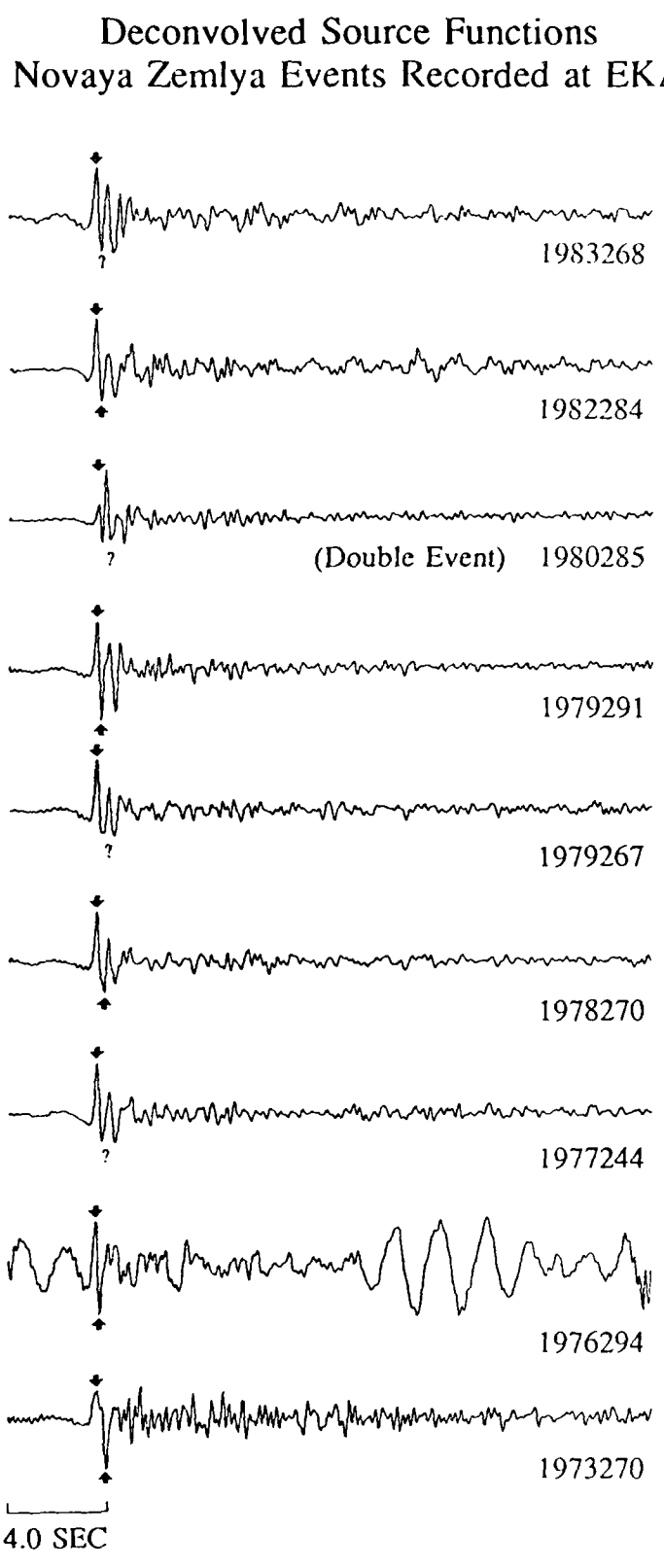

Figure 5b. Deconvolutions of P phases recorded at the array EKA from events located at the Novaya Zemlya test sites.

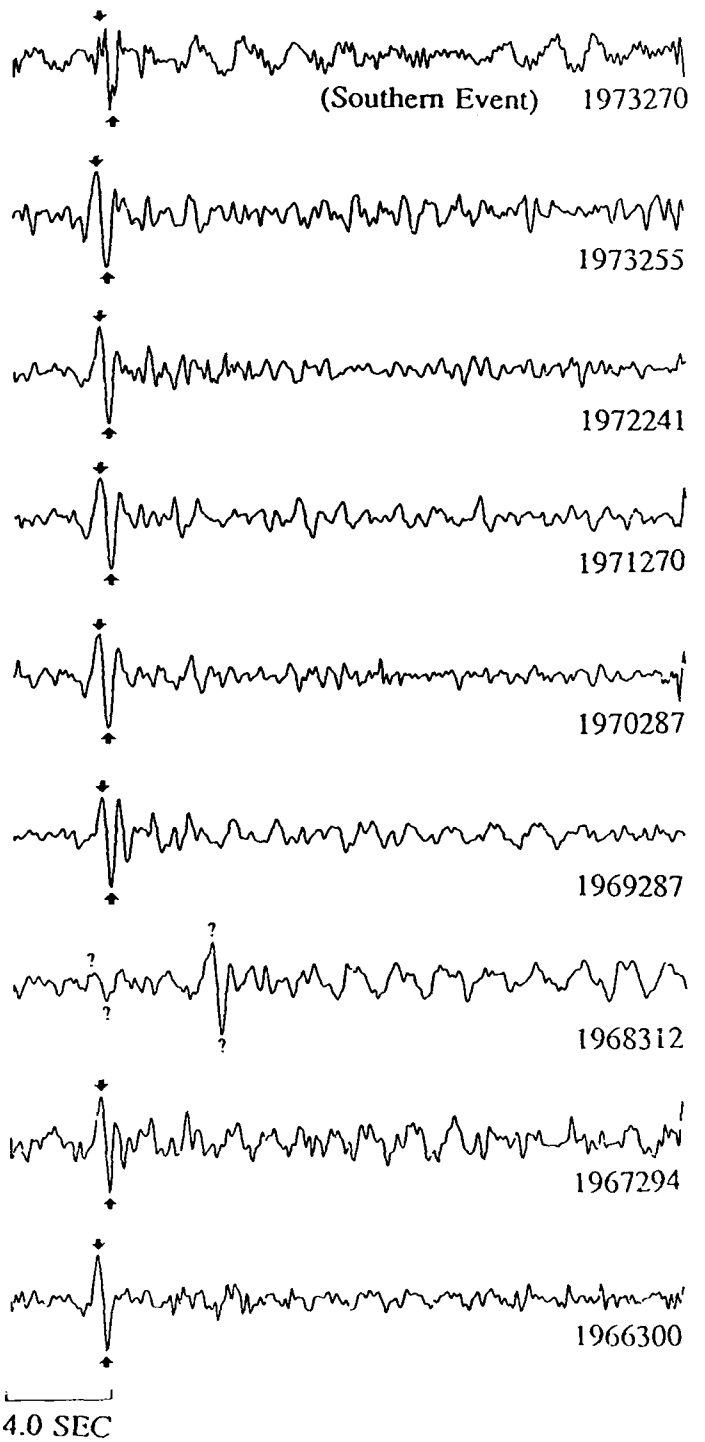

Figure 5c. Deconvolutions of PcP phases recorded at the array EKA from events located at the Novaya Zemlya test sites.

Deconvolved PcP Source Functions
Novaya Zemlya Events Recorded at EKA

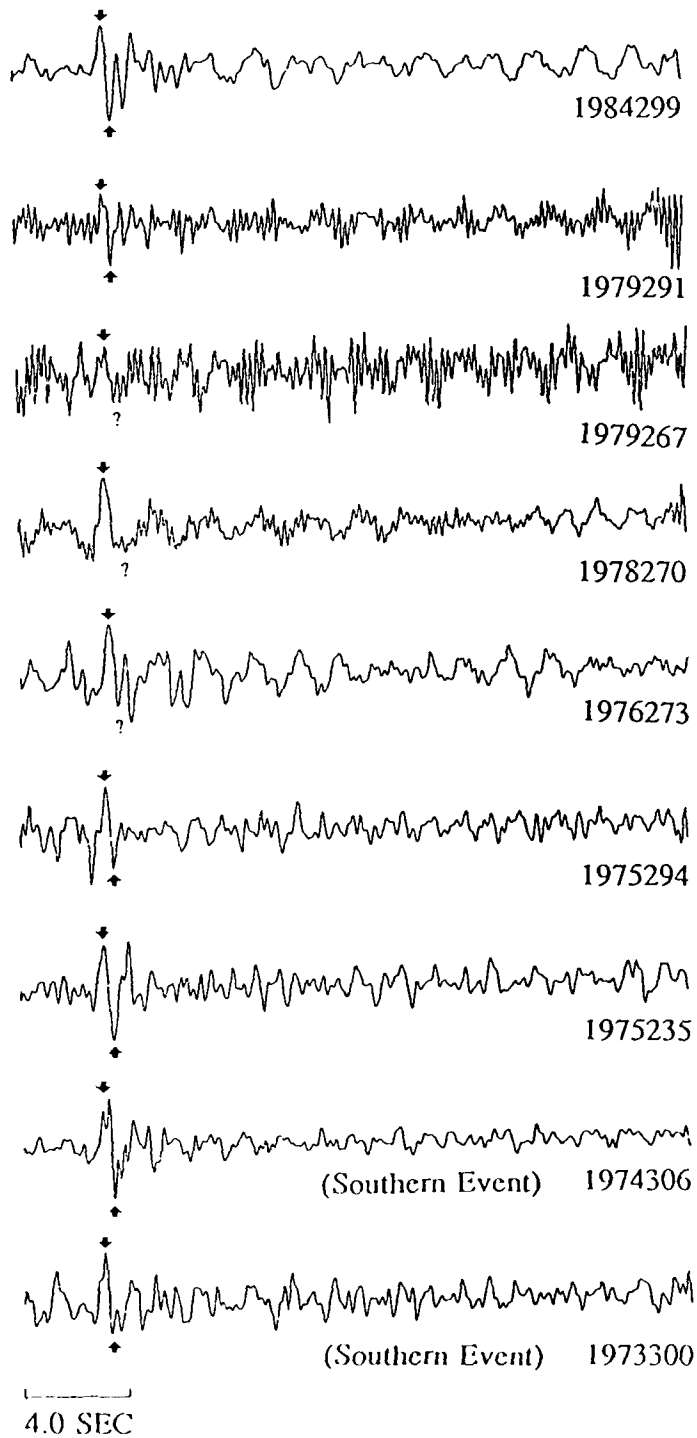

Figure 5c. (cont'd)

Deconvolved P_{diff} Source Functions
Novaya Zemlya Events Recorded at WRA

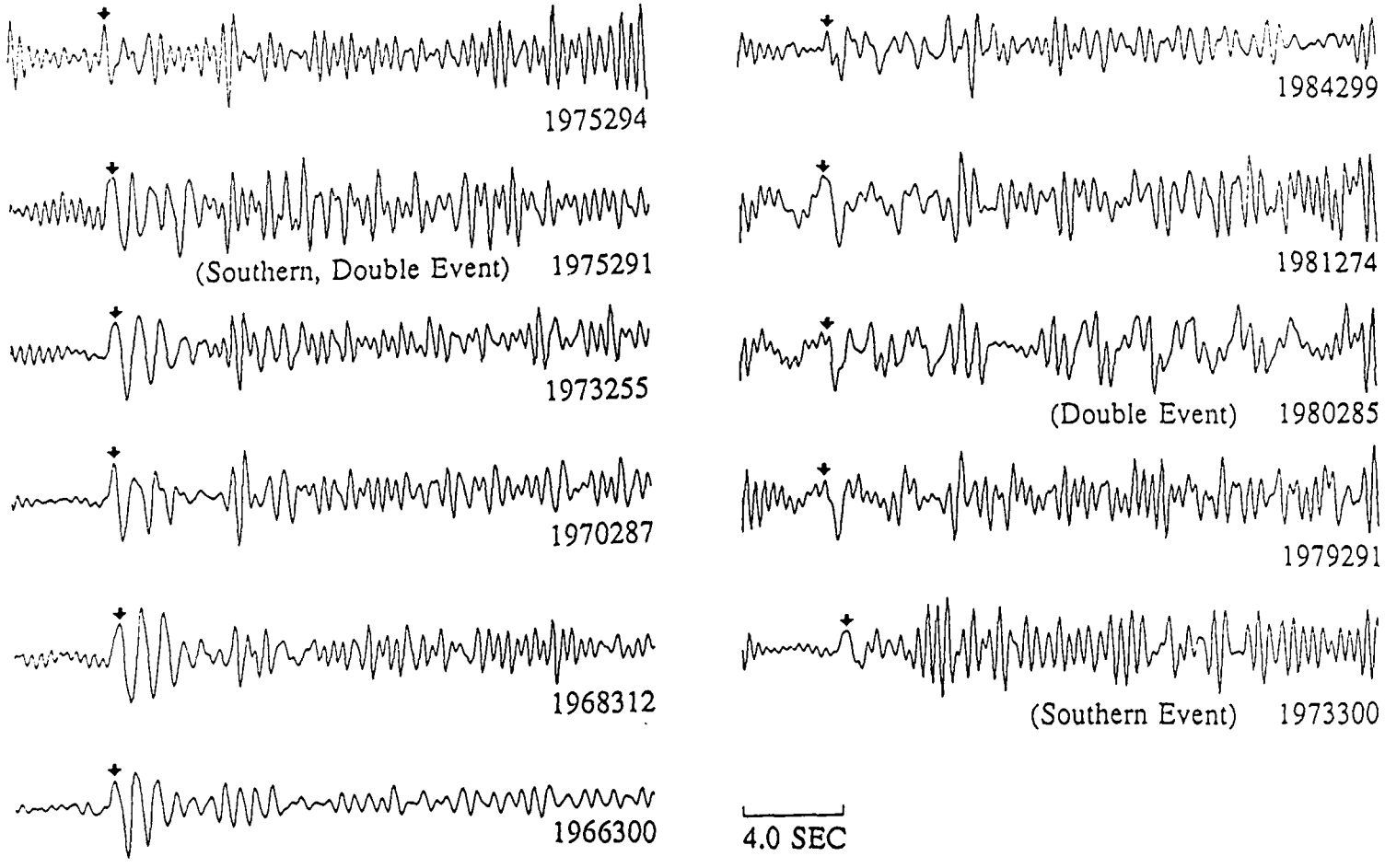

Figure 5d. Deconvolutions of P_{diff} phases recorded at the array WRA from events located at the Novaya Zemlya test sites.

Table 4. Novaya Zemlya pP and pPcP Amplitudes and Delays

Date	m_b Lilwall and Marshall (1986)	Relative Amplitude	Delay (sec)	Phase
1966300	6.47	-0.7	0.35	PcP
1967294	5.99	-0.75	0.30	PcP
1968312	6.11	-1.1	0.40	PcP
1969287	6.18	-1.2	0.35	PcP
1970287	6.77	-0.75	0.40	PcP
1971270	6.63	-0.75	0.40	PcP
1972241	6.46	-0.7	0.37	PcP
1973255	6.96	-0.7	0.45	PcP
1973270(S)	5.84	-1.45	0.40	P
1973270(S)	5.84	-1.8	0.35	PcP
1973300(S)	6.89	-0.65	0.62	PcP
1974306(S)	6.73	-0.75	0.62	PcP
1975235	6.55	-1.0	0.43	PcP
1975291(S-D)	6.69			P&PcP clipped
1975294	6.59	-0.4	0.40	PcP
1976273	5.77	-0.9	0.37	PcP
1976294	4.89	-1.05	0.2	P
1977244	5.71	-0.5	0.25	P
1978270	5.68	-0.85	0.33	P
1978270	5.68	-0.55	0.25	P
1979267	5.80	-0.65	0.30	P
1979267	5.80	-0.27	0.50	PcP(?)
1982284	5.52	-0.6	0.60	P
1983268	5.71	-0.4	0.90	P
1984299	5.90	-1.9	0.32	PcP

The time delays are plotted with respect to the Lilwall and Marshall m_b's in Figure 6. Except for the two largest southern events, the data show a trend for the depth phase time delays to increase gradually with increasing event size. The two largest southern events stand out from the population with depth phase delays of 0.6 sec. The time resolution of the deconvolution procedure is estimated to be about ±0.15 sec. This is the half-width-half-maximum of the Shumway-Der resolution kernel. This indicates that the depth phase time delay may be a weak function of the source size and not wholly dependent on the burial depth of the explosion unless the biggest two events were overburied.

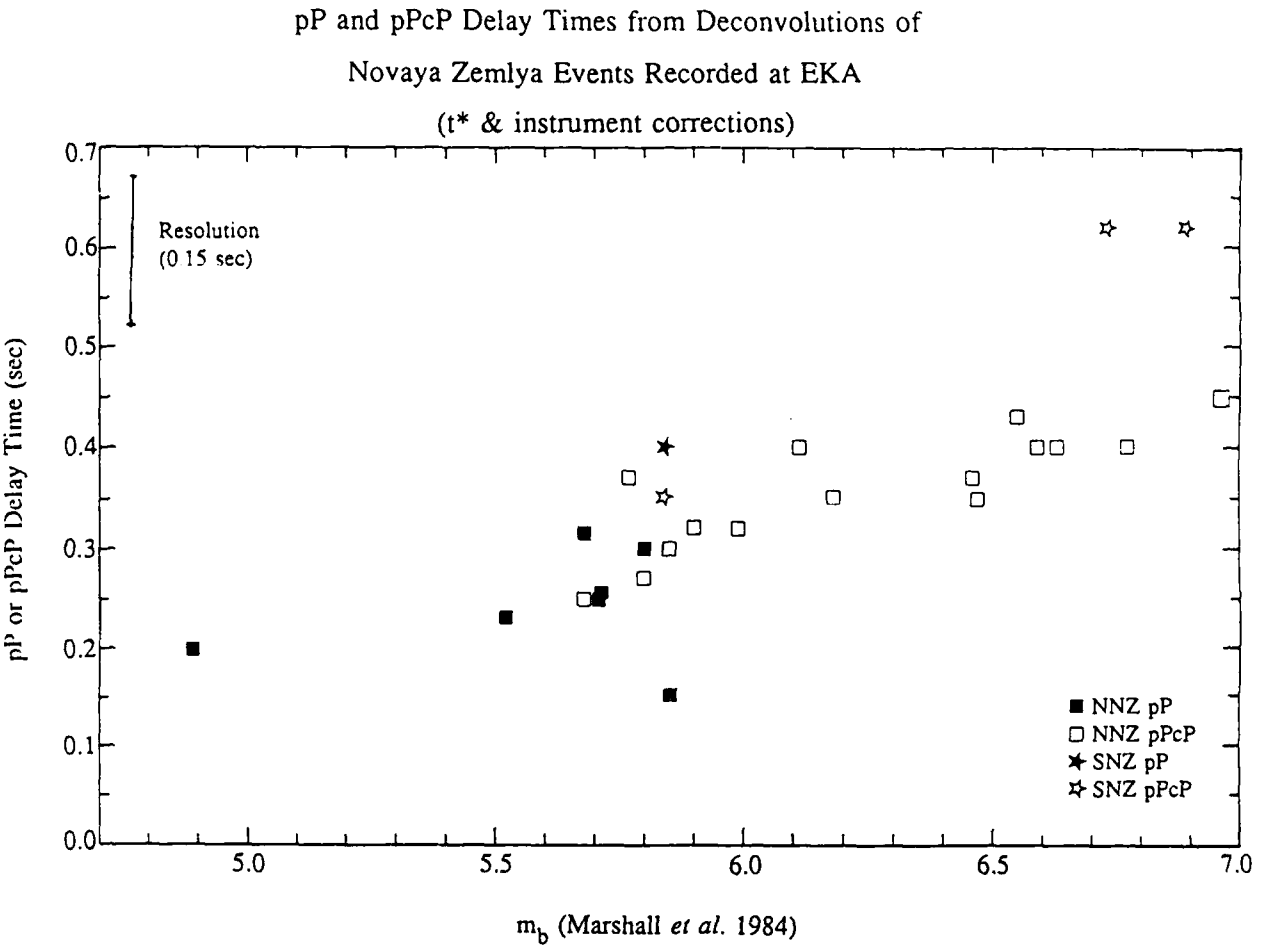

Figure 6. pP-P and pPcP-PcP time delays versus Lilwall and Marshall (1986) m_b measured from the P and PcP deconvolutions of Figure 5. Events at the southern Novaya Zemlya test site are indicated with "stars", northern Novaya Zemlya test site events are indicated with "boxes". Measurements made on deconvolved PcP waves are indicated by open stars or boxes, while those made on deconvolved P waves are solid stars or solid boxes. With the exception of one northern event and the two large southern events, the data exhibit a trend indicating larger events have longer delay times.

P- and PcP-wave Spectral Estimates

Gupta *et al.* (1985) used the average spectral level of the P-wave and P-coda for NTS and Eastern Kazakh explosions at a single station, NA0, to derive an explosion source size estimator. They found that the single station spectral estimator had an excellent correlation with ISC m_b and known yields for NTS explosions. The source size estimate is made from a log-average of the spectral amplitude in a selected bandwidth after corrections have been made for instrument, attenuation, and a von Seggern and Blandford (1972) source spectral shape. These corrections pre-whiten the spectral amplitude, and if a bandwidth is chosen that has good signal-to-noise ratio, then the average spectral level is an estimate of the far-field explosion size. This level can be corrected for geometrical spreading and the free-surface effect at the receiver to yield an estimate of the explosion RDP or moment, Ψ_∞ or M_0 respectively.

This procedure was applied to P and PcP data recorded at the EKA array. A frequency independent t* of 0.23 seconds was assumed as an attenuation correction, and the Bache (1982) m_b:Log(Y) relation was applied to estimate yield-dependent parameters for the von Seggern and Blandford RDP. The maximum-likelihood P- and PcP-wave averaged spectra before pre-whitening are shown in Figures 7a and 7b. After correcting for instrument response, attenuation, and estimated RDP, the corresponding spectra are shown in Figures 7c and 7d.

Because the P-wave was clipped at EKA for many of the events of interest, we performed the procedure on both P and PcP arrivals at the EKA array. The results are presented in Table 5, with uncertainties estimated from the scatter of the spectral levels

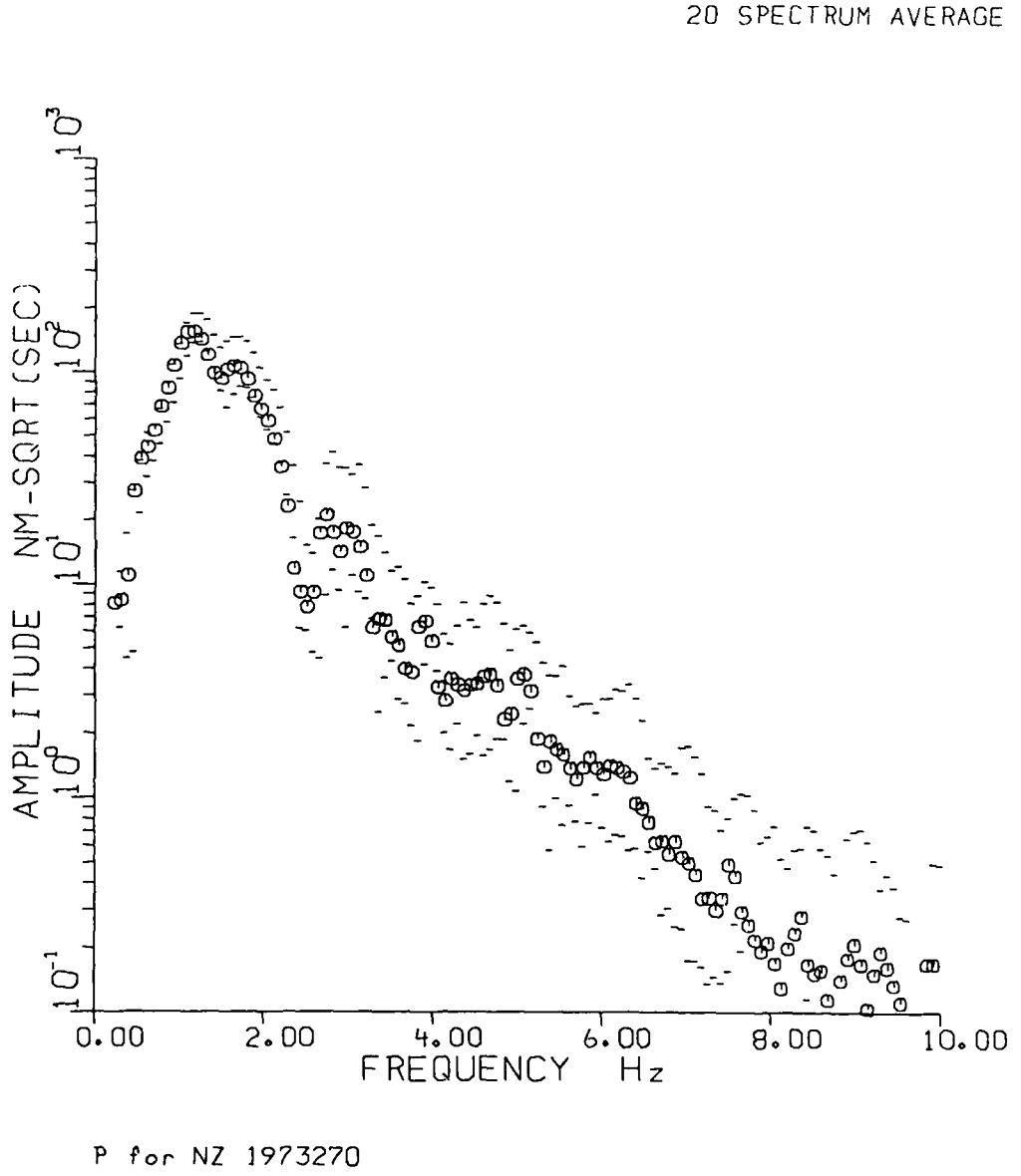

Figure 7a. Maximum-likelihood P-wave averaged spectra for Novaya Zemlya event 73270 recorded at 19 EKA stations. The upper and lower error bars are indicated for each discrete spectral amplitude.

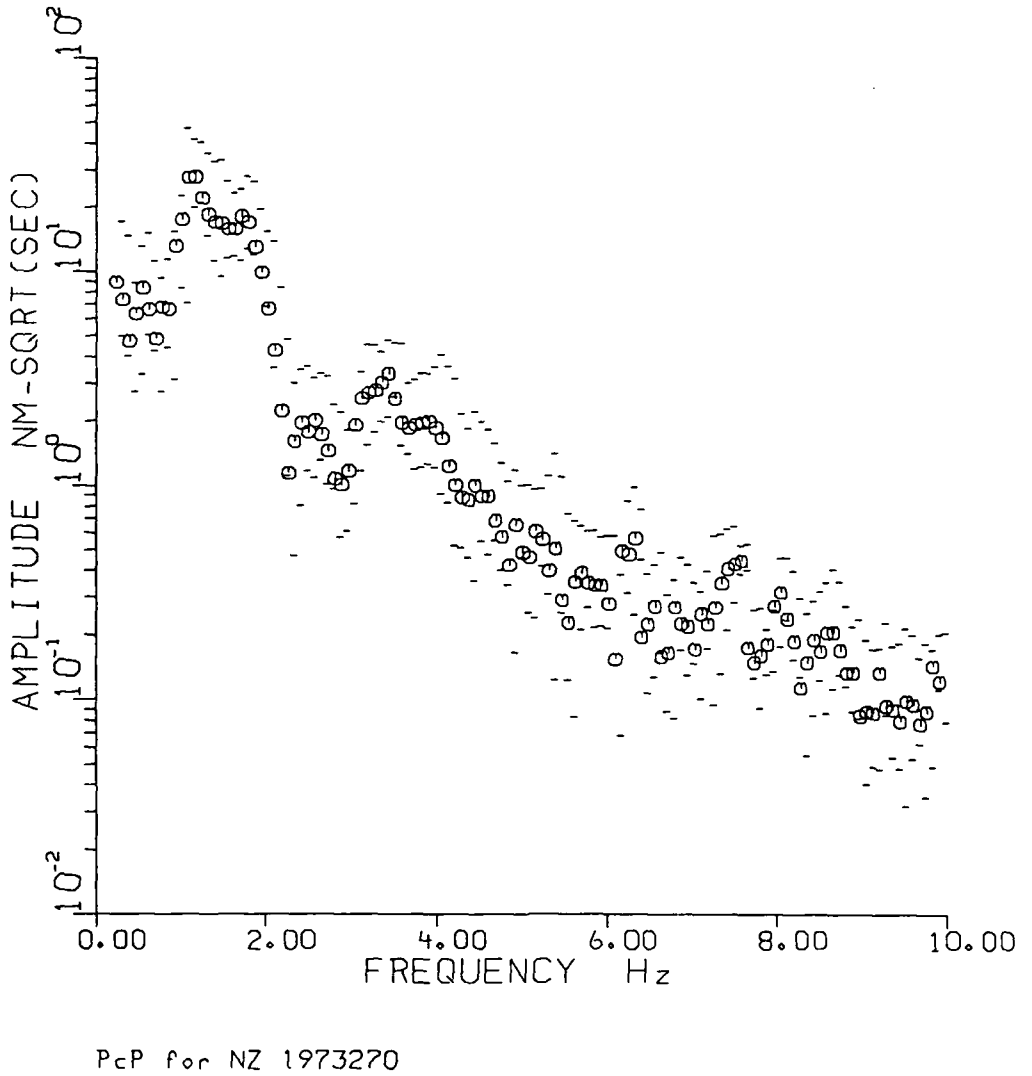

Figure 7b. Maximum-likelihood PcP-wave average spectra for Novaya Zemlya event 73270 recorded at 20 EKA stations. The upper and lower error bars are indicated for each discrete spectral amplitude.

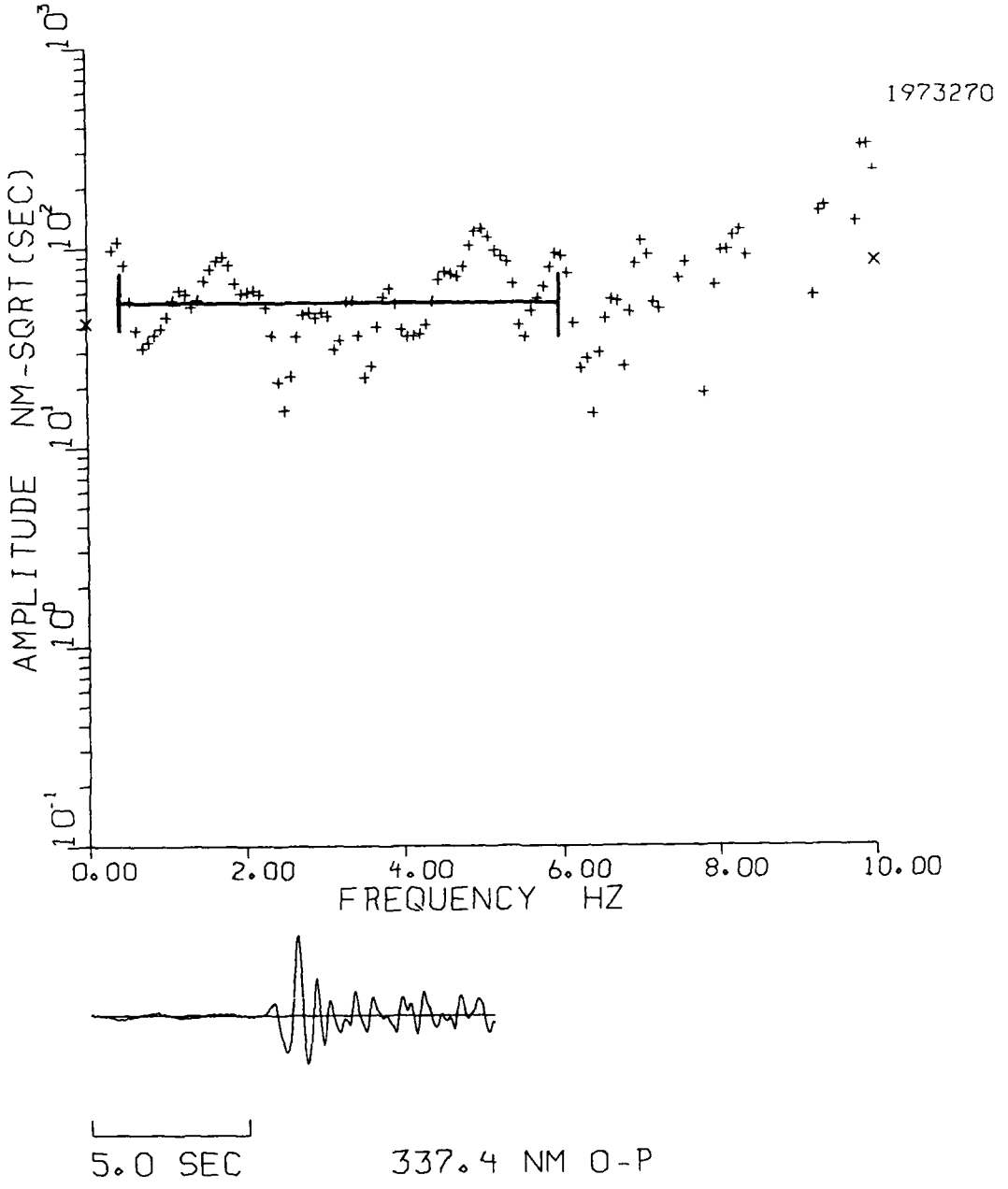

Figure 7c. P-wave spectra for event in Fig. 7a recorded at EKA. The spectra is corrected for instrument response, attenuation, and estimated RDP. The horizontal bar indicates the bandwidth used to estimate the spectral amplitude of the phase.

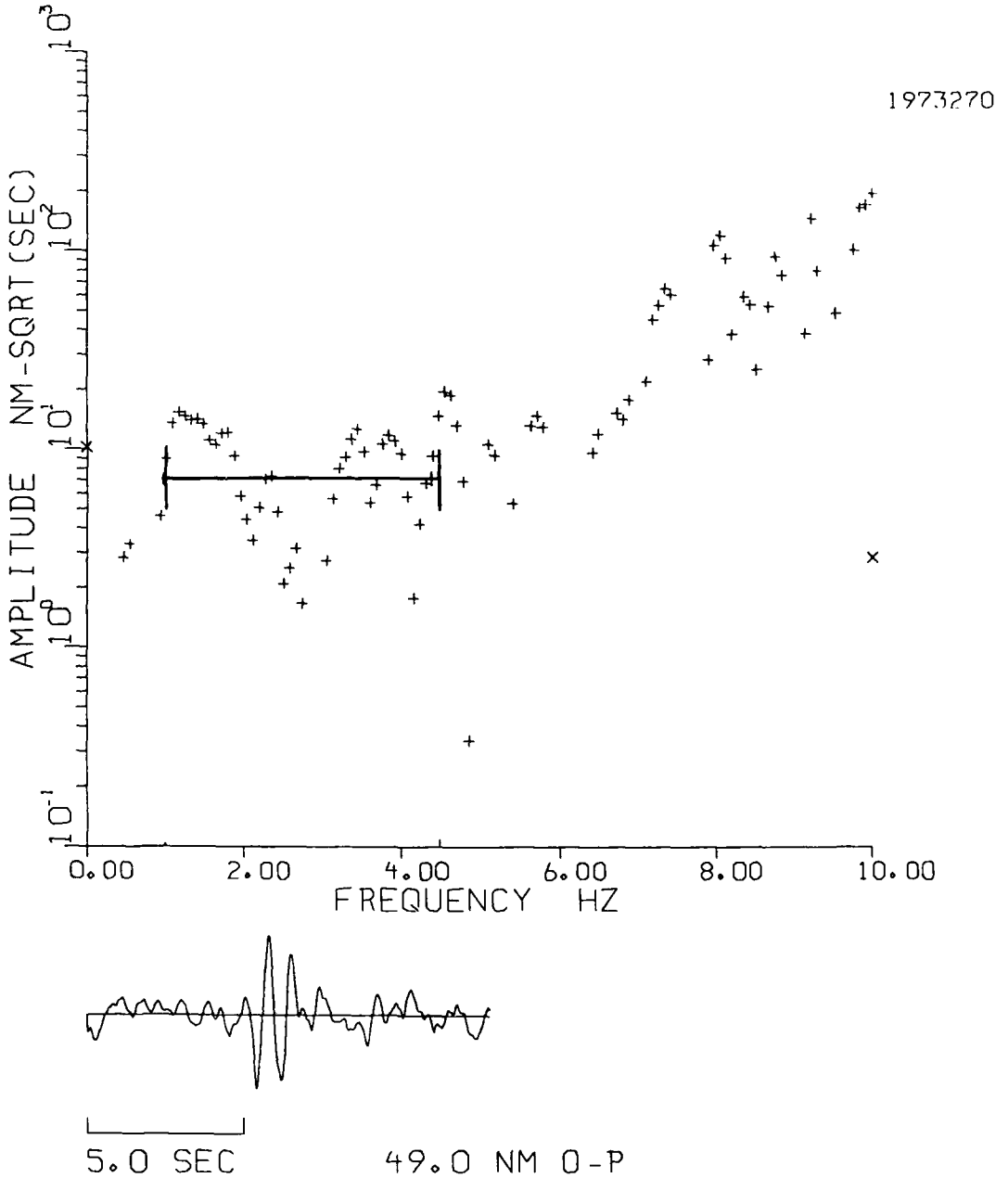

Figure 7d. PcP-wave spectra for event in Fig. 7a recorded at EKA. The spectra is corrected for instrument response, attenuation, and estimated RDP. The horizontal bar indicates the bandwidth used to estimate the spectral amplitude of the phase.

across the array of stations. The four southern events are denoted with an "(S)". The southern event identified as a double event by Lilwall and Marshall (1986) is denoted by an "(SD)" in the table. The average log(P/PcP) is estimated directly from the data for the four events with both P and PcP recordings on scale. For all others events, Log(P) was either extrapolated from Log(PcP) or the reverse. The arrows ($\Rightarrow$ and $\Leftarrow$) indicate the direction of extrapolation for each event. The value Log(P/PcP) = 0.69±0.16 was used for the southern test site and Log(P/PcP) = 0.91±0.09 was used for the northern test site. In the cases of the extrapolated Log(P), the stated error includes both the uncertainty in the estimate of the original Log(PcP) estimate and the uncertainty in the Log(P/PcP) estimate. The Log(P) estimates are plotted in Figure 8 against the Lilwall and Marshall (1986) m_b for each event. The largest events (1973255, 1973300, 1974306, and 1975291) may still be biased due to the censoring imposed by PcP-phase clipping at stations within the array and their consequent removal from the processing. For example, the southern event 1975291 clipped all but one station on the PcP signal and is therefore certainly biased low.

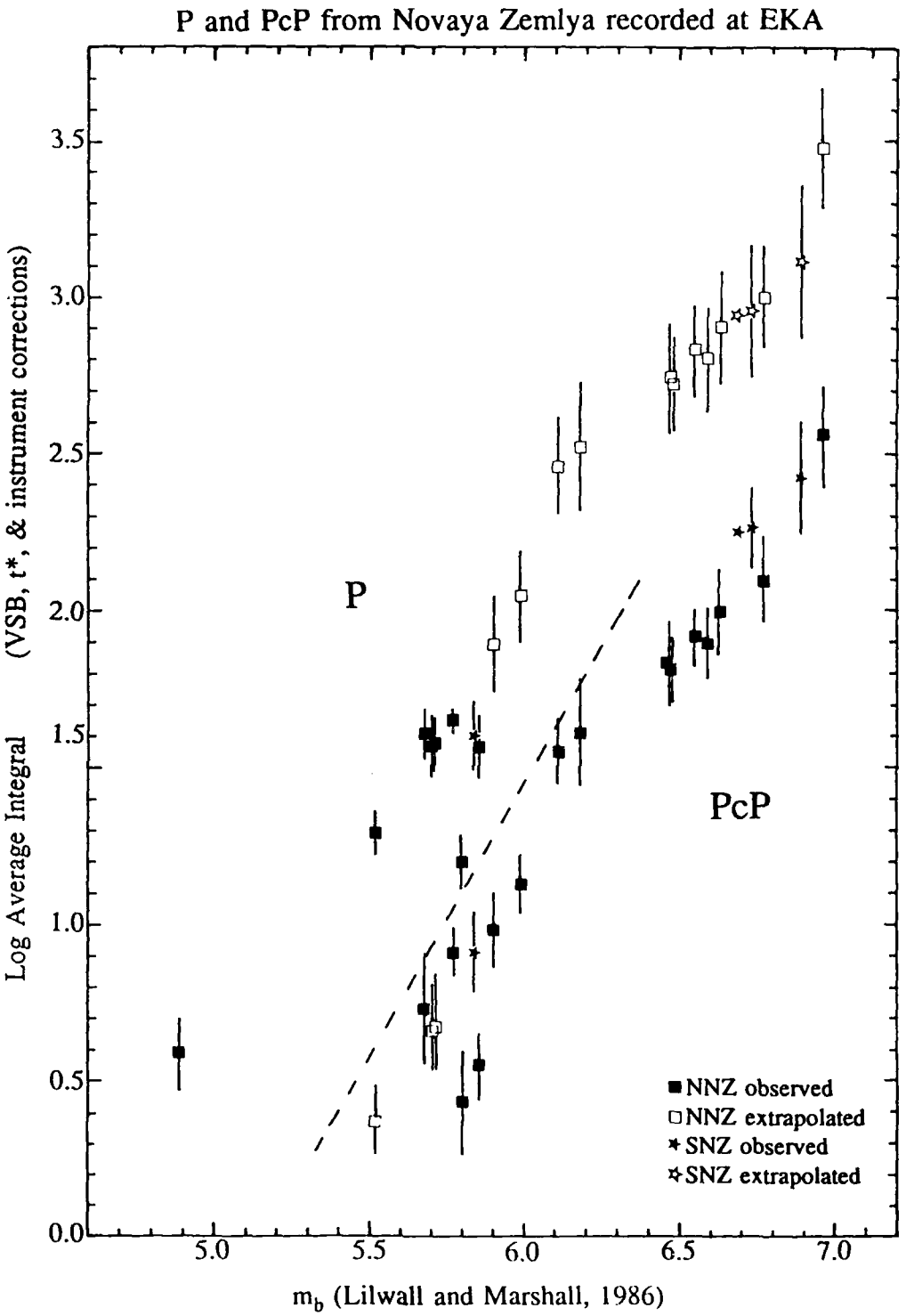

Figure 8. P and PcP spectral estimates at EKA versus Lilwall and Marshall (1986) m_b. The dotted line serves to separate P and PcP spectral level estimates. Events at the northern test site are identified with "boxes", the southern test site with "stars". P-wave spectral levels inferred from PcP spectral levels are identified by either open "stars" or "boxes".

Table 5. Novaya Zemlya Explosion P and PcP Spectral Levels [Log(nm-sec)] at EKA (Δ = 29°; t* = 0.23 sec)

Date	Lilwall and Marshall m_b	Log(P)	σ		Log(PcP)	σ	$\text{Log}(\frac{P}{PcP})$	σ
1966300	6.47	2.72	0.15	⇐	1.81	0.10		
1967294	5.99	2.04	0.14	⇐	1.13	0.09		
1968312	6.11	2.46	0.15	⇐	1.55	0.10		
1969287	6.18	2.52	0.20	⇐	1.61	0.17		
1970287	6.77	3.00	0.16	⇐	2.09	0.12		
1971270	6.63	2.90	0.18	⇐	1.99	0.14		
1972241	6.46	2.74	0.17	⇐	1.83	0.13		
1973255	6.96	3.47	0.19	⇐	2.56	0.15		
1973270(S)	5.84	1.60	0.10		0.91	0.12	0.69	0.16
1973300(S)	6.89	3.11	0.24	⇐	2.42	0.18		
1974306(S)	6.73	2.95	0.21	⇐	2.26	0.13		
1975235	6.55	2.83	0.14	⇐	1.92	0.08		
1975291(SD)	6.69	2.94	0.16	⇐	2.25			
1975294	6.59	2.80	0.16	⇐	1.89	0.11		
1976273	5.77	1.82	0.13	⇐	0.91	0.06		
1976294	4.89	0.59	0.11	⇒	0.32	0.14		
1977244	5.71	1.58	0.08	⇒	0.67	0.12		
1978270	5.68	1.61	0.06		0.73	0.16	0.88	0.17
1979267	5.80	1.20	0.07		0.43	0.16	0.77	0.17
1979291	5.85	1.56	0.09		0.55	0.10	1.01	0.13
1982284	5.52	1.29	0.05	⇒	0.38	0.10		
1983268	5.71	1.57	0.09	⇒	0.66	0.13		
1984299	5.90	1.89	0.16	⇐	0.98	0.11		

⇒ Log(P) extrapolated from Log(PcP)

⇐ Log(PcP) extrapolated from Log(P)

P_{diff}-Wave Spectral Estimates

The procedure used in the P and PcP yield estimates was subsequently applied to diffracted P-waves (P_{diff}) recorded at the WRA array (Δ = 106°). Because these P-waves are diffracted by the core-mantle boundary, it is less certain how to estimate appropriate geometrical spreading and attenuation factors. An attenuation operator with

a t* of 0.45 seconds was found to flatten the spectrum adequately. Some of the estimates are listed in Table 6. Again, the three largest events (1973255, 1973300, and 1975291) may be biased due to censoring by clipping at the stations within the array recording the largest amplitudes. The spectral estimates are plotted versus Lilwall and Marshall m_b in Figure 9.

Table 6. Novaya Zemlya P_{diff} Spectral Estimates [Log(nm-sec)] at WRA (Δ = 106°; t*=0.45 sec)

Date	Lilwall and Marshall m_b	Log(P)	
1966300	6.47	2.16	0.20
1968312	6.11	1.22	0.21
1970287	6.77	2.18	0.36
1973255	6.96	2.08	0.22
1973300(S)	6.89	2.35	0.33
1975291(S-D)	6.69	1.35	0.14
1975294	6.59	1.03	0.11
1979294	5.85	0.33	0.14
1980285(D)	5.80	0.32	0.23
1981274	5.90	0.42	0.20
1984299	5.90	0.30	0.16

Comparison with Amchitka Events

Douglas *et al.* (1987) estimated Ψ_∞ for the three Amchitka events LONGSHOT, MILROW, and CANNIKIN using the geometrical spreading factors of Carpenter (1967). They estimated Log(Ψ_∞) for LONGSHOT, MILROW, and CANNIKIN as 3.84, 4.70, and 5.27 (Log(m^3)) from P-waves recorded at EKA, YKA, GBA, and WRA. We have applied the same geometrical spreading corrections to the Novaya Zemlya events for EKA data. The estimates are presented in Table 7. The largest Novaya Zemlya Log(Ψ_∞) is estimated to be 5.31±0.19 for the 1973255 event. We are

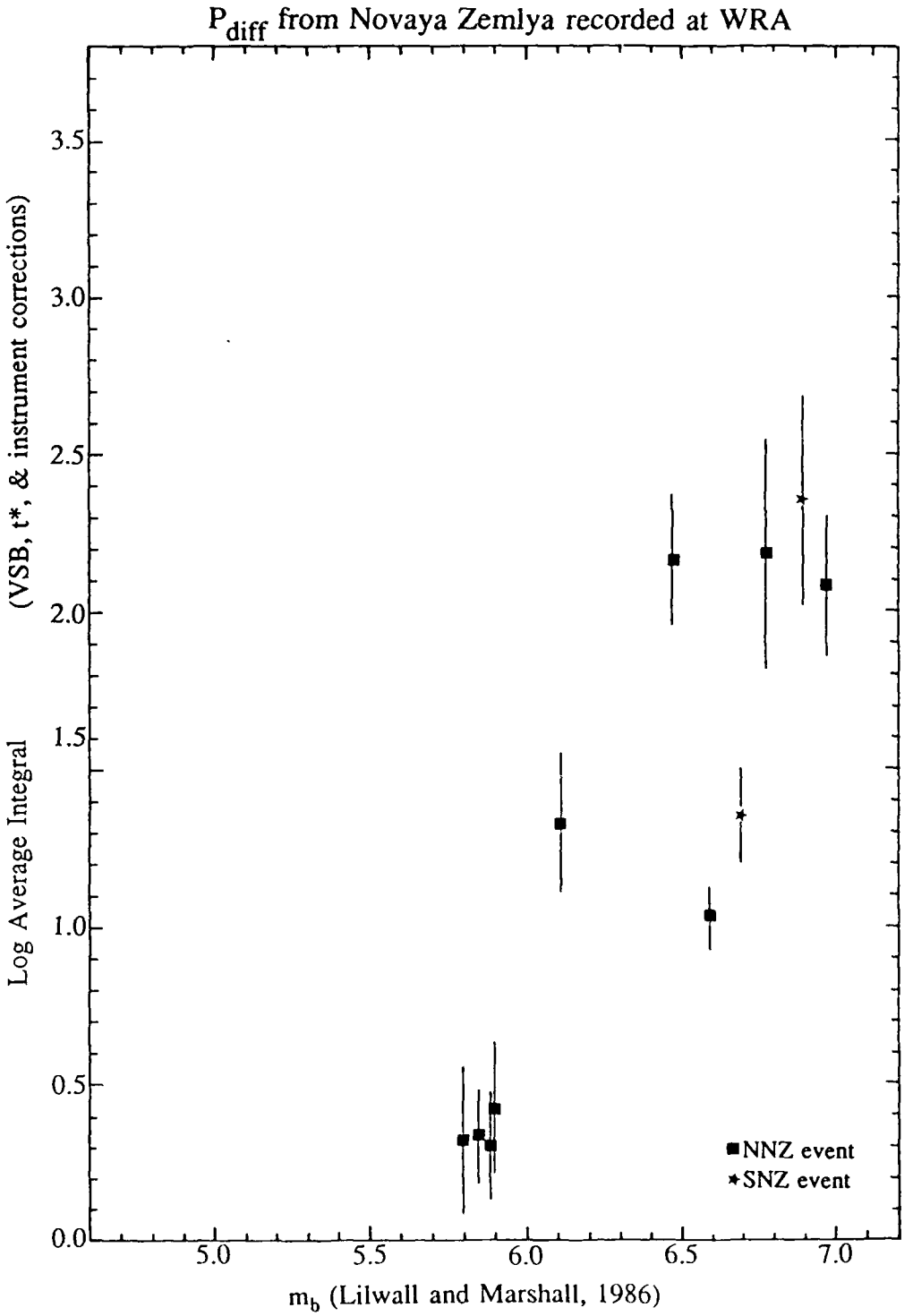

Figure 9. P spectral levels at WRA corrected for t*=0.45 sec, and estimated RDP, versus Lilwall and Marshall (1986) m_b.

justified in making this comparison, since McLaughlin *et al.* (1988) have shown that the time domain method used by Douglas *et al.* (1987) and the frequency domain method used here are equivalent. Given that the large events are biased low by clipping at stations recording high amplitude in the array, and given the scatter of $\mathrm{Log}(\Psi_\infty)$ with respect to the MLE-GLM m_b's in Figure 8, it may be concluded that the largest Novaya Zemlya events are larger than CANNIKIN. This comparison assumes that the corresponding shot point acoustic impedance for the CANNIKIN and Novaya Zemlya shots are the same and that coupling is uniform for constant RDP. If we assume that shot point velocities are higher for the Novaya Zemlya test site than for Amchitka, then we must question whether it is more valid to compare RDP or moment. We have reason to believe that shot point velocities are higher at the two Novaya Zemlya test sites and that with changing rock type, the yield coupling is more nearly constant with respect to moment than to RDP. Both of these corrections will increase the yield estimates for Novaya Zemlya explosions.

Table 7. Log(Ψ_∞) Spectral Estimates (Log(m^3)) Geometrical Spreading from Carpenter (1967)

	Lilwall and Marshall	EKA	
Date	m_b	Log(Ψ_∞)	σ
1966300	6.47	4.56	0.15
1967294	5.99	3.88	0.14
1968312	6.11	4.30	0.15
1969287	6.18	4.36	0.20
1970287	6.77	4.84	0.16
1971270	6.63	4.74	0.18
1972241	6.46	4.58	0.17
1973255	6.96	5.31	0.19
1973270(S)	5.84	3.44	0.10
1973300(S)	6.89	4.95	0.24
1974306(S)	6.73	4.79	0.21
1975235	6.55	4.67	0.14
1975291(SD)	6.69	4.78	0.16
1975294	6.59	4.64	0.16
1976273	5.77	3.66	0.13
1976294	4.89	2.43	0.11
1977244	5.71	3.42	0.08
1978270	5.68	3.45	0.06
1979267	5.80	3.04	0.07
1979291	5.85	3.40	0.09
1979294	5.85		
1980285(D)	5.80		
1981274	5.90		
1982284	5.52	3.13	0.05
1983268	5.71	3.41	0.09
1984299	5.90	3.73	0.16

Stevens (1986) estimates Log(M_0) for the Amchitka events as 23.05±0.07, 24.13±0.04, and 24.88±0.04 (log(dyne-cm)) from surface waves for LONGSHOT, MILROW, and CANNIKIN, respectively. In order to convert properly the Douglas *et al.* (1987) Amchitka Ψ_∞ estimates for these three shots to moment using shot-point velocities and density from Stevens (1986), we must impose a slight digression.

Carpenter (1967) expresses the far-field amplitude as

$$A(t) = \left(\frac{\rho_1\alpha_1}{\rho_0\alpha_0}\right)^{1/2} G(\Delta)\ R\ B\ \dot{\Psi}(t),$$

$B \approx 2$ is the free surface effect and $R \approx 1$ is the transmission coefficient across interfaces in the Earth. The factor $\rho_0\alpha_0$ is the acoustic impedance at the receiver, and $\rho_1\alpha_1$ is the acoustic impedance at the source. $\dot{\Psi}(t)$ is the time derivative of the RDP. $G(\Delta)$ is Carpenter's tabulated geometrical spreading coefficient for a surface source and receiver. Moment and RDP are related by the definition, $M = 4\pi\rho_1\alpha_1^2\Psi$. Therefore, in order to compare RDP estimates of Douglas *et al.* (1987) with Steven's (1986) moments, we estimate the velocity and density at the ARWE arrays to be about 5.0 km/s and 2.5 gm/cc respectively and make the necessary conversions. Douglas *et al.* (1987) assume that $\frac{\rho_1\alpha_1}{\rho_0\alpha_0} \approx 1$, so we also estimated an impedance-"corrected" RDP.

The results presented in Table 8, serve to demonstrate that the P wave moments are systematically lower than the surface wave moments by about a factor of 5. This discrepancy between P-wave moment derived from deconvolved short-period records and the moment derived from surface waves or near-field RDP measurements is larger than previous moment estimates for Piledriver and the southern Sahara explosions in granite (McLaughlin *et al.*, 1988) compared to near-field RDP measurements. The comparison would be much the same if we convert moment to RDP. Since these estimates are based on only one array, care should be taken in interpreting their absolute levels. The discrepancy between the body wave and surface waves moments may be attributed to the use of a frequency independent t* in the body wave estimation. In

addition, a single station average may have quite large or small magnitudes compared to a network average in the case of the body wave estimation.

Another interesting result of this calculation is that the moment estimates, whether from surface waves or from P-waves, are consistent with a slope of 1.0 with respect to yield, whereas the RDP estimates, whether impedance corrected or not, are not consistent with a slope of 1.0.

Table 8. Comparison of Amchitka Surface Waves and P-Wave $Log(M_0)$ (dyne-cm) Estimates

EVENT	α_1 (km/sec)	Stevens surface-waves $Log(M_0)$	Douglas Ψ corrected to P-wave $Log(M_0)$	$Log(\Psi)+Log(\frac{\alpha_0}{\alpha_1})/2$
LONGSHOT	3.0	23.05±0.07	22.41	3.95
MILROW	3.7	24.13±0.04	23.39	4.76
CANNIKIN	4.2	24.88±0.04	24.09	5.34

MAGNITUDE SCALING FOR NOVAYA ZEMLYA EXPLOSIONS FROM P'P'

In addition to the PcP signals that remain on scale at stations where the P-wave is clipped, we have found that the P'P' phase is an excellent candidate for magnitude determination for events larger than m_b = 6.0. The phase is the PKP equivalent of PP, often referred to as PKPPKP, whose raypath is indicated in Figure 10. The ray emerges as a P phase, travels through the outer core, is reflected off the Earth's surface, and then resumes its passage through the core before surfacing through the mantle. P'P' is mostly associated with its precursor, designated as P'dP', which is P'P' reflecting off the upper mantle discontinuity as identified by Whitcomb (1973) and by Whitcomb and Anderson (1970). These phases have been used extensively to study the properties of the upper mantle structure and their scattering effects (Teng and Tung, 1973; Whitcomb, 1973; Haddon *et al.*, 1977; Sobel, 1978).

The P'P' phase is prominent in the epicentral distance range of 40° to 80°. The familiar 145° PKP caustic appears for P'P' at 70° stretched out over twice the epicentral distance. The P'P' phase is easily seen on a short-period WWSSN record between 25 and 35 minutes after the P arrival. P'P' are stretched out in time due to the doubled PKP triplication, precursors, and non-minimum phase nature of the arrivals. The peak amplitude of the phase appears, however, to be a stable measurement. Another interesting aspect of the P'P' phase propagation is that it emerges from the source at the opposite azimuth of the direct P-wave and arrives at the station 180° in azimuth from the direct P wave. Consequently, the P'P' becomes another independent P-wave measure of the source that can be made at the same station.

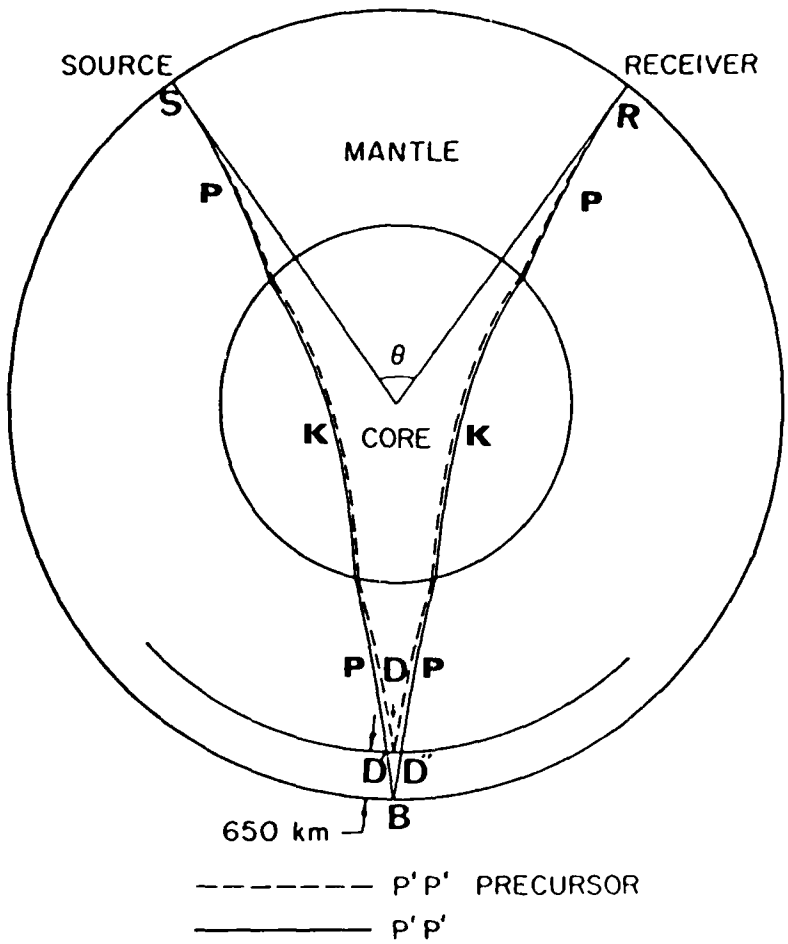

Figure 10. Ray paths for P'P' (PKPPKP). The phase is best recorded at distance range of 40° to 80°. The underside reflection from the 650 discontinuity is generally denoted as the P'P' precursor.

A large number of WWSSN stations across north America and Europe fall within the optimal epicentral distance window for the P'P' phase from Novaya Zemlya and can therefore contribute two phase readings at each station: P and P'P'. Although in principle these stations could also provide PcP and PP measurements, the large Novaya Zemlya events often produced an extended P coda that obscured the PcP and PP arrivals.

P'P' Amplitude–Distance Relationship

P'P' is a prominent secondary P phase in the 40° to 80° range for large events ($m_b > 6.0$). By studying the P'P' amplitude as a function of distance, we may construct an amplitude-distance scaling function. The P'P' trace from the WWSSN station BOZ ($\Delta = 60.6°$) is shown in Figure 11. The measured peak amplitude is indicated on the figure. Note that the wavetrain is stretched out over a full minute on the WWSSN recording. The measurement is simple and straightforward since only the maximum of the phase need be identified. The analysis is performed on eight Novaya Zemlya events to obtain the peak amplitude-distance relationship. The amplitude-distance relationship is shown in Figure 12 for each event. As noted in the figure, there is a maximum at around 60° to 70°, which corresponds to the caustics at 70°. A similar feature may also be seen in the composite amplitude-distance plot for all events after they are scaled to an m_b of 6.0 in Figure 13. The composite P'P' data are grouped in distance bins of 6° and then fitted with a smooth curve where data are averaged. The distance-amplitude relationship may then be used to correct the observed P'P' data. This observation appears to be in agreement with the predicted P'P' amplitudes from WKBJ

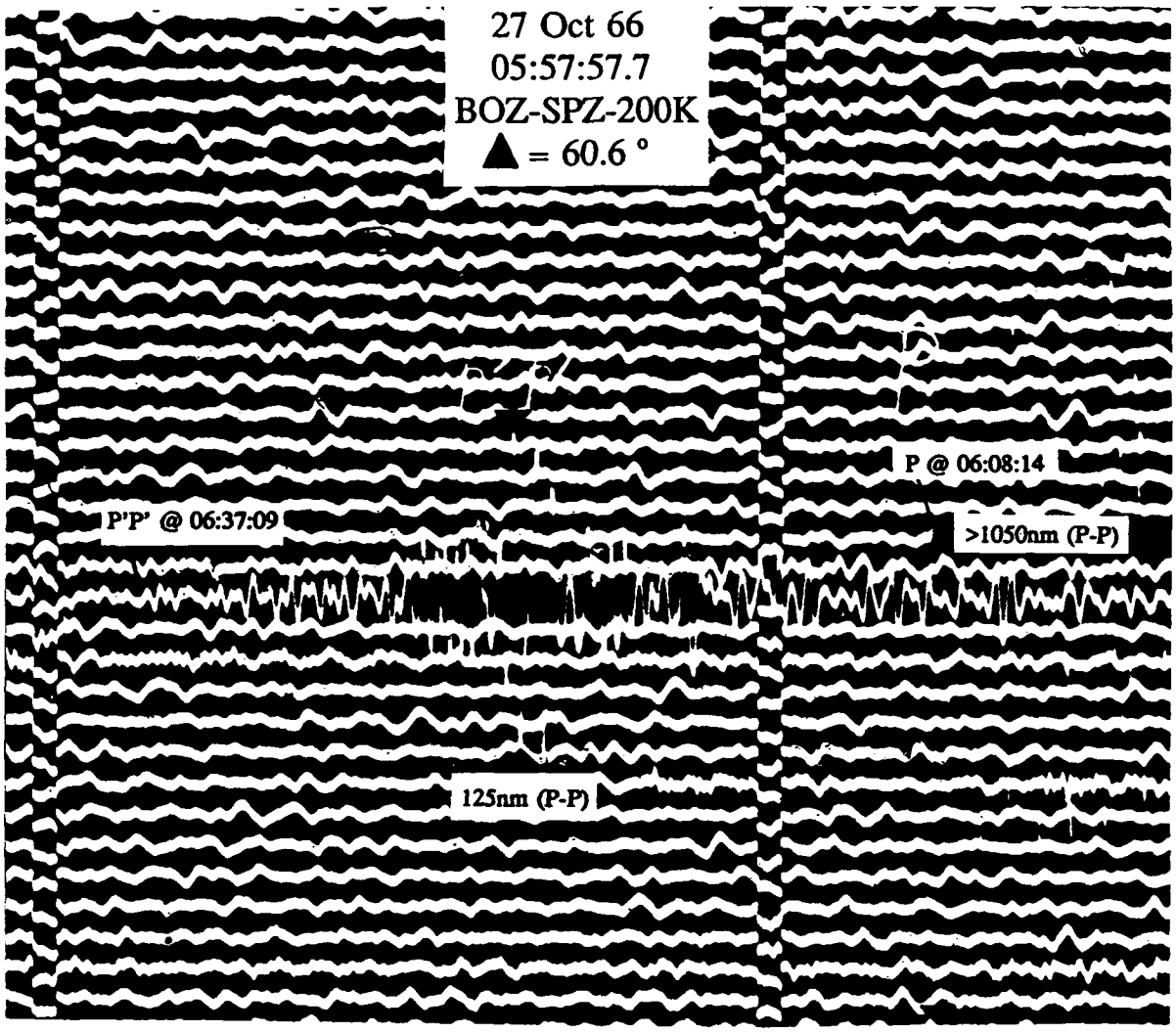

Figure 11. An example of P'P' trace from the WWSSN station BOZ (Δ = 60.6°)

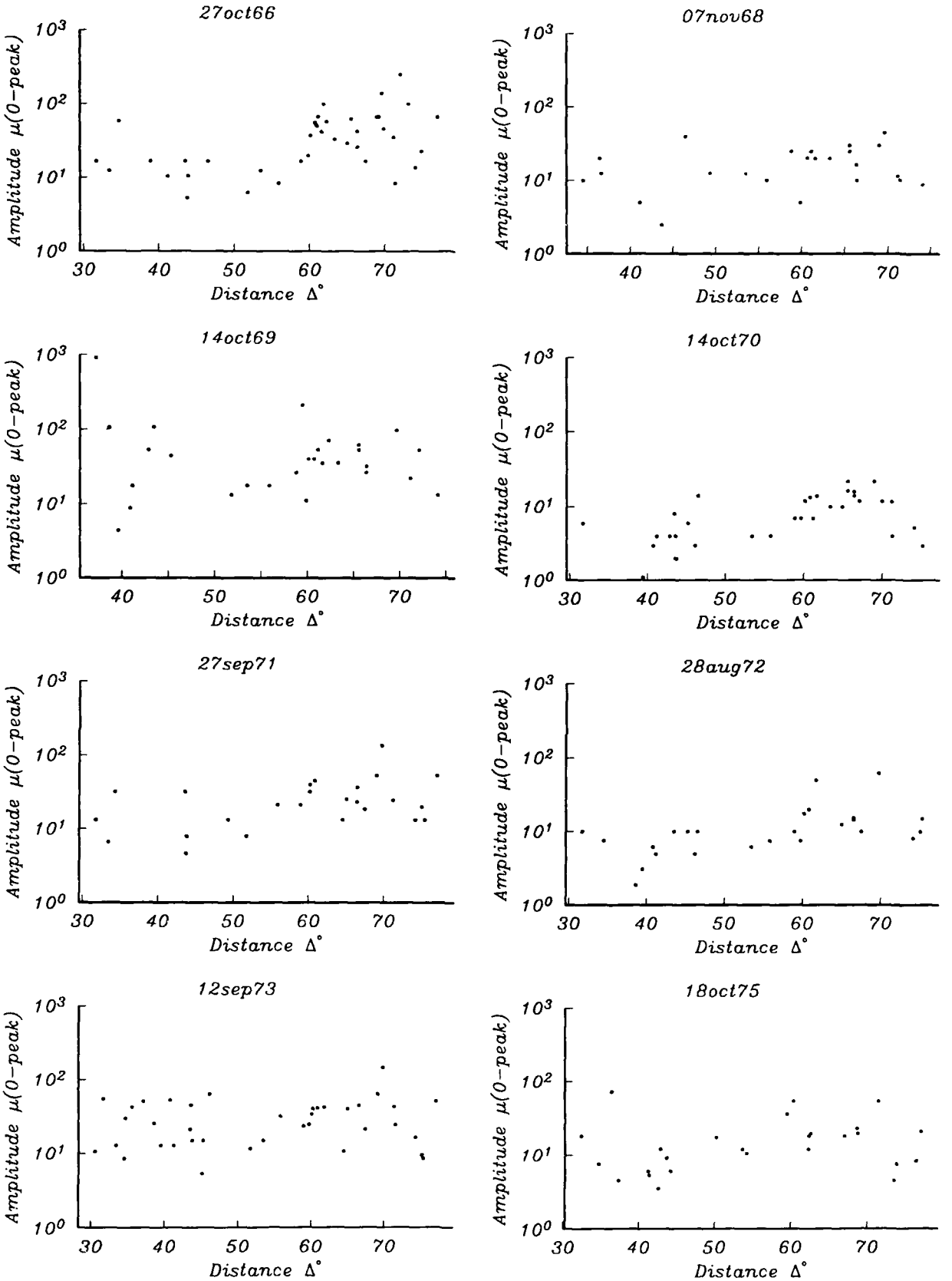

Figure 12. P'P' amplitude-distance relationship for eight events in Novaya Zemlya. These are uncorrected amplitudes measured from the analog WWSSN film chips.

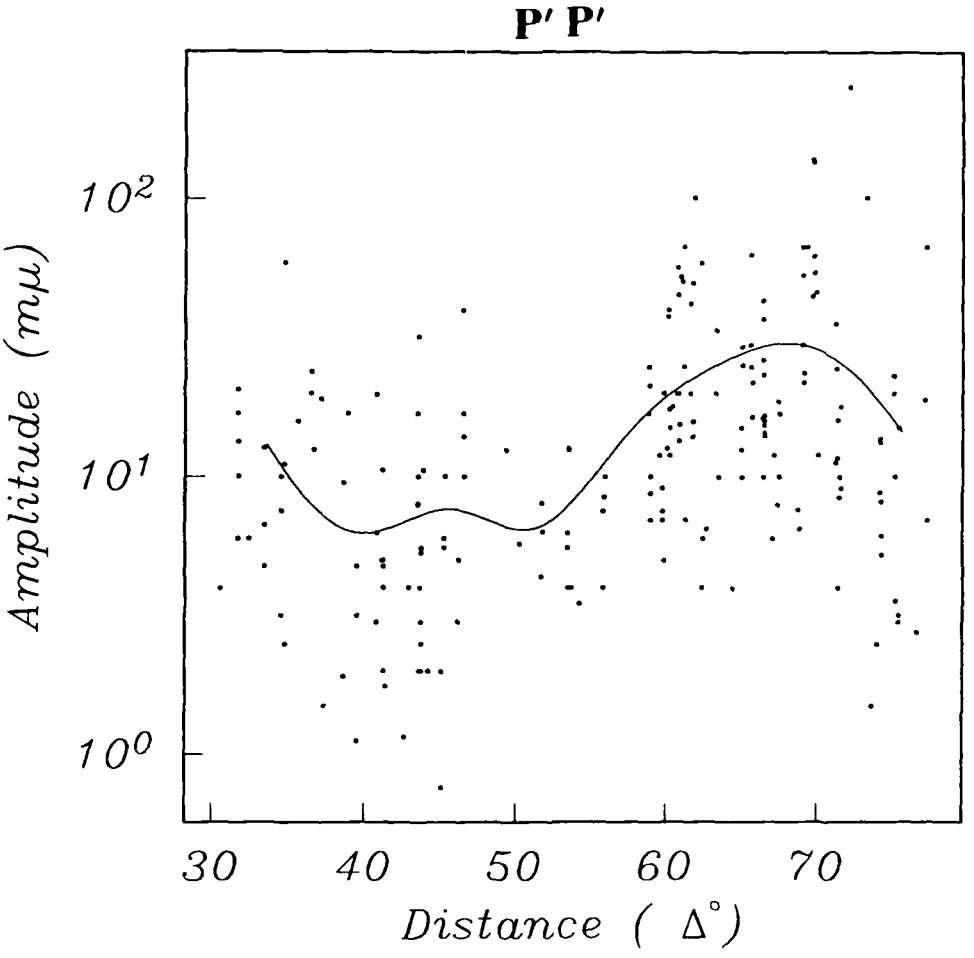

Figure 13. Composite P′P′ data scaled to m_b = 6 after correcting for instrument response and gain. A rms fit to the data yields an empirical distance-amplitude relationship for P'P'.

theory shown in Figure 14 together with the P and PKP amplitudes for a perturbed Preliminary Earth Model (PEM) of Choy and Cormier (1983). The caustics at 70° are clearly visible in both the theoretical and empirical curves for P′P′.

The amplitude ratios between the P′P′ and P phases are also studied for distance dependence. Since the peak P′P′ amplitude is measured, it is convenient to use the P_{max} phase for the ratios. The P/P′P′ ratios for the 8 events are shown in Figure 15. The data shown are observed ratios from stations where P and P′P′ were both on scale, and above the noise. By not considering censoring information, these ratios would probably be biased low since the clipped P_{max} and noisy P′P′ phases producing potentially large ratios are not considered. The observed P/P′P′ ratio has a minimum near 70°, as would be expected from the location of the P′P′ caustic. This minimum P/P′P′ ratio averages about 3, whereas values above 10 in the 40° to 60° range are more common. From Figure 14, we notice that the expected ratio of P/P′P′ in the distance range of 60° to 70° is about 2.5, roughly in agreement with the observed ratios in Figure 15. Sobel (1978) studied P′P′ and P′P′ precursors from earthquakes recorded at WWSSN stations and at the LASA and NORSAR arrays, and found a nearly constant amplitude of P′P′ between epicentral distances of 50° and 100° with m_b = Log(P′P′ in nm) + 3.76. The present study rests on an expanded data set and is able to provide broader azimuthal coverage than the study of Sobel (1978) which failed to detect the P′P′ caustic.

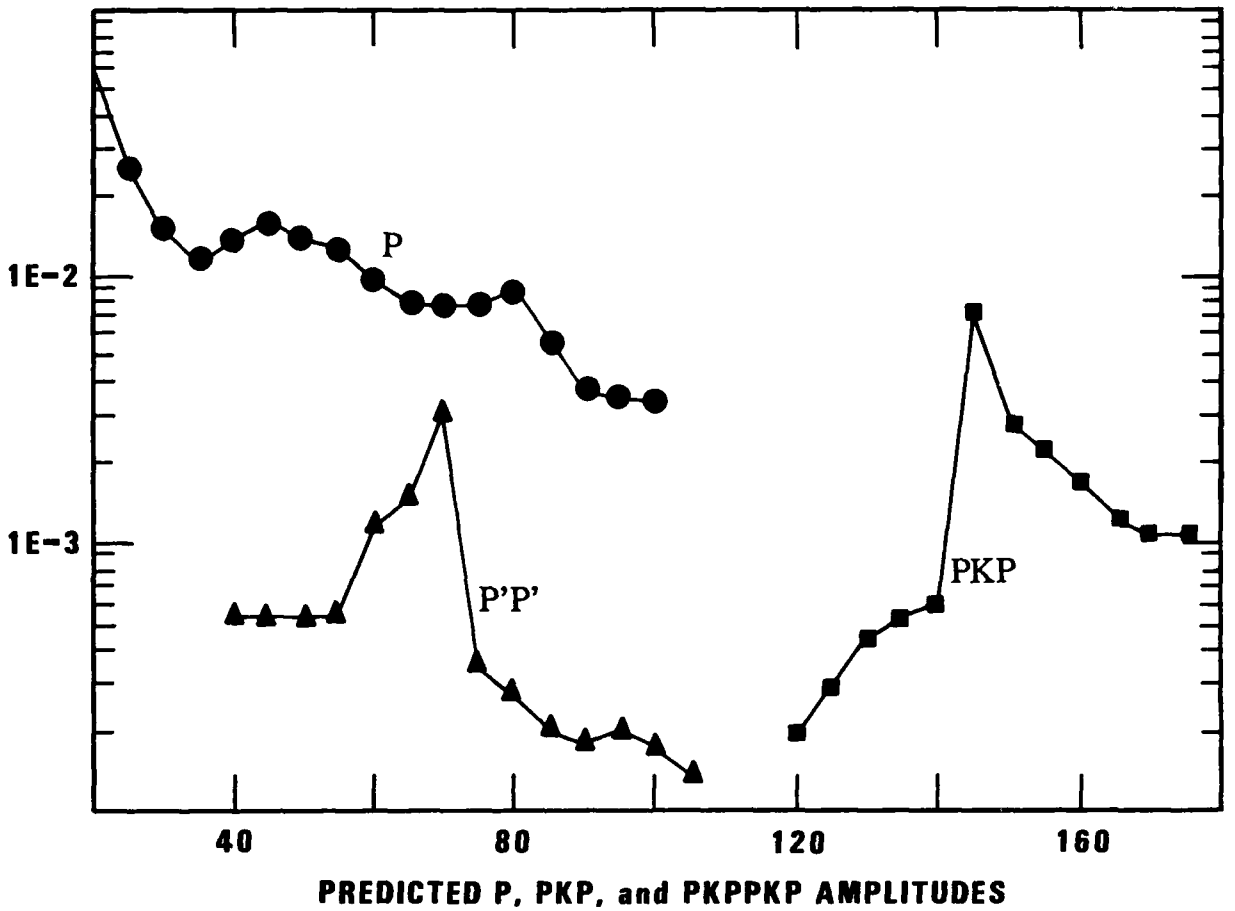

Figure 14. Predicted P, PKP, and P'P' peak amplitudes from WKBJ theory for a perturbed PEM (Choy and Cormier, 1983). Note the PKP caustic at 145° and the P'P' caustic at 70° .

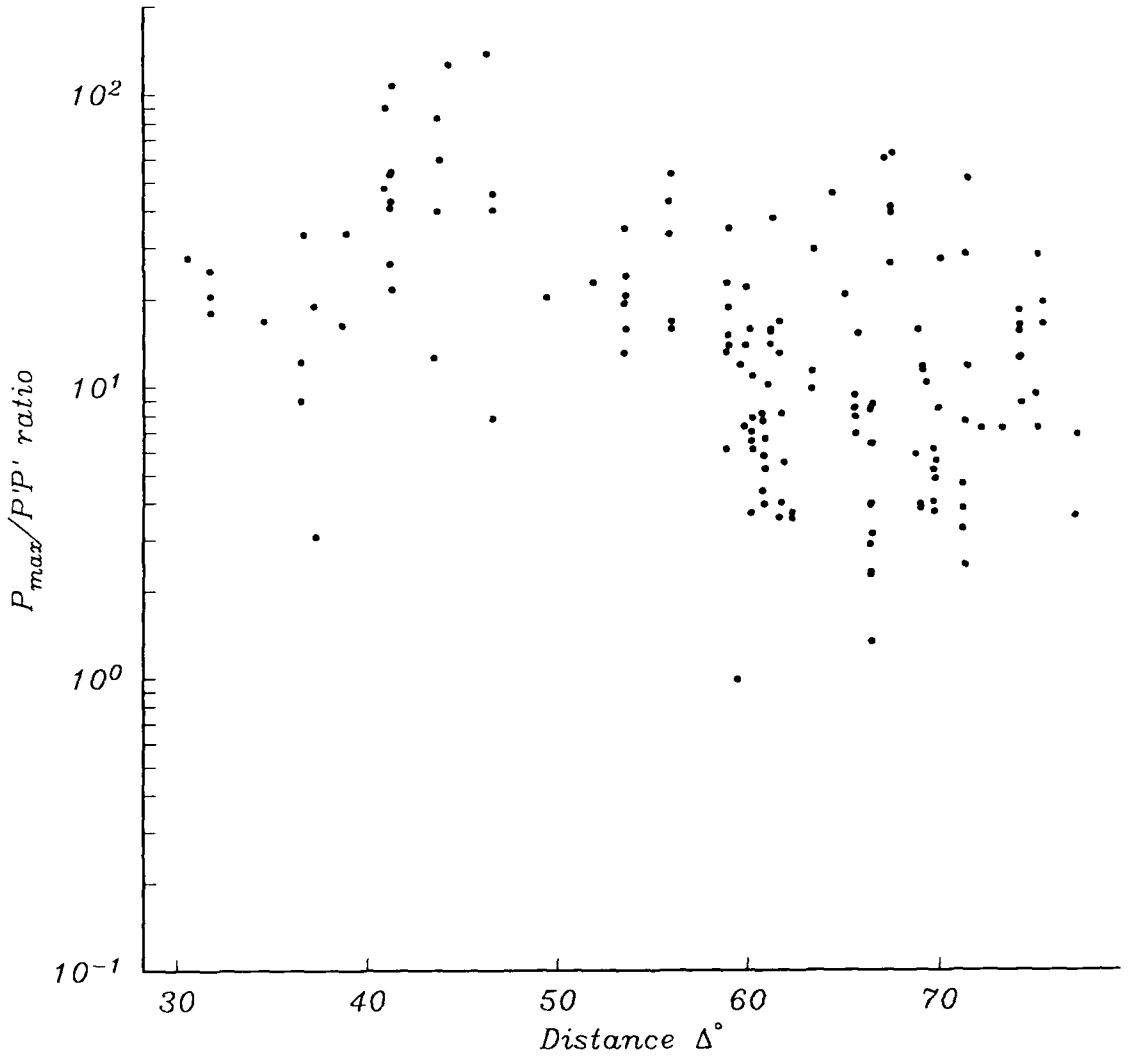

Figure 15. Observed P(max)/P'P' amplitude ratios at WWSSN stations between 30° and 80°, for the eight large Novaya Zemlya explosions. Only on scale P(max) and P'P' data are plotted. The ratios decrease drastically near the caustics of about 60° to 70°.

Maximum-Likelihood Estimates of $m_b(P'P')$

In order to estimate the $m_b(P'P')$ for the Novaya Zemlya events, we undertake two approaches. In both, the P'P' event magnitudes are adjusted to agree on average with events in the m_b = 6 range. The first method is to make use of the distance-amplitude relationship obtained in Figure 13 and the station corrections from Chan *et al.* (1988). The P'P' amplitudes in millimicrons are corrected for these parameters in addition to the instrument response. After correcting for these *a priori* parameters, the data are then input to the MLEGLM model (Chan *et al.*, 1988) to solve for the $m_b(P'P')$. The absolute value of the $m_b(P'P')$ is not a major concern here, since we are only interested in establishing a relationship between the $m_b(P)$ and $m_b(P'P')$.

Assuming a linear relationship between the $m_b(P)$ and $m_b(P'P')$, we performed a least squares fit to the data. From the correlation between the m_b's , the following relationships are obtained:

$$m_b(P_a) = 1.928 + (0.789 \pm 0.246)(m_b(P'P'))$$

$$m_b(P_b) = 1.585 + (0.899 \pm 0.239)(m_b(P'P'))$$

$$m_b(P_{max}) = 2.028 + (0.843 \pm 0.252)(m_b(P'P')).$$

The parameters are presented in Figure 16a and Table 9 between the various m_b's. Within standard errors, the slopes obtained from the above relationships do not deviate statistically from unity which is assumed in the following analysis. The linear intercepts are scaled such that the average $m_b(P'P')$ is the same $m_b(P)$.

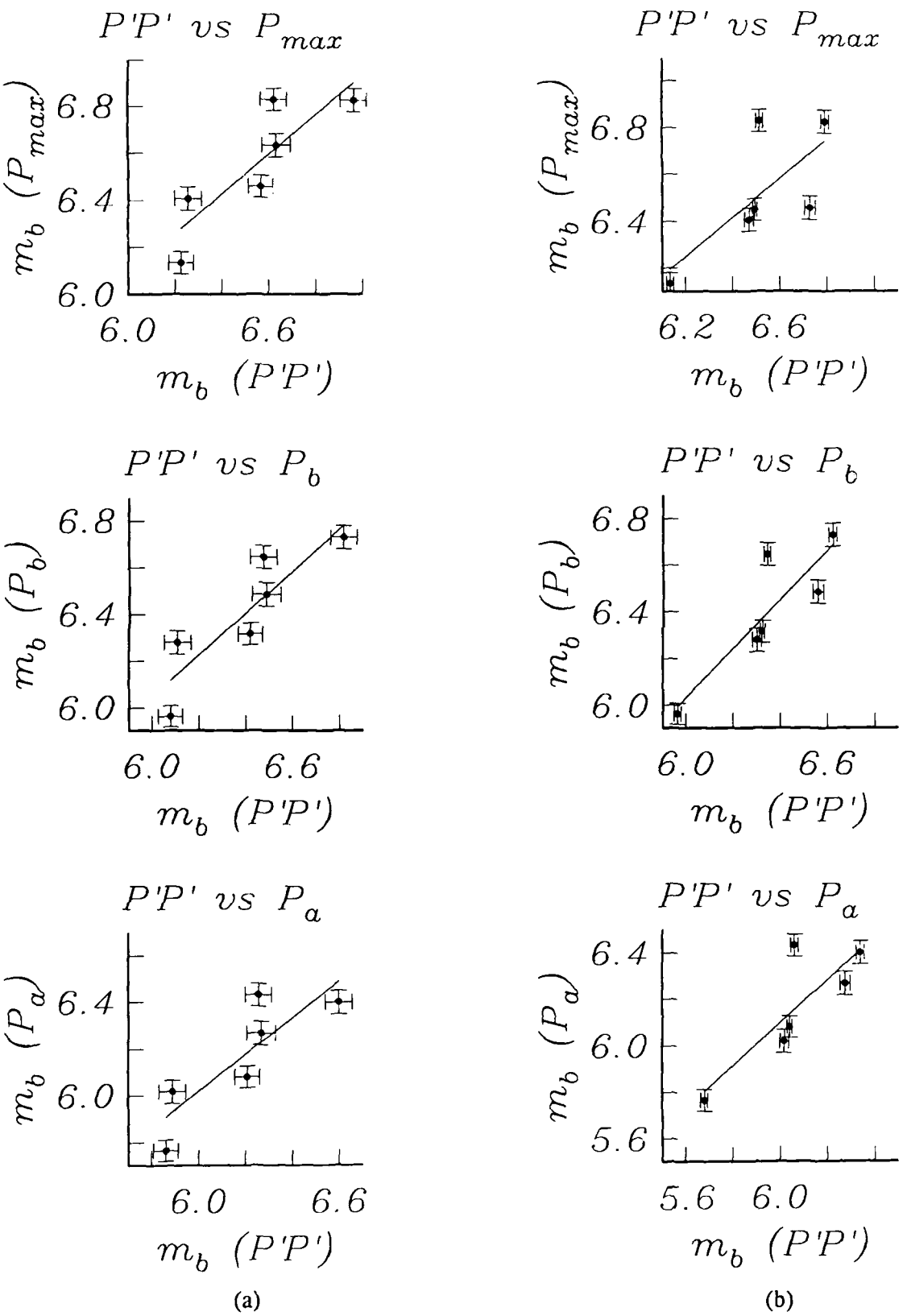

(a) (b)

Figure 16. Least squares fit of m_b(P)'s versus m_b(P'P') using (a) *a priori* constraints from estimated station corrections and amplitude-distance correction (left) and (b) no station and path constraints (right).

Table 9. $m_b(P'P')$ Estimates Using Amplitude-Distance Corrections

Date	$m_b(P_a)$	$m_b(P_b)$	$m_b(P_{max})$	$m_b(P'P')$
27 Oct 66	6.081±0.046	6.317±0.046	6.450±0.047	6.210±0.052
14 Oct 69	5.766±0.046	5.964±0.046	6.135±0.046	5.043±0.053
14 Oct 70	6.433±0.048	6.647±0.048	6.830±0.048	6.258±0.056
27 Sep 71	6.268±0.050	6.317±0.050	6.634±0.050	6.268±0.061
28 Aug 72	6.019±0.050	6.280±0.050	6.407±0.050	5.073±0.057
12 Sep 73	6.401±0.050	6.731±0.050	6.826±0.050	5.782±0.057

From the fit to the data, there is an indication that the $m_b(P)$ estimate for event 14 Oct 70 may possibly be biased high. However, the scatter of the data weakens such a conclusion. Judging from the quoted uncertainties for the estimated slopes, the $m_b(P'P')$ data is consistent with a unit slope between the $m_b(P_a)$, $m_b(P_b)$, $m_b(P_{max})$. The best estimates for the differences in Table 9, $m_b(P'P')$-$m_b(P_a)$, $m_b(P'P')$-$m_b(P_b)$, $m_b(P'P')$-$m_b(P_{max})$ are -0.40±0.18, -0.60±0.20, and -0.78±0.18, respectively. The $m_b(P'P')$ estimates are best correlated with the $m_b(P_a)$ estimates.

The second approach is to use the raw P'P' data from the northern Novaya Zemlya events recorded at common stations to solve for both the $m_b(P'P')$ and the station-path terms simultaneously using the maximum-likelihood estimation MLEGLM model (Chan *et al.*, 1988). The station-path terms may then be studied for distance dependence to be evaluated in light of the P'P' distance-amplitude curve obtained in Figure 13. The station-path terms are different from the P'P' distance-amplitude relationship in that they contain the additional station corrections, while preserving the dominating caustics at around 70°. Judging from the quoted uncertainties for the estimated slopes, the $m_b(P'P')$ data is consistent with a unit slope between the $m_b(P_a)$, $m_b(P_b)$, $m_b(P_{max})$. The best estimates for the differences in Table 9, $m_b(P'P')$-$m_b(P_a)$, $m_b(P'P')$-$m_b(P_b)$,

$m_b(P'P')$-$m_b(P_{max})$ are -0.12±0.06, -0.09±0.07, and -0.27±0.06, respectively. The $m_b(P'P')$ estimates are again correlated best with the $m_b(P_a)$ estimates.

The data are better constrained in this than in the earlier case. The least squares fits to the data give the following relationships between the $m_b(P)$'s and $m_b(P'P')$'s:

$$m_b(P_a) = 4.122 + (0.919\pm0.301)(m_b(P'P'))$$

$$m_b(P_b) = 3.542 + (1.051\pm0.292)(m_b(P'P'))$$

$$m_b(P_{max}) = 5.009 + (0.835\pm0.399)(m_b(P'P')).$$

The $m_b(P'P')$'s data presented in Figure 16d and listed in Table 10 are scaled by the intercept values in the above relationships in order to be compared with the $m_b(P)$'s.

Table 10. $m_b(P'P')$ Estimates Corrected for Station-Path Effects

Date	$m_b(P_a)$	$m_b(P_b)$	$m_b(P_{max})$	$m_b(P'P')$
27 Oct 66	6.081±0.046	6.317±0.046	6.459±0.046	6.254±0.010
14 Oct 69	5.766±0.046	5.964±0.046	6.135±0.046	5.895±0.015
14 Oct 70	6.433±0.048	6.647±0.048	6.830±0.048	6.276±0.015
27 Sep 71	6.268±0.050	6.317±0.050	6.634±0.050	6.489±0.022
28 Aug 72	6.019±0.050	6.280±0.050	6.407±0.050	6.232±0.019
12 Sep 73	6.401±0.050	6.731±0.050	6.826±0.050	6.553±0.017

Based on $m_b(P_{max})$-$m_b(P_{max})$-$m_b(P_a)$ and $m_b(P'P')$, the 27 Sep 1971 event has a smaller $m_b(P_{max})$ compared to other events of comparable size. The $m_b(P_{max})$ for this event may be underestimated by 0.1 magnitude units. The $m_b(P'P')$-$m_b(P)$ is anomalous for the 14 Oct 70 event when compared to the other events of similar size. Regression analyses of the two sets of results in Tables 9 and 10 show that the $m_b(P'P')$: $m_b(P_a)$, $m_b(P'P')$: $m_b(P_b)$, and $m_b(P'P')$: $m_b(P_{max})$ correlation coefficients all fail the 95% F-statistic test for the first approach using the amplitude-distance correction whereas for the second approach using the station-path corrections, only the $m_b(P'P')$: $m_b(P_a)$

correlation coefficient fails the 95% F-statistic. The multivariate regression analysis shows that the latter approach is a more stable. The m_b's appear to correlate best between the P'P' and P_a phases in both cases.

The station-path corrections are shown as a function of distance in Figure 17. The scaled P'P' distance-amplitude curve obtained in Figure 13 for is also plotted. The station-path correction is a combination of the station effects, geometrical spreading and attenuation factors. Since the station effects are independent of distance, therefore the relationship between the station-path terms and distance is obscure. As expected, no clear relationship may be established due to the strong scatter in the data, but there is an indication of a possible caustic at around 60° to 70°, as shown from the theoretical and empirical studies. With the scatter in the data, the station-path terms appear to follow the general trend of the P'P' distance-amplitude curve. Although we are not able to delineate any distance information using just the station-path terms, the m_b(P'P')'s corrected using these estimates appear to be better correlated with the m_b(P)'s since both the m_b(P'P')'s and the station-path corrections are inverted simultaneously using the same data set.

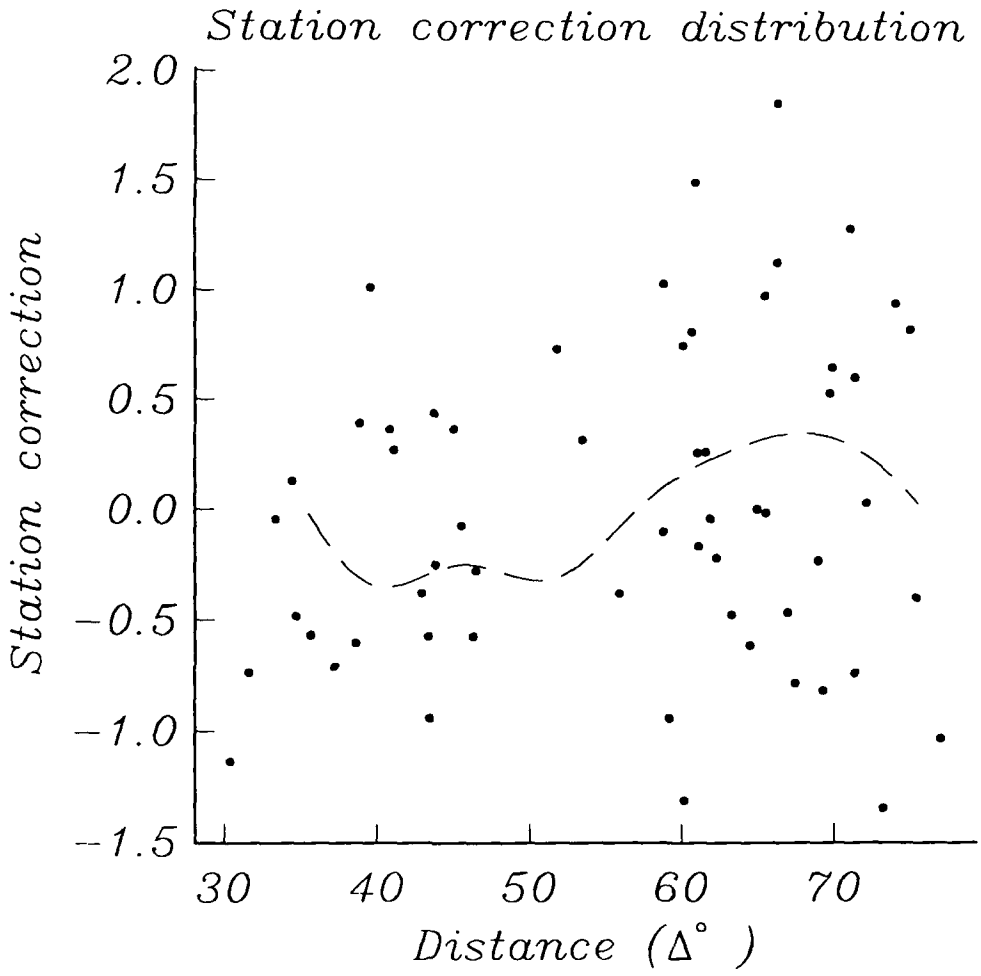

Figure 17. Station-path effects versus distance obtained from ML-GLM estimates of m_b(P'P') using 7 northern Novaya Zemlya events. The dashed line indicates the P'P' distance-amplitude relationship from Figure 13.

CONCLUSIONS

A variety of analyses was performed in order to gain better understanding of the characteristics of Novaya Zemlya explosions using body wave phases and to calibrate their source size. The azimuthal variations in amplitude for most Novaya Zemlya explosions may be modeled using a sin(2θ) curve. This pattern may be attributed to a combination near-source effects including local structural heterogeneity, tectonic release, focusing and defocusing, or source anisotropy. Deviations from the sin(2θ) model may be indicative of multiple events characterized by an asymmetrical m_b distribution. The m_b bias estimated by azimuthal quadrants for the known double event of 14 Oct 70 may be biased high by 0.4 magnitude units.

Source time function deconvolution show that the time delays of the depth phase are up to 0.6 seconds and are a function of source size. An understanding of the interference of the depth phase will aid in the determination of the spectral amplitude to correlate with the m_b estimates from P-waves. The spectral energy measurements of P, PcP and P_{diff} at EKA and WRA arrays are well correlated with the m_b's and provide an added constraint on the source size. The source size for the largest Novaya Zemlya events was found to be larger than CANNIKIN by studying the moment estimates from both sites.

A distance-amplitude relationship for P′P′ was derived empirically using data for Novaya Zemlya explosions recorded teleseismically at WWSSN stations. Using this distance-amplitude correction, relationships between the m_b's for P and P′P′ were established. In addition, by solving for the m_b(P′P′) and station-path corrections simul-

taneously using a maximum-likelihood generalized linear model, a similar relationship between the m_b's was also obtained. The empirical relationship between m_b(P) and m_b(P'P') may be used independently to calibrate the less well constrained magnitudes for the large Novaya Zemlya events.

The magnitude relationships derived in this study provide constraints on the scaling of the source size of the large Novaya Zemlya explosions. In spite of the paucity of available data for these explosions, we have succeeded in obtaining empirical relationships between m_b's, P_{diff}, and PcP spectral amplitudes, and P'P' time domain amplitudes. These auxiliary diffracted and core-related phases were shown to be useful in calibrating the large explosions for which the direct P arrivals are mostly saturated.

REFERENCES

Aki, K. (1964). A note on surface waves from the HARDHAT nuclear explosions, *J. Geophys. Res.*, **69**, 1131-1134.

Aki, K. and Y.-B. Tsai (1972). Mechanism of Love-wave excitation by explosive source, *J. Geophys. Res.*, **77**, 1452-1475.

Archambeau, C.B. (1972). The theory of stress wave radiation from explosions in prestressed media, *Geophys. J.*, **29**, 329-366.

Azimi, Sh.A., A.V. Kalinin, and B. L. Pivovarov (1968). Impulse and transient characteristics of media with linear and quadratic absorption laws, *Izv., Earth Phys.*, **2**, 42-54 (English translation).

Bache, T.C. (1976). The effects of tectonic release on explosion P-wave signatures, *Bull. Seism. Soc. Am.*, **66**, 1441-1457.

Bache, T.C. (1982). Estimating the yield of underground nuclear explosions, *Bull. Seism. Soc. Am.*, **72**, S131-S168.

Bakun, W.H., and L.R. Johnson (1973). The deconvolution of teleseismic P waves from explosions MILROW and CANNIKIN, *Geophys. J. R. astr. Soc.*, **34**, 321-342.

Brune, J.N. and P.W. Pomeroy (1963). Surface wave radiation patterns for underground nuclear explosions and small-magnitude earthquakes, *J. Geophys. Res.*, **68**, 5005-5028.

Burger, R.W., L.J. Burdick, and T. Lay (1986). Estimating the relative yields of Novaya Zemlya tests by waveform intercorrelation, *Geophys. J. R. astr. Soc.*, **87**, 775-800.

Carpenter, E.W. (1967). Teleseismic signals calculated for underground, underwater, and atmospheric explosions, *Geophysics*, **32**, 17-32.

Chan, W.W. and B.J. Mitchell (1985). Surface wave dispersion, crustal structure, and sediment thickness variations across the Barents shelf, *Geophys. J. R. astr. Soc.*, **80**, 329-344.

Chan, W.W, K.L. McLaughlin, R.-S. Jih, M.E. Marshall, and R.A. Wagner (1988). Comprehensive magnitude yield estimation for nuclear explosions: A maximum likelihood general linear model (MLE-GLM88), *TGAL-87-05*, Teledyne Geotech, Alexandria, Virginia.

Choy, G. and V. Cormier (1983). The structure of the inner core inferred from short-period and broadband GDSN data, *Geophys. J. R. astr. Soc.*, **72**, 1-21.

Der, Z.A., T.W. McElfresh, R.A. Wagner, and J. Burnetti (1985), Spectral characteristics of P waves from nuclear explosions and yield estimation. *Bull. Seism. Soc. Am.*, **75**, 379-390. Errata, *Bull. Seism. Soc. Am.*, **75**, 1222.

Der, Z.A., A.C. Lees, W.W. Chan, R.H. Shumway, K.L. McLaughlin, E. Smart, T.W. McElfresh, and M.E. Marshall (1987a). Maximum-likelihood multichannel deconvolution of P waves at seismic arrays, *TGAL-87-3*, Teledyne Geotech, Alexandria, Virginia.

Der, Z.A., R.H. Shumway, and A.C. Lees (1987b). Multichannel deconvolution of P waves at seismic arrays, *Bull. Seism. Soc. Am.*, **77**, 195-211.

Douglas, A., P.D. Marshall, and J.B. Young (1987). The P waves from the Amchitka Island explosion, *Geophys. J. R. astr. Soc.*, **90**, 101-117.

Eldholm, O. and M. Talwani (1977). Sediment distribution and structural framework of the Barents Sea, *Bull. Geol. Soc. Am.*, **88** 1015-1029.

Gupta, I.N., R.R. Blandford, R.A. Wagner, J.A. Burnetti, and T.W. McElfresh (1985). Use of P coda for determination of yield of nuclear explosions, *Geophys. J. R. astr. Soc.*, **83**, 541-553.

Haddon, R.A.W., E.S. Husebye, and D.W. King (1977). Origins of precursors to P'P', *Phys. Earth Planet. Inter.*, **14**, 41-70.

Hirasawa, T. (1971). Radiation patterns of S waves from underground nuclear explosions, *J. Geophys. Res.*, **76**, 6440-6454.

Hurley, R.W. (1977). Anomalous seismic signals from Novaya Zemlya, *AWRE Report No. O21/77*, HMSO, London, England.

Langston, C.A. and D.V. Helmberger (1975). A procedure for modeling shallow dislocation sources, *Geophys. J.*, **42**, 117-130.

Lay, T., T.C. Wallace, and D.V. Helmberger (1984). The effects of tectonic release on short-period P waves from NTS explosions, *Bull. Seism. Soc. Am.*, **74**, 819-842.

Lilwall, R.C., and P.D. Marshall (1986). Body wave magnitudes and locations of Soviet underground explosions at the Novaya Zemlya test site, *AWRE Report No. O17/86*, AWRE, MOD(PE), Aldermaston, Berkshire, England.

Masse, R.P. (1981). Review of seismic source models for underground nuclear explosions, *Bull. Seism. Soc. Am.*, **71**, 1249-1268.

McLaughlin, K.L., A.C. Lees, Z.A. Der, and M.E. Marshall (1988). Teleseismic spectral and temporal M_0 and Ψ_∞ estimates for four French explosions in southern Sahara, *Bull. Seism. Soc. Am.*, **78**, 1580-1586.

Murphy, J.R., C.B. Archambeau, and H.K. Shah (1983). Magnitude/yield variability in the western United States: Analysis of the Rulison/Gasbuggy anomaly, Final Technical Report, *SSS-R-83-5978*, S-Cubed, La Jolla, California.

Nuttli, O.W. (1969). Travel times and amplitudes of S waves from nuclear explosions in Nevada, *Bull. Seism. Soc. Am.*, **59**, 385-398.

Nuttli, O.W. (1988). L_g magnitudes and yield estimates for underground Novaya Zemlya nuclear explosions, *Bull. Seism. Soc. Am.*, **78**, 873-884.

Press, F. and C.B. Archambeau (1962). Release of tectonic strain by underground nuclear explosions, *J. Geophys. Res.*, **67**, 337-343.

Shumway, R.H. and Z.A. Der (1985). Deconvolution of multiple time series, *Technometrics*, **27**, 385-393.

Sobel, P. (1978). The phase P'dP' as a means for determining upper mantle structure, Ph.D. thesis, 129pp., University of Minnesota, Minneapolis, Minnesota.

Stevens, J.L. (1986). Analysis of explosion-generated Rayleigh and Love waves from the East Kazakh, Amchitka, and Nevada test sites, *AFGL-TR-86-0043*, S-Cubed, La Jolla, California.

Teng, T.-L. and J.P. Tung (1973). Upper-mantle discontinuity from amplitude data of P'P' and its precursors, *Bull. Seism. Soc. Am.*, **63**, 587-597.

Toksöz, M.N. and Kehrer, H.H. (1972). Tectonic strain release by underground nuclear explosions and its effects on seismic discrimination, *Geophys. J. R. astr. Soc.*, **31**, 141-161.

Veith, K.F. and G.E. Clawson (1972). Magnitude from short-period P-wave data, *Bull. Seism. Soc. Am.*, **62**, 435-452.

von Seggern, D.H., and R.R. Blandford (1972). Source time functions and spectra for underground nuclear explosions, *Geophys. J. R. astr. Soc.*, **31**, 83-97.

Wallace, T.C., D.V. Helmberger, and G.R. Engen (1983). Evidence of tectonic release from underground nuclear explosions in long-period P waves, *Bull. Seism. Soc. Am.*, **73**, 593-613.

Whitcomb, J.H. (1973). Asymmetric P'P': an alternative to P'dP' reflections in the uppermost mantle (0 to 110 km), *Bull. Seism. Soc. Am.*, **63**, 133-143.

Whitcomb, J.H. and D.L. Anderson (1970). Reflection of P'P' seismic waves from discontinuities in the mantle, *J. Geophys. Res.*, **75**, 5713-5728.

DISTRIBUTION LIST
FOR UNCLASSIFIED REPORTS
DARPA-FUNDED PROJECTS
(Last Revised: 26 October 1988)

RECIPIENT	NO. OF COPIES
DEPARTMENT OF DEFENSE	
DARPA/GSD ATTN: Dr. R. Alewine and Dr. R. Blandford 1400 Wilson Boulevard Arlington, VA 22209-2308	2
DARPA/PM 1400 Wilson Boulevard Arlington, VA 22209-2308	1
Defense Intelligence Agency Directorate for Scientific and Technical Intelligence Washington, D.C. 20301	1
Defense Nuclear Agency Shock Physics Washington, D.C. 20305-1000	1
Defense Technical Information Center Cameron Station Alexandria, VA 22314	12
DEPARTMENT OF THE AIR FORCE	
AFGL/LWH ATTN: Dr. J. Cipar and Mr. J. Lewkowicz Terrestrial Sciences Division Hanscom AFB, MA 01731-5000	2

AFOSR/NPG
ATTN: Director
Bldg. 410, Room C222
Bolling AFB, Washington, D.C. 20332

1

AFTAC/DA
ATTN: STINFO Officer
Patrick AFB, FL 32925-6001

1

AFTAC/TT
Patrick AFB, FL 32925-6001

3

AFWL/NTESG
Kirtland AFB, NM 87171-6008

1

DEPARTMENT OF THE NAVY

NORDA
ATTN: Dr. J.A. Ballard
Code 543
NSTL Station, MS 39529

1

DEPARTMENT OF ENERGY

Department of Energy
ATTN: Mr. Max A. Koontz (DP-52)
International Security Affairs
1000 Independence Avenue
Washington, D.C. 20545

1

Lawrence Livermore National Laboratory
ATTN: Dr. J. Hannon and Dr. M. Nordyke
University of California
P.O. Box 808
Livermore, CA 94550

2

Los Alamos Scientific Laboratory 2
ATTN: Dr. K. Olsen and Dr. T. Weaver
P.O. Box 1663
Los Alamos, NM 87544

Sandia Laboratories 1
ATTN: Mr. P. Stokes
Geosciences Department 1255
Albuquerque, NM 87185

OTHER GOVERNMENT AGENCIES

Central Intelligence Agency 1
ATTN: Dr. L. Turnbull
OSI/NED, Room 5G48
Washington, D.C. 20505

U.S. Arms Control and Disarmament Agency 1
ATTN: Dr. M. Eimer
Verification and Intelligence Bureau, Rm 4953
Washington, D.C. 20451

U.S. Arms Control and Disarmament Agency 1
ATTN: Mr. Alfred Lieberman
VI-OA, Rm 5726
State Department Building
320 - 21st Street, NW
Washington, DC 20451

U.S. Arms Control and Disarmament Agency 1
ATTN: Mrs. M. Hoinkes
Multilateral Affairs Bureau, Rm 5499
Washington, D.C. 20451

U.S. Geological Survey 1
ATTN: Dr. T. Hanks
National Earthquake Research Center
345 Middlefield Road
Menlo Park, CA 94025

U.S. Geological Survey 1
ATTN: Dr. R. Masse
Global Seismology Branch
Box 25046, Stop 967
Denver Federal Center
Denver, CO 80225

UNIVERSITIES

Boston College 1
ATTN: Dr. A. Kafka
Western Observatory
381 Concord Road
Weston, MA 02193

California Institute of Technology 1
ATTN: Dr. D. Harkrider
Seismological Laboratory
Pasadena, CA 91125

Columbia University 1
ATTN: Dr. L. Sykes
Lamont-Doherty Geological Observatory
Palisades, NY 10964

Cornell University 1
ATTN: Dr. M. Barazangi
INSTOC
Snee Hall
Ithaca, NY 14853

Harvard University 1
ATTN: Dr. J. Woodhouse
Hoffman Laboratory
20 Oxford Street
Cambridge, MA 02138

Massachusetts Institute of Technology 3
ATTN: Dr. S. Soloman, Dr. N. Toksoz, and Dr. T. Jordan
Department of Earth and Planetary Sciences
Cambridge, MA 02139

Southern Methodist University 1
ATTN: Dr. E. Herrin
Geophysical Laboratory
Dallas, TX 75275

State University of New York at Binghamton 1
ATTN: Dr. F. Wu
Department of Geological Sciences
Vestal, NY 13901

St. Louis University 2
ATTN: Dr. O. Nuttli and Dr. R. Herrmann
Department of Earth and Atmospheric Sciences
3507 Laclede
St. Louis, MO 63156

The Pennsylvania State University 1
ATTN: Dr. S. Alexander
Geosciences Department
403 Deike Building
University Park, PA 16802

University of Arizona 1
ATTN: Dr. T. Wallace
Department of Geosciences
Tucson, AZ 85721

University of California, Berkeley 1
ATTN: Dr. T. McEvilly
Department of Geology and Geophysics
Berkeley, CA 94720

University of California Los Angeles 1
ATTN: Dr. L. Knopoff
Department of Earth and Space Sciences
3806 Geology
Los Angeles, CA 90024

University of California, San Diego 1
ATTN: Dr. J. Orcutt
Scripps Institute of Oceanography
La Jolla, CA 92093

University of Colorado 1
ATTN: Dr. C. Archambeau
CIRES
Boulder, CO 80309

University of Illinois 1
ATTN: Dr. S. Grand
Department of Geology
1301 West Green Street
Urbana, IL 61801

University of Michigan 1
ATTN: Dr. T. Lay
Department of Geological Sciences
Ann Arbor, MI 48109-1063

University of Nevada 1
ATTN: Dr. K. Priestley
Mackay School of Mines
Reno, NV 89557

University of Southern California 1
ATTN: Dr. K. Aki
Center for Earth Sciences
University Park
Los Angeles, CA 90089-0741

DEPARTMENT OF DEFENSE CONTRACTORS

Applied Theory, Inc. 1
ATTN: Dr. J. Trulio
930 South La Brea Avenue
suite 2
Los Angeles, CA 90036

Center for Seismic Studies 2
ATTN: Dr. C. Romney and Mr. R. Perez
1300 N. 17th Street, Suite 1450
Arlington, VA 22209

ENSCO, Inc.
ATTN: Mr. G. Young
5400 Port Royal Road
Springfield, VA 22151

1

ENSCO, Inc.
ATTN: Dr. R. Kemerait
445 Pineda Court
Melbourne, FL 32940

1

Gould Inc.
ATTN: Mr. R. J. Woodard
Chesapeake Instrument Division
6711 Baymeado Drive
Glen Burnie, MD 21061

1

Pacific Northwest Laboratories
ATTN: Dr. Wes L. Nicholson
Battelle Memorial Institute
P. O. Box 999
Richland, WA 99352

1

Pacific Sierra Research Corp.
ATTN: Mr. F. Thomas
12340 Santa Monica Boulevard
Los Angeles, CA 90025

1

Rockwell International
ATTN: B. Tittmann
1049 Camino Dos Rios
Thousand Oaks, CA 91360

1

Rondout Associates, Inc.
ATTN: Dr. P. Pomeroy
P.O. Box 224
Stone Ridge, NY 12484

1

Science Applications, Inc.
ATTN: Dr. T. Bache, Jr.
P.O.Box 2351
La Jolla, CA 92038

Science Horizons
ATTN: Dr. T. Cherry and Dr. J. Minster
710 Encinitas Blvd.
Suite 101
Encinitas, CA 92024 2

Sierra Geophysics, Inc.
ATTN: Dr. R. Hart and Dr. G. Mellman
11255 Kirkland Way
Kirkland, WA 98124 2

SRI International
ATTN: Dr. A. Florence
333 Ravensworth Avenue
Menlo Park, CA 94025 1

S-Cubed, A Division of
Maxwell Laboratories Inc.
ATTN: Dr. S. Day
P.O. Box 1620
La Jolla, CA 92038-1620 1

S-Cubed, A Division of
Maxwell Laboratories Inc.
ATTN: Mr. J. Murphy
11800 Sunrise Valley Drive
Suite 1212
Reston, VA 22091 1

Teledyne Geotech
ATTN: Dr. Z. Der and Mr. W. Rivers
314 Montgomery Street
Alexandria, VA 22314 2

Woodward-Clyde Consultants
ATTN: Dr. L. Burdick and Dr. J. Barker
556 El Dorado St.
Pasadena, CA 91105 2

NON-U.S. RECIPIENTS

National Defense Research Institute FOA 290 — 1
ATTN: Dr. O. Dahlman
Box 27322
S-10254 Stockholm, Sweden

Blacknest Seismological Center — 1
ATTN: Mr. P. Marshall
Atomic Weapons Research Establishment
UK Ministry of Defence
Brimpton, Reading, Berks. RG7-4RS
United Kingdom

NTNF NORSAR — 1
ATTN: Dr. F. Ringdal
P.O. Box 51
N-2007 Kjeller
Norway

OTHER DISTRIBUTION

To be determined by the project office — 9